



This is to certify that the

thesis entitled

EVALUATING ISOSTATIC AND QUASI-ISOSTATIC PROCEDURES DETERMINING THE ORGANIC VAPOR BARRIER PROPERTIES THROUGH POLYMER MEMBRANES

presented by

SHU-JUNG HUANG

has been accepted towards fulfillment of the requirements for

M. S. degree in PACKAGING

Date 8/15/96

Major professor

O-7639

MSU is an Affirmative Action/Equal Opportunity Institution

LIBRARY Michigan State University

PLACE IN RETURN BOX to remove this checkout from your record. TO AVOID FINES return on or before date due.

DATE DUE	DATE DUE	DATE DUE
73 A		
AN 1 1 2000 - AN 1 1 2000		

MSU is An Affirmative Action/Equal Opportunity Institution ctoirclassdus.pm3-p.1

EVALUATING ISOSTATIC AND QUASI-ISOSTATIC PROCEDURES FOR DETERMINING THE ORGANIC VAPOR BARRIER PROPERTIES THROUGH POLYMER MEMBRANES

by

Shu-Jung Huang

A THESIS

Submitted to
Michigan State University
in partial fulfillment of the requirements
for the degree of

MASTER OF SCIENCE

School of Packaging

1996

ABSTRACT

EVALUATING ISOSTATIC AND QUASI-ISOSTATIC PROCEDURES FOR DETERMINING THE ORGANIC VAPOR BARRIER PROPERTIES THROUGH POLYMER MEMBRANES

bv

Shu-Jung Huang

The permeability of ethyl acetate, toluene, limonene, methyl ethyl ketone, and α -pinene through a series of commodity films was determined by an isostatic procedures utilizing the MAS Technology Model 2000 Permeability Test System. Studies considered the concentration and temperature dependency of the mass transfer process, as well as the application of the Arrhenius expression for determining permeance values of high barrier polymer structures. The temperature dependency of the transport processes, over the temperature range studied, was found to follow well the Arrhenius relationship. For penetrant/polymer systems, permeability tests were also carried out at selected vapor concentrations by a quasiisostatic procedure, based on a test system of our own design. The permeance values obtained by the two procedures were found to be in acceptable agreement.

In addition to determining the permeability and diffusion coefficient values, a consistency analysis was also performed on experimental permeability data to examine the variation in system parameters and to provide a better understanding of the mechanism of the diffusion process associated with penetrant permeability.

To My Dear Family.

ACKNOWLEDGMENTS

I would like to gratefully thank Dr. Giacin for his guidance and endless patience while acting as my advisor.

Appreciation is expressed to Dr. Hernandez and Dr. Beaudry for serving on the guidance committee.

A special thank you is extended to Chai-Hung Lin for her sharing of knowledge and skill and my family for their support and understanding.

Finally I am indebted to the MAS Technology company for the technical support throughout this research study.

TABLE OF CONTENTS

LIST OF TABLES	viii
LIST OF FIGURES	xi
INTRODUCTION	1
LITERATURE REVIEW	
Importance of The Permeation of Organic Vapor Through Polymer Films	
Permeation Process of Organic Vapor Through Polymer Membranes	
Permeation Mechanism for Organic Vapor Through Polymer Membranes	· · · · · · · · · · · · · · · · · · ·
Diffusion of Organic Vapors Through Polymer Membranes	12
Theory of diffusion	13
Equilibrium sorption	14
Steady of solution	15
Time lag technique	16
Characteristics of diffusion coefficient	18
Free volume theory	20
Factors Affecting Permeation of Organic Vapors Through Polymer Films	22
Natural of polymer	22
Nature of penetrant	25
Concentration	26
Temperature	27
Organic Vapor Permeation Measurement and Techniques	28

Gravimetric technique 29
Absolute procedure method 29
Quasi-isostatic procedure
Isostatic procedure 33
MAS 2000 Organic Vapor Permeation Test System 35
Evaluating The Consistency of The Permeability Experimental Data
MATERIALS AND METHODS
Packaging Materials 40
Permeability Test Methods
Quasi-isostatic procedure 42
Isostatic procedure 44
Determining vapor pressure
Determining partial pressure 47
RESULTS AND DISCUSSION
Permeability of Packaging Films by an Isostatic Procedure 54
Effect of vapor activity and temperature on organic vapor permeability
Estimation of permeance values at vapor activity levels impractical to measure experimentally 101
Permeability of Packaging Films by a Quasi- Isostatic Procedure
A Comparison of Organic Vapor Permeance Values by Isostatic and Quasi-Isostatic Procedures 113
Evaluation of The Consistency of The Continuous Flow Permeability Data 116
Evaluation The Application of MAS 2000 Organic Vapor Permeation Test System

ERROR ANALYSIS	129
SUMMARY AND CONCLUSIONS	132
Appendix A: Calibration curve for penetrants by Gas Chromatograph	134
Appendix B: Permeation rate of various permeants for a series of packaging films by quasi-isostatic procedure	139
BIBLIOGRAPHY	142

LIST OF TABLES

Tables				
1.	Permeance constant of ethyl acetate through packaging films as a function of temperature and vapor activity	. 55		
2.	Diffusion coefficient of ethyl acetate through packaging films as a function of temperature and vapor activity	. 56		
3.	Permeance constant of toluene through packaging films as a function of temperature and vapor activity	. 57		
4.	Diffusion coefficient of toluene through packaging films as a function of temperature and vapor activity	. 58		
5.	Permeance constant of limonene through packaging films as a function of temperature and vapor activity	. 59		
6.	Diffusion coefficient of limonene through packaging films as a function of temperature and vapor activity	. 60		
7.	Permeance constant of methyl ethyl ketone through packaging films as a function of temperature and vapor activity	. 61		
8.	Diffusion coefficient of methyl ethyl ketone through packaging films as a function of temperature and vapor activity			
9.	Permeance constant of $\alpha\text{-pinene}$ through packaging films as a function of temperature and vapor activity	. 63		
10.	. Diffusion coefficient of α -pinene through packaging films as a function of temperature and vapor activity	. 64		
11.	Activation energy values for the permeation of ethyl acetate through packaging films	. 95		
12.	Activation energy values for the permeation of toluene through packaging films	. 96		
13.	Activation energy values for the permeation of limonene through packaging films	. 96		
14.	Activation energy values for the permeation of methyl ethyl ketone through packaging films	. 97		

15.	Activation energy values for the permeation of $\alpha\text{-pinene}$ through packaging films	. 97
16.	Estimated permeance values of test packaging structures for limonene at 24°C	102
17.	Permeability parameters for high density polyethylene by quasi-isostatic procedure at 24°C	111
18.	Permeability parameters for oriented polypropylene by quasi-isostatic procedure at 24°C	111
19.	Permeability parameters for Saran coated OPP by quasi-isostatic procedure at 24°C	112
20.	Permeability parameters for Acrylic coated OPP by quasi-isostatic procedure at 24°C	112
21.	Permeability parameters for glassine by quasi-isostatic procedure at 24°C	113
22.	A comparison of permeance values determined by isostatic and quasi-isostatic procedures for ethyl acetate at 24°C \dots	114
23.	A comparison of permeance values determined by isostatic and quasi-isostatic procedures for toluene at 24°C	114
24.	A comparison of permeance values determined by isostatic and quasi-isostatic procedures for limonene at 24°C	115
25.	A comparison of permeance values determined by isostatic and quasi-isostatic procedures for methyl ethyl ketone at 24°C	115
26.	A comparison of permeance values determined by isostatic and quasi-isostatic procedures for $\alpha\text{-pinene}$ at 24°C	116
27.	Experimental date for limonene and α -pinene in high density polyethylene and oriented polypropylene structures at a=0.4, 50°C	127
28.	Calibration data for ethyl acetate in acetonitrile with a 1 μl injection volume	134
29.	Calibration data for toluene in ortho-dichlorobenzen with a 1 μ l injection volume	135

		data for limonene in acetonitrile	
	with a 1 μ l	injection volume	136
31.	Calibration	data for methyl ethyl ketone in xylenes	
	with a 1 μ l	injection volume	137
32.	Calibration	data for α -pinene in acetonitrile	
	with a 1 μ l	injection volume	138

LIST OF FIGURES

Figures		
1.	The effect of ethyl acetate vapor activity on permeance for high density polyethylene	65
2.	The effect of ethyl acetate vapor activity on permeance for oriented polypropylene	65
3.	The effect of ethyl acetate vapor activity on permeance for Saran coated OPP	66
4.	The effect of ethyl acetate vapor activity on permeance for Acrylic coated OPP	66
5.	The effect of toluene vapor activity on permeance for high density polyethylene	67
6.	The effect of toluene vapor activity on permeance for oriented polypropylene	67
7.	The effect of toluene vapor activity on permeance for Saran coated OPP	68
8.	The effect of toluene vapor activity on permeance for glassine	68
9.	The effect of limonene vapor activity on permeance for high density polyethylene	69
10.	The effect of limonene vapor activity on permeance for oriented polypropylene	69
11.	The effect of limonene vapor activity on permeance for Saran coated OPP	70
12.	The effect of limonene vapor activity on permeance for glassine	70
13.	The effect of methyl ethyl ketone vapor activity on permeance for high density polyethylene	71
14.	The effect of methyl ethyl ketone vapor activity on permeance for oriented polypropylene	71
15.	The effect of methyl ethyl ketone vapor activity on permeance for Saran coated OPP	72

16.	The effect of methyl ethyl ketone vapor activity on permeance for Acrylic coated OPP	72
17.	The effect of methyl ethyl ketone vapor activity on permeance for glassine	73
18.	The effect of α -pinene vapor activity on permeance for high density polypropylene	73
19.	The effect of $\alpha\text{-pinene}$ vapor activity on permeance for oriented polypropylene	74
20.	The effect of $\alpha\text{-pinene}$ vapor activity on permeance for glassine	74
21.	Temperature dependence of permeance for ethyl acetate in high density polyethylene	80
22.	Temperature dependence of permeance for ethyl acetate in oriented polypropylene	80
23.	Temperature dependence of permeance for ethyl acetate in Saran coated OPP	81
24.	Temperature dependence of permeance for ethyl acetate in Acrylic coated OPP	81
25.	Temperature dependence of permeance for ethyl acetate in glassine	82
26.	Temperature dependence of permeance for toluene in high density polyethylene	82
27.	Temperature dependence of permeance for toluene in oriented polypropylene	83
28.	Temperature dependence of permeance for toluene in Saran coated OPP	83
29.	Temperature dependence of permeance for toluene in Acrylic coated OPP	84
30.	Temperature dependence of permeance for toluene in glassine	84
31.	Temperature dependence of permeance for limonene in high density polyethylene	85
32.	Temperature dependence of permeance for limonene in oriented polypropylene	85

33.	Temperature dependence of permeance for limonene in glassine
34.	Temperature dependence of permeance for methyl ethyl ketone in high density polyethylene
35.	Temperature dependence of permeance for methyl ethyl ketone in oriented polypropylene
36.	Temperature dependence of permeance for methyl ethyl ketone in Saran coated OPP
37.	Temperature dependence of permeance for methyl ethyl ketone in Acrylic coated OPP
38.	Temperature dependence of permeance for methyl ethyl ketone in glassine
39.	Temperature dependence of permeance for α -pinene in high density polyethylene
40.	Temperature dependence of permeance for α -pinene in oriented polypropylene
41.	Temperature dependence of permeance for α -pinene in glassine
42.	The effect of limonene vapor activity on permeance for different polymer structures at 24°C
43.	Permeation rate curve of limonene through Saran coated OPP at a=0.4
44.	Permeation rate curve of α -pinene through Acrylic coated OPP at a=0.4
45.	Permeation rate curve of ethyl acetate through glassine at a=0.05
46.	Permeation rate curve of toluene through high density polyethylene a=0.05
47.	Permeation rate curve of methyl ethyl ketone through oriented polypropylene at a=0.05
48.	1/X as a function of time for system HDPE/limonene at a=0.4, T=50°C

49.	Best estimation for diffusion coefficient as a function of sum of squared estimated D for HDPE/limonene system at a=0.4, T=50°C	120
50.	1/X as a function of time for system OPP/limonene at a=0.4, T=50°C	
51.	Best estimation for diffusion coefficient as a function of sum of squared estimated D for OPP/limonene system at a=0.4, T=50°C	122
52.	1/X as a function of time for system HDPE/ α -pinene at a=0.4, T=50°C	123
53.	Best estimation for diffusion coefficient as a function of sum of squared estimated D for HDPE/ α -pinene system at a=0.4, T=50°C	124
54.	$1/X$ as a function of time for system OPP/ $\alpha\text{-pinene}$ at a=0.4, T=60°C	125
55.	Best estimation for diffusion coefficient as a function of sum of squared estimated D for OPP/α -pinene system at a=0.4, T=60°C	126
56.	Calibration curve for ethyl acetate by GC-FID	134
57.	Calibration curve for toluene by GC-FID	135
58.	Calibration curve for limonene by GC-FID	136
59.	Calibration curve for methyl ethyl ketone by GC-FID	137
60.	Calibration curve for α -pinene by GC-FID	138

INTRODUCTION

A large number of polymeric materials are employed in food packaging today. In most of these applications, the permeability of flexible packaging films to organic vapors, water vapor, and gases such as oxygen, and carbon dioxide is of great importance. In order to avoid the acquisition of undesirable odors from the external environment or from the package itself, or the loss of favorable flavor compounds to the atmosphere (Kontominas, 1985), knowledge of the barrier characteristics of the package structure is critical. Understanding the barrier properties of polymeric materials and their proper selection is important in preventing off-flavor, as well as prolonging the shelf life of packaged food products.

A number of experimental methods and test systems for determination of the solubility, diffusion and permeability coefficients of organic vapors through polymeric materials have been described in the literature (Murrat, 1985; Baner, 1986; Hernandez et al., 1986; DeLassus, 1985). Until recently, there was a lack of instrumentation available commercially for performing organic vapor permeability measurements and since organic vapor and aroma permeability measurements are very complicated procedures, there were no standard methods. Within the past three years; however, two commercially available systems have come on the market. One is the MAS 2000 Permeation Test System which is marketed by Testing Machines

Inc. (Amityville, NY) and the other unit, the Aromatran which is marketed by Modern controls Inc. (Minneapolis, MN).

In the present study, an isostatic procedure utilizing the MAS 2000 Organic Vapor Permeation Test System and a quasi-isostatic procedure, based on a permeability test system of our own design were employed. Permeation studies were carried out on a series of organic vapor/polymer membrane combinations. The permeants selected for study include the following: ethyl acetate; toluene; methyl ethyl ketone; α -pinene; and limonene. The first three permeants were selected based on their common use as solvents in the converting industry and their presence as residuals from laminating and printing processes. α -Pinene was selected to simulate supermarket storage conditions, where packaged foods might be affected by their proximity to non-food products (Kontominas, 1985). Limonene was selected as it represents a major flavor volatile for citrus oil and essence (Sadler, 1991). Parameters to be evaluated include vapor activity levels, the nature of the permeant molecule and temperature. For each temperature, three vapor activity levels were evaluated. The specific activity levels varied as a function of both the specific polymer and temperature of test. Permeation studies were carried out at three temperatures to allow evaluation of the Arrhenius relationship. Also, the effect of temperature were estimated at each permeant concentration level. Diffusion coefficients for the test materials will be determined using the MAS Technology Permeability System.

In addition to determining the permeability and diffusion coefficients, it is also important to evaluate the consistency of the experimental data obtained. The numerical consistency of the permeability data will be evaluated to determine the consistency of the system parameters, such as temperature, and vapor activity throughout the permeation experiment. In this study, the consistency analysis described by Gavara and Hernandez (1993) was applied to a set of experimental continuous-flow permeability data, to provide a better understanding of the mechanism of the diffusion and sorption processes associated with the permeation process.

The objectives of this study are, in terms of practical importance, to investigate the general utility and applicability of the MASTM Technologies Inc. Model 2000 Organic Vapor Permeation Test System for evaluating the organic vapor barrier properties of polymer membranes, and in terms of theoretical importance, to provide a better understanding of the diffusion process and the effect of penetrant/polymer interaction on the transport properties of polymer membranes. The specific objectives of the study include:

- Determine the temperature and concentration dependence of a series
 of organic permeants of varying polarity and molecular structure
 through a series of commodity packaging structures utilizing the
 MASTM Technologies Inc. Model 2000 Organic Vapor Permeation Test
 System.
- 2. Compare the agreement of permeance values for a series of organic vapor/polymer membrane combinations by the MAS 2000 Permeation

Test System isostatic procedure and a quasi-isostatic procedure.

3. Evaluate the experimental permeability data to determine the consistency of the test parameters and diffusion processes, to establish whether it follows Fickian behavior.

LITERATURE REVIEW

Importance of the Permeation of Organic Vapor Through Polymer Film

The packaging industry in the United States (U.S.) is very large and very broad-based. The total U.S. packaging market is a \$78 billion industry (Fishman, 1995). Of this, food packaging is the largest and most important single segment of the worldwide packaging market, and one increasingly moving to plastics. However, the absence or presence of organic volatiles in the product or package may create a major or minor problem with the food product properties. Eighty percent of food products demand a barrier to gases, flavors and odors (Shalaby, 1978). In biological type products, such as food and pharmaceuticals, packaging requirements are more complex and stricter than for other products. Flavor and aroma give foods and beverages their individual distinction and affects the decision of consumers as to what products they will buy, repeatedly. It is therefore important to minimize the gain or loss of flavor or aroma compounds by the product, before it reaches the consumer.

The use of polymeric packaging materials for food packaging requires a knowledge of their transport properties. Whereas, while extensive studies have been conducted on the permeability of non-interactive gases (e.g. O₂ and CO₂) and water vapor through plastic films, permeability data on organic compounds are limited (Liu, 1988). When considering interactions involving a foodstuff/organic volatile/polymeric package system, product-package interaction and

compatibility is typically associated with one of two mechanisms: (i) The mass transfer or permeability of the vapor into or out of the package; and (ii) sorption or migration of organic volatiles. The loss of product volatiles can thus occur as a result of sorption by the polymeric packaging material or permeation to the environment. However, when dealing with possible exposure of the packaged food system to foreign odors, the mechanism of interest is permeability. Here, concern deals with the levels of penetrant that diffuse through the polymer into the food system. Sorption of volatile product flavor and aroma compounds by polymeric packaging materials can also cause the loss of perceived product quality. The loss of aroma volatiles from the food product may reduce the flavor or sensory response below a threshold concentration of the aroma, which is one of the important characteristics of food products. The phenomena of permeation and sorption are especially applicable to the semi-permeable package systems constructed from polymeric materials (Baner, 1987).

Permeation Process of Organic Vapors Through Polymer Membranes

Permeation denotes the transfer of gases or vapors through a membrane in response to a gradient (i.e. pressure or concentration gradient). For a polymeric material free of microvoids, mass transfer occurs primarily when there exists a partial pressure differential across the polymeric matrix. The transport of permeant gases and vapors can be described by Fick's first and second laws of diffusion (Crank, 1975). Mass transport through polymeric materials, typically

occurs by a diffusion process rather than by a Knudsen flow, which describes the process whereby the pore diameter of a porous material is smaller than the mean of the gas molecule (Vieth, 1991).

Meares (1965a) described the diffusion process as one which occurs randomly throughout the polymer and is dependent on the gradient or the chemical potential of the diffusate. Because of the unequal partial pressures on each side of the polymer sheet, more diffusing substances dissolve in the polymer at the high pressure side than the low pressure side. This generates a concentration gradient across the polymer film and diffusion takes place down the gradient. After a steady state rate of transfer is attained with a constant transmission rate, a constant pressure difference is maintained across the film. Further, some flow may also take place through any interconnecting capillaries or pinholes in the macrostructure, as a result of the pressure gradient, or the nature of the polymer structure.

In general, for the permeation of a gas or vapor through a polymer membrane to occur, several processes are involved:

- (1) Adsorption a gas or vapor is sorbed at the high concentration surface, dissolving there, with equilibrium rapidly being established between the two phases.
- (2) Diffusion the dissolved penetrant molecules then diffuse through the membrane by a random walk or a hopping mechanism, creating a concentration gradient across the polymer bulk base.
- (3) Desorption the penetrant molecules evaporate from the low

concentration surface of the polymer membrane.

The mechanism of permeation, then, involves both dissolution and diffusion procedures.

The permeation of a substance through a polymeric material is usually described by the permeability coefficient (P), which is a measure of the permeation rate of a gas or vapor through a polymer membrane at steady state. It is relative to the speed of the molecule advancing through the polymer matrix and the number of molecules absorbed in the polymer being tested. The former is the so-called diffusion coefficient (D) and the latter is the solubility coefficient (S). The permeability constant is therefore a function of the diffusion coefficient (D) and solubility coefficient (S). Functionally, the diffusion coefficient is a kinetic term and describes how rapidly the permeant molecules are advancing and the time required to reach steady state, and the solubility coefficient is a thermodynamic term, describing how many permeant molecules are sorbed by the polymeric structure (Vieth, 1991).

It has also been found that the permeability varies with temperature according to an Arrhenius relationship. The apparent activation energy for permeation is the sum of diffusion activation energy and enthalpy of solution, each in turn is related to the temperature dependence of the diffusivity and solubility coefficients. These mechanisms will be reviewed in the following section.

Permeation Mechanism for Organic Vapors Through Polymer Membranes

There is now quite an extensive number of studies dealing with the development of permeability theory, especially for the permeability of gases and vapors through solids, such as polymeric films and sheets (Demorest, 1992; Franz, 1993; Mason, 1991; Nielsent et al., 1994; Theodorou, 1991). The relationships described are related back to the fundamental equations of diffusion derived by Fick (1855), who perceived the analogy between mass transfer and heat transfer processes. Eyring (1936), proposed a theory of diffusion in solids involving an activated transition state. Barrer (1937), later, developed an activated zone theory to apply to the diffusion of gases and vapors through polymeric microstructures. Several recent reviews firmly substantiate that the permeation process consists of both sorption and a diffusion procedure (Apostolopoulos, 1990; DeLassus, 1993; Nielsent et al., 1994).

The general theory of permeation can be described by a series of mathematical expressions, which are summarized from Rogers (1964). The transmission rate or flux, F, is defined as the amount of penetrant passing during unit time, through a surface of unit area normal to the direction of flow:

$$F = \frac{Q}{At} \tag{1}$$

.

Where Q is the total amount of permeant which has passed through area (A) during time (t). Given a unit area of film with thickness I, exposed to a penetrant at pressure p_1 on one side and a lower pressure p_2 on the other side, the penetrant concentration in the first layer of film (x=0) is c_1 and in the last layer (x=I) is c_2 . The rate of transmission through a slab, at a distance x+dx, will be $F+(\partial F/\partial x)\,dx$. Therefore, the amount retained per unit distance of polymer is equal to the rate of change of concentration with time:

$$-\frac{\partial F}{\partial x} = \frac{\partial c}{\partial t} \tag{2}$$

In the steady state of flow, $\partial c/\partial t$ is equal to zero, F is constant, and the rate of permeation is directly proportional to the concentration gradient, as expressed by Fick's first law of diffusion:

$$F = -D \left[\frac{\partial c}{\partial x} \right]$$
 (3)

Where D is the diffusion coefficient and the negative sign in Eqn. 3 indicates that the diffusion occurs spontaneously in the direction of concentration decrease. Assuming D to be constant, this can be integrated between the concentrations c_1 and c_2 to give:

$$F = \frac{D(C_1 - C_2)}{I} \tag{4}$$

The equilibrium concentrations c_1 and c_2 of penetrant in the surface layers of the polymer can be related to the partial pressures p_1 and p_2 in the gaseous phase by Henry's law:

$$c = S \times p \tag{5}$$

where c is the concentration of gas in the polymer, p is the partial pressure of penetrant at the interface, and S is the solubility coefficient of the penetrant in the polymer. When Henry's law is obeyed, a linear relationship is found between concentration and pressure, and S is constant, so that:

$$F = \frac{DS(p_1 - p_2)}{l} = \frac{DS \Delta p}{l}$$
 (6)

therefore:

$$P = \frac{F l}{\Delta p} = \frac{Q}{t} \frac{l}{A \Delta p}$$
 (7)

or

$$P = D \times S \tag{8}$$

Where P is the permeability coefficient, which is defined as the quantity of penetrant permeated through a film of thickness l, per unit membrane area, per unit permeant driving force, per unit time.

The above derivation only considers the case where D and P are functions of concentration and S is constant, as well as the following assumptions (Vieth, 1991):

- Diffusion must be really unidirectional, i.e., there exists a concentration gradient only along the x-axis. Compared to film surface area, the thickness is usually very small.
- Polymeric film microstructure is homogeneous and isotropic.
- Equilibrium is found between the gas phase and the polymer surface.
- Diffusing gases or vapors reach a steady state of transfer.
- Henry's law is applicable, i.e., the solubility coefficient is not a function of concentration.

However, in many organic permeant-polymer systems, S is a function of the concentration of permeant in the polymer and does not always follow Henry's law, particularly at high permeant concentration levels (Baner, 1987).

Diffusion of Organic Vapor Through Polymer

The diffusion process is the result of polymer molecules having a random kinetic agitation or heat motion. Above the glass transition temperature (T_g) , polymer chain segments have vibration, rotation and translation properties which continually create temporary "holes" or voids within the polymer matrix. The "holes" allow penetrant molecules to pass through the matrix under a concentration gradient. For polymer membranes below T_g , the rate of diffusion will be a

function of the size and frequency of preexisting "holes" or the void volume between the respective polymer chains. Whereas, the solubility involves the affinity of the permeant for the polymer (Baner, 1986; Imalzane et al., 1991)

Theory of diffusion

Fick's first law is the fundamental law of diffusion. It states that the flux (F) in the x-direction is proportional to the concentration gradient $(\partial c/\partial x)$.

$$F = -D \left[\frac{\partial c}{\partial x} \right]$$
 (3)

Flux is defined as the amount of substance diffusing across a unit area, in unit time and D is the diffusion coefficient. Fick's first law can only be directly applied to diffusion in the steady state, in other words, where concentration is not varying with time (Crank, 1975).

Fick's second law of diffusion describes the non-steady state and it has several forms. The flux gradients are obtained from the first law equation. For example, $\partial F_x/\partial x=-D\partial^2 c/\partial x^2$, so that

$$\frac{\partial c}{\partial t} = D \left[\frac{\partial^2 c}{\partial x^2} + \frac{\partial^2 c}{\partial y^2} + \frac{\partial^2 c}{\partial z^2} \right]$$
 (9)

Eqn. 9 is known as Fick's second law of diffusion. Under circumstances where diffusion is limited to the x-direction it simplifies to:

$$\frac{\partial c}{\partial t} = D \left[\frac{\partial^2 c}{\partial x^2} \right]$$
 (10)

In any case involving mass transfer, the problem is to find a solution to the appropriate form of the second law equation. Various solutions have been described by Crank (1975).

Two methods commonly used to evaluate molecular diffusion in polymers are: (1) transmission through a thin membrane, and (2) sorption of gases or vapors by a film or thick slab (Crank and Park, 1968).

Equilibrium sorption

In sorption kinetics, the results can be presented graphically with $t_{1/2}$ as the independent variable and M_t/M_{∞} as the dependent variable, where M_t/M_{∞} represents the fraction of material sorbed at time t, relative to the amount sorbed at infinite time (equilibrium). Crank and Park (1968) and a number of other investigators have used the kinetic study of the sorption and desorption of gases and vapors in polymers as a means for determining the diffusion coefficient. In the McBain procedure (Crank and Park, 1968), a sample of polymer film is suspended from a quartz spring in the penetrant atmosphere and the change in length of the spring is followed with a cathetometer, as

the polymer sample takes up the vapor. The well known Cahn electrobalance obviates the latter and automates the procedure. The diffusion approximation expression for short times is:

$$\frac{M_t}{M_m} = \frac{4}{l} \left[\frac{Dt}{\pi} \right]^{1/2} \tag{11}$$

A plot of M_t/M_∞ verses $(t/\emph{l}^2)^{1/2}$ is initially linear and from the slope, D can be determined.

Steady state solution

The simplest solution to the diffusion equation occurs at steady state, when

$$\frac{\partial}{\partial x} \left[D \frac{\partial C}{\partial x} \right] = 0 \tag{12}$$

or:

$$F = -D \frac{\partial c}{\partial t} = a \text{ constant}$$
 (13)

If the flux and concentration gradient can be accurately determined, then the diffusion coefficient can be evaluated directly. The concentration of penetrant just within the gas/membrane interface is not known unless the solubility of the gas in the polymer has been determined. In many simple cases, it is customary to assume that the gas/polymer system follows the quation of $c = S \times p$ (Eqn. 5). This

assumption is valid only if an equilibrium is established, since S is essentially an equilibrium partition coefficient of gas between the gaseous and polymer phases. Fick's law at the steady state is written as:

$$F = D \cdot S \cdot \frac{\Delta p}{I}$$
 (14)

Since diffusion coefficients may not be independent of concentration, and Henry's law may not apply, the permeability of a polymer is, in general, not a fundamental property, being dependent on the permeability coefficient, which must be known in practice, for it is a measure of the barrier protection or separation potential offered by the polymer.

Time lag technique

This method combines evaluation of the steady transport rate with analysis of the earlier transient state region. Its importance lies in the fact that the two values P and D can be determined be one single experiment. S can then be deduced from the two known constants by substitution in Eqn. 8. Barrer (1939), assuming a constant value for D, was able to solve Fick's second law by deriving the following relationship.

$$Q_{t} = \frac{DC_{1}}{l} \left[t - \frac{l^{2}}{6D} \right] - \frac{2lC_{1}}{\pi^{2}} \sum_{n=1}^{n=\infty} \frac{(-1)^{n}}{n^{2}} \exp \frac{-Dn^{2}\pi^{2}t}{l^{2}}$$
 (15)

where Q_{t} is the amount of permeant passing through a film in time t, \emph{I} is the film thickness, and \emph{c}_{1} is the penetrant concentration at the upstream face.

When the steady state is achieved, t becomes large enough to make the exponential term negligibly small. Eqn. 15 can thus be simplified to:

$$Q_{t} = \frac{DC_{1}}{l} \left[t - \frac{l^{2}}{6D} \right]$$
 (16)

The necessary conditions are: (i) an initially permeant-free film; (ii) attainment of equilibrium at the permeant/polymer interface; and (iii) zero concentration of permeant gas or vapor at the outflow face. Under these conditions, a plot of Q_t vs. t yields a straight line where the intercept (θ) on the t axis is represented by following equation:

$$\theta = \frac{l^2}{6 \, \mathrm{D}} \tag{17}$$

where θ = time lag.

l =thickness of membrane.

D = diffusion coefficient.

The diffusion coefficient thus can be determined by solution of Eqn. 17. The slope of the steady state portion of the plot, which is linear, can be directly related to the permeability constant, P. And

since the values for P and D can be calculated, the solubility coefficient, S, can be determined directly from Eqn. 8.

Characteristics of diffusion coefficient:

The diffusion process is influenced by the characteristics of the polymer and diffusant molecule, temperature and the concentration of diffusant in the polymer.

The temperature dependence of the diffusion coefficient, at a constant vapor concentration, can be represented by an Arrhenius relationship:

$$D = D_0 \exp\left[-\frac{E_d}{RT}\right]$$
 (18)

Where E_d is the activation energy of the diffusion process, D_0 is the pre-exponential factor, R is gas constant, and T is Kelvin temperature. The activation energy of D is a measure of the energy required to act against the cohesive forces of the polymer in forming the "holes" through which diffusion will occur. The pre-exponential factor is associated with the frequency and magnitude of the holes in the polymer matrix in the absence of penetrant.

The concentration dependence of the diffusion coefficient at a given temperature can be represented by the equation:

$$D = D_0 \exp(\gamma c) \tag{19}$$

Where γ is a characteristic constant, D_0 is the pre-exponential factor at zero concentration, and c is the concentration of permeant in the polymer. The diffusion coefficient may deviate significantly from a linear or exponential dependence over a wide range of temperature and vapor activity levels. The concentration dependence in these systems can be represented as a function of vapor activity:

$$D = D_0 \exp(\alpha a_h) \tag{20}$$

Where α is a constant and a_h is the vapor activity on high concentration side or up stream surface of the film (Roger, 1960).

For the diffusion of a series of homologous hydrocarbon vapors in various elastomers at a given temperature, γ and α increase as the size and shape of the diffusing molecules decrease, and as the chemical similarity of the penetrant polymer structure increases. A penetrant molecule with a branched structure decreases the diffusion coefficient more than the effect on D caused by an increase in its carbon chain length. This indicates that diffusion occurs preferentially along the direction of greatest length of the permeant molecule (Roger, 1964). The molecular weight of a polymer has little effect on the diffusion rate, whereas chemical modification and morphology of the polymer gave a much greater effect. The diffusion coefficient also decreases with an increased degree of crosslinking and crystallization (Roger, 1964).

Free volume theory:

The effect of the polymer structure on diffusion can usually be described in term of the free volume theory. Fujita et al., (1968) applied the free volume theory to provide an explanation for the concentration and temperature dependence of the diffusion of organic vapors in amorphous polymers above their glass transition temperature T_{σ} . The theory states that "the mobility of both the polymer chain segment and the diffusant molecule in a polymer/penetrant system is primarily determined by a discrete free volume or hole, which may be either mobile or fixed within and throughout a polymer matrix. These voids or holes are created by the Brownian movement of the molecular segments of the polymer chains. A molecule of penetrant can move only when there is a space available to allow it to pass through. Because the mobility of diffusant molecules and polymer chain segments are exceedingly sensitive to changes in the average free volume of the polymer/penetrant system, the diffusion coefficients of polymer/organic penetrant system are quite concentration-dependent" (Fujita et al., 1968).

Meares (1958) and Fujita (1961) have shown that the free volume approach provides an additional understanding of the segmental motion of polymers and diffusion in polymeric materials. Meares assumed a direct proportionality between D and the dependence of the latter quantity on the polymer free volume. Fujita et al. (1961) defined a mobility term, m_d, which was dependent upon the free volume of the system, through an expression of the Doolittle type:

$$m_{d} = A_{d} \exp\left[-\frac{B_{d}}{f}\right]$$
 (21)

where m_d = the mobility of diffusant component(relative to the polymer component) = D/RT.

f = average fractional free volume of the system.

 \mathbf{A}_{d} , \mathbf{B}_{d} = parameters independent of diffusant concentration and temperature.

The two principal assumptions made were that a penetrant molecule requires some constant critical value, $B_{\rm d}$, of free volume to promote diffusion and that the fractional free volume, f, in the system increases linearly with penetrant volume fraction, ϕ_1 :

$$f = f_0 + \beta \phi_1 \tag{22}$$

where f_0 is the mean fractional free volume of pure polymer at a given temperature, and $\beta = \lambda - f_0$, λ being the corresponding fractional free volume of pure solvent. In general, as $\lambda >> f_0$, the diffusion coefficient D will increase with ϕ_1 .

Based on energy consideration, Meares (1986) observed that, "The jumping frequency of the gas molecules is far higher than that of the polymer segments, which are consequently rate controlling. These jumping frequencies are strongly temperature dependent and they involve, like viscous flow, a free volume of activation." Stuk

(1990), also proposed that the diffusion coefficient is related to a diffusive jump length, which is characteristic of the polymer, and a jump frequency, which is related to segmental mobility of polymer chain. The theory was fit to experimental diffusion data for a number of gases in natural and butyl rubbers and partial molar volumes were calculated from the fitting parameters. Good agreement with experimental partial molar volumes was obtained.

Factors Affecting Permeation of Organics Through Polymer Films

The rate of permeation of organic vapor through a polymeric film is affected by the type of permeant, the structure of the polymeric film, as well as environmental conditions. These include the nature of the permeating molecule, its size and shape; the nature of the barrier material and its physical properties, such as degree of crosslinking, percent crystallinity and molecular orientation. Other parameters are the permeant concentration, thickness of the membranes or laminations and its surface area, temperature, and relative humidity (Lee, 1988).

Natural of polymer

Various properties of the polymer itself play a major role in the process of vapor transport. The chemical composition and molecular structure greatly influences the permeability of a polymeric material to organic vapors or gases. The relationship between penetrant transfer characteristics and the basic molecular structure and

chemical composition of a polymer is rather complex, and a number of factors contribute to the permeability and diffusion processes, among the most important being;

- cohesive energy density, which creates strong intermolecular bonds, Van der Waals or hydrogen bonds.
- the glass transition temperature (Tg) of the polymer, associated with vibration and rotational motion of polymer chains.

With respect of the Tg of barrier polymer structures, DeLassus (1993) proposed that glassy polymers have very low diffusion coefficients for flavor, aroma and solvent molecules at low concentrations.

Typically, these values are too low to measure by standard analytical procedures. The diffusion coefficient determines the dynamics of the permeation process and thus the time to reach steady state, which accounts for glassy polymers exhibiting high barrier characteristics to organic permeants. Polyolefins, being well above their glass transition temperature, are non-glassy polymers and have high diffusion coefficients for organic permeants, and steady state permeation is established quickly in such structures.

Solid state polymer chains can by found in a random arrangement to yield an amorphous structure or a highly ordered crystalline phase. Most polymers used in packaging are semicrystalline or amorphous materials. Morphology refers to the physical state by which amorphous and semicrystalline regions coexist and relate to each other in a polymer, and depends not only on its stereochemistry, but also on whether the polymer has been oriented, and at which

conditions of temperature, strain rate and cooling, as well as the melt cooling rate. Fundamental properties which are associated with polymer morphology and will therefore influence the permeability and diffusivity characteristics of the polymer include:

- structural regularity or chain symmetry, which can readily lead to a three dimensional order of crystallinity. This is determined by the type of monomer and the conditions of the polymerization reaction.
- chain alignment or orientation which allows laterally bonding groups to approach each other to the distance of the best interaction, enhancing the tendency to form crystalline materials.

Morphology is thus important in determining the barrier properties of semicrystalline polymerd. The degree or percent crystallinity of a polymer plays an important part in both its barrier and physical properties. With respect to its barrier properties, since a gas or vapor is soluble only in the amorphous phase and the diffusion coefficient for an unannealed film decreases as the amorphous volume decreases, an increase in percent crystallinity yields a decrease in diffusivity and solubility through a polymer. Crystallinity decreases permeability, not only by reducing the volume of amorphous region available for flow, but also by restricting pathways for a diffusing molecule.

Molecular orientation also has a profound effect on polymer morphology, especially for semi-crystalline polymers. Polymeric materials that are highly ordered pack more tightly and generally have lower permeability. Pascat (1985) investigated the influence of orientation on oxygen permeability and found reduction of the permeability value reached 50% for oriented semi-crystalline polymers, while only a decrease of 10 to 15% was obtained for amorphous polymers. The orientation level will depend on the extent of elongation, the temperature, the strain rate etc., Deformation of polymeric structure does not appreciably affect S or D, until elongation results in crystallization. At higher elongation, the sorption and transport processes can be significantly affected by deformation of the crystalline domain structure (Vieth, 1991).

Nature of penetrant

The rate of passage of a permeating species through a polymer matrix depends on the size, shape and polarity of the permeant molecule, together with its facility of condensation. Size and shape particularly affect diffusivity, while solubility is typically influenced by polarity and ease of condensation of the permeating molecule.

An increase in size (e.g., average diameter, molar volume) of the penetrant molecule for a homologous series generally leads to an increase in solubility and a decrease in diffusion coefficients.

Since the permeability coefficient is the product of these two

factors, its variation with penetrant size is often much less (Rogers, 1985). The decrease in D is a reflection in the need to create a critical activation volume in the polymer. Additionally, the activation energy for diffusion is also found to be proportional to the molecular dimensions of the penetrant. Berens and Hopfenberg (1982), found that the diffusivities of elongated or flattened molecules are higher than the diffusivities of spherical molecules of similar volume or molecular weight.

A comparable dependence on penetrant shape (linear, branched or cyclic) has also been found for solubility by Rogers (1959), with the result that very small differences in shape may cause important differences in permeability. This is the case for the permeability of polyethylene to o-xylene, which is considerably lower than to p-xylene (Pascat, 1985).

Concentration

For gases and some vapors of very limited solubility, the diffusion coefficient can be thought as a constant, independent of the permeant concentration, e.g. Fickian in nature. For organic permeants with relatively high solubility in polymers; however, the concentration dependence of D becomes important, since the organic penetrants are capable of plasticizing the polymer chain segments, resulting in a rapid increase of D with increasing permeant concentration.

Studies by Huang and Lin (1968) on the permeation characteristics of binary mixtures of hydrocarbons through low density polyethylene showed that for a mixture of benzene and n-hexane, the membrane selectivity decreased with increasing concentration of benzene. This is explained on the basis that benzene has a higher solubility and consequently more plasticizing effect on polyethylene than n-hexane.

Temperature

Permeability, diffusion and solubility coefficients vary with temperature according to the Arrhenius relationships, as given in the following equations:

$$P = P_0 \exp(-E_p/RT) \tag{23}$$

$$D = D_0 \exp(-E_D/RT)$$
 (19)

$$S = S_0 \exp(-H_S/RT) \tag{24}$$

An increase in temperature provides energy for a general increase in segmental motion. If the energy density is sufficient, the polymer may pass through structural transition, (i.e. glass and melting transition), which affect solution and diffusion processes. The effects of an increase in temperature, may be equal to the term describing the increase in free volume, which is directly related to the increased segmental mobility in the polymer (Rogers, 1985).

According to Eyring's hole theory of diffusion (1936), the thermal motion of polymer chains randomly produces "holes" through

which the permeating molecules can diffuse. The formation of "holes" requires enough energy to break a number of secondary valence or non-covalent bonds. At low temperature, there is higher frequency of smaller holes than larger holes in the amorphous regions. With a temperature increase, thermal agitation of polymer chain segments increases and the diffusive "holes" become larger, which causes more molecules to diffuse through the membrane. Rogers (1985) also proposed that temperature is one of the major factors which affects polymer chain segmental motion by its temporal distribution of sorbed penetrant in the polymer. An increase in temperature provides energy for an increase in segmental motion or in free volume. When above the glass transition temperature (T_g), vibration and rotational motions of the polymer chain segments, continually create temporary "holes" or voids in the polymer matrix.

Organic Vapor Permeation Measurement and Technology

Experimental methods and test apparatus for measuring permeability of organic vapor through polymers have been described by a number of investigators. These methods are (i) a gravimetric technique; (ii) the absolute pressure method; (iii) the quasi-isostatic procedure; and (iv) the isostatic procedure. Generally, the latter three methods can be described as partition cell methods, where the permeant being tested is isolated on one side of the film and then detected on the other side.

Gravimetric technique

In the gravimetric procedure, the weight gain or loss of the penetrant permeating through a known area of polymer film is measured. Lebovits (1966) described a gravimetric procedure, where by the polymer membrane is sealed to the lip of the test cup to which the liquid permeant had been added. The cup is placed in a constant temperature and atmosphere environment, and the loss of permeant through the membrane is measured by weight loss. A variation of this method involves filling a polymer pouch with absorbent, exposing the package to an organic vapor atmosphere and measuring the vapor transmission rate by the gain in weight over time (Laine and Osburn, 1977). When the permeation rate reaches steady state in these methods, the pouch or the dish maintains a constant weight gain or loss. However, these gravimetric methods have low sensitivity, especially for high barrier polymers which exhibit low permeation rates, and are applicable over a limited vapor pressure range. Gravimetric methods, therefore, lack the ability to evaluate concentration dependent permeability and diffusion processes (Baner, 1987).

Absolute pressure method

The absolute pressure method is designed to measure permeability by mounting the sample film between two hermetic test cell chambers. A fixed and constant organic permeant is introduced into one cell

chamber and the mass penetrating through the polymer film will be detected on the other side as a function of time.

The absolute pressure method directly measures the pressure of the permeating gas or vapor by utilizing volumetric or manometric techniques. The sample film is mounted in a permeation cell and the organic vapor is introduced into another chamber of the permeation cell The steady state permeation rate is determined from the conditions when there is a constant increase in pressure over time in the low pressure side of the cell. Rogers et al. (1956), Meters et al. (1957), and Meanness (1958a) have made modifications and refined the technique for measuring the permeation and diffusion of organic vapors through polymer films by the absolute pressure method. A number of theoretical studies involving permeation and diffusion of specific organic vapor/polymer systems have used the manometric and volumetric methods (Stannett, 1972). These methods have been widely employed for measuring the permeability of gases and vapors through polymer membranes. There are, however, a number of problems associated with the absolute pressure method. Because the test system requires evacuating the low concentration chamber of the cell to low pressure, the system requires high seal integrity during the period of testing, particularly for high barrier polymers. Furthermore, since there is a total pressure differential between respective cell chambers, it restricts the usage of thin, easily distorted, or pressure sensitive films.

The American Society for Testing and Methods Standard, ASTM D3985-81 designated that for this method, a total pressure gradient between the two cell chambers is established which provides the driving force for the mass transfer process.

The majority of the problems associated with determining the permeability of organic vapor, either by gravimetric or absolute pressure method can be avoided by application of the quasi-isostatic or isostatic test procedures. Indeed, more recently, researchers have extensively employed both the quasi-isostatic and isostatic methods for studying the permeability of organic vapors through barrier membranes. Since the measurement of organic vapor permeability rates is quite complicated, and there are no standard procedures for performing such analyses, most research in this field has been conducted on permeation systems of the researcher's own design (Baner, 1986; Blakesley, 1974; DeLassus et al., 1979; Franz, 1993; Hatzidimitriu et al., 1987; Hernandez et al., 1986; Kontominas, 1985; Liu et al., 1991; Niebergall et al., 1979; and Stannett et al., 1972). Most of these test systems have been designed to measure the transmission rate of organic vapor through barrier film by creating a constant partial pressure differential across the test film. The partial pressure differential of the test vapor or gas provides the driving force, with the total pressure on both sides of the membrane being constant at one atmosphere.

Quasi-isostatic procedure

One common method for determining permeability is the quasiisostatic method (or accumulation method). In this method, the

permeated gas or vapor is accumulated and measured as a function of

time. A polymer film is mounted tightly between two cell chambers,

where a partial pressure differential is established. The gas or

vapor being tested is allowed to flow through the high concentration

cell chamber at atmospheric pressure. The partial pressure gradient,

provides a driving forces for vapor permeating into the low

concentration cell chamber, where gas samples in the static cell are

removed periodically and injected directly into a gas chromatograph

equipped with flame ionization detector for quantification (Baner et

al., 1986).

Using this procedure, the quantity of permeant accumulated in the static cell chamber increases over time. When the relationship between quantity accumulated per unit of time is constant, the steady-state rate of permeation has been reached. From the flux at steady state and test constants, to include film thickness, surface area and permeant partial pressure, the permeability constant for the permeation/polymer system is determined. The diffusion coefficient (D) can also be determined by the lag time method, by the expression, D = $I^2/6\theta$, where θ is the lag time and I is film thickness. The lag time (θ) is obtained from the intersection of the projection of the steady state portion of the transmission curve to the time axis (Hernandez, et al., 1986; Wangwiwatsilp, 1993).

The permeability coefficient, P is expressed as:

$$P = \frac{Q \times l}{t \times A \times \Delta p} \tag{7}$$

where Q is the total quantity of permeant that has penetrated during unit time (t). A is a unit film area with a thickness (I) exposed to the permeant and Δp is the driving force, given by the concentration or partial pressure gradient.

Isostatic procedure

In the isostatic method, a polymer membrane is mounted in a permeation cell system and the desired permeant concentration is flowed continually through the high concentration cell chamber. The total pressure in the permeation cell system is kept constant by maintaining the same pressure in both cell chambers. An inert carrier gas stream (the same as the permeant carrier gas) is flowed simultaneously through the low concentration cell chamber and the permeant vapor is conveyed to a detector for quantification. Steady state is reached when the transmission rate monitored continually under constant conditions of temperature and permeant vapor pressure remains constant.

The isostatic test system allows the continuous collection of permeation data of a vapor or gas through a polymer membrane from the initial time zero to steady state conditions over time, as a function of temperature and permeant concentration.

A number of studies have described isostatic permeation systems, with various detection devices. Thermal conductivity detectors to measure the increasing amount of permeant in the lower chamber sweep stream (Pasternak et al., 1970; Ziegel et al., 1969). Small thermistors were also used to detect the presence of permeant in the sweep stream (Giacin et al., 1981; Yasuda and Rosengren, 1970). Both thermal conductivity detectors and small thermistors worked well for single permeants. However, one major problem of both systems was their inability to quantify co-permeant concentrations in the sweep stream. Also, these detectors were associated with problems of calibration for the specific permeant vapor and concentrations, as well as the effect of the sweep gas on calibration. The use of a flame ionization detector (FID) has the advantage of not being affected by the presence of the carrier gas and water vapor (Zobel, 1982). A gas chromatography sampling system interfaced with FID was used to separate and detect a complex mixture of organic permeants (Caskey, 1967; DeLassus, 1985; Hernandez, 1984; Pye et al., 1976).

The permeability coefficient, P can be calculated from the transmission rate at steady state, by the expression:

$$P = \frac{[C]_{\infty} \times f \times l}{A \times \Delta p}$$
 (25)

where $[C]_{\infty}$ = steady-state concentration of permeant conveyed to the detector, in mass per unit of volume f = rate of carrier gas flow passing through the lower

concentration permeation cell, in volume per unit of time

l = thickness of the film, in length unit

A = film surface area, in area unit

The diffusion coefficient, D is expressed by Equation:

$$D = \frac{l^2}{7.199 \times t_{1/2}}$$
 (26)

where l = film thickness, in length unit

 $t_{1/2}$ = time required to reach a rate of transmission value equal to half the steady state, in time unit

MAS 2000 Organic Vapor Permeation Test System

Permeation theory incorporated by the MAS 2000 Organic Vapor Permeation Test System is based on Fick's law, as well as Henry's Law. The steady state permeability value, P, is also assumed to be directly proportional to a material's solubility coefficient, S, and it's diffusion coefficient, D ($P = D \times S$). The solution to the differential equations describing the mass transport rate through a planer surface is:

$$R_{t} = RC^{1/2} \sum_{k=1,3,5,...} exp(-k^{2} C)$$
 (27)

where R_t is the mass transport rate at time t, R is a constant associated with the permeation coefficient, and C is a constant associated with the diffusion coefficient.

In experiments associated with the solution to this equation, other parameters need to be considered:

- (i) B, the initial baseline value associated with organic trapped in the material and which are dissolving from the material at a steady state, when the test is initiated.
- (ii) t_0 , the time associated with the initiation of the test. This parameter is usually known only approximately due to instrumentation lag time. The equation to be solved is therefore:

$$R_t = B + RC^{1/2} \sum_{k=1,3,5...} exp(-k^2 C)$$
 (28)

where $C = 1/(4D(t-t_0))$ and $R = 4P/Pi^{1/2}$. Thus, the above equation involves 4 parameters: the baseline value (B), the permeation coefficient (P), the diffusion coefficient (D), and the test initiation time (t_0) . The temperature control function is incorporated in the following equation:

$$H = H_0 + C_1 + C_2 \tag{29}$$

H is the amount of time corresponding heater will be set to on, H_0 is the amount of time from the previous cycle, c_1 is a time correction factor related to the current temperature value, and c_2 is the time correction factor related to the current temperature slope vs. time.

$$c_1 = A * (freq/del)*[set-(T + del* D)]$$
 (30)

$$c_2 = B * (freq/del) * D$$
 (31)

The parameter definitions include:

- freq the set cycle rate. (5 sec)
- del the temperature time response of the unit to be controlled.

 this value is set under the system program.
- set the temperature set point value.
- T the current temperature of the unit to be controlled.
- D the current temperature slope vs. time.
- A a constant describing the relation of Heater setting (H) to temperature.
- B a constant describing the relation of Heater setting (H) to the temperature derivative with respect to time.

Evaluating The Consistency of The Permeability Experimental Data

Since the steady-state permeability experiment provides a method to determine the permeability and diffusion coefficients, it is important to evaluate the consistency of the experimental data obtained from the continuous flow permeability experiment. The numerical consistency of the permeability data will affect the values of both the diffusion and permeability coefficients and would indicate variations in the system parameters, such as temperature or permeant concentration, during the course of the experiment. Furthermore, the consistency test is a useful tool to establish if the penetrant/polymer system follows Fickian behavior, and its

application may assist in identifying the presence of complex diffusion mechanisms associated with the permeation process.

Gavara and Hernandez (1993) have described a simple procedure for performing a consistency analysis on a set of experimental permeability data from a continuous-flow study. This procedure can be applied to the continuous-flow permeation data obtained to provide a better understanding of the mechanism of the diffusion and sorption processes associated with the permeation process. The consistency test for continuous flow permeability data has been described in detail by Gavara and Hernandez (1993) and is summarized briefly below.

The value of the permeation rate (F_t) at any time (t), during the unsteady state portion of the permeability experiment varies from zero, at time equal to zero, up to the transmission rate value (F_{∞}) reached at the steady state. For non-interacting penetrant/polymer systems, permeability data and diffusion coefficients can be expressed by the following (Pasternak et al., 1970)

$$\frac{F_{t}}{F_{xx}} = \frac{4}{\sqrt{\pi}} \sqrt{\frac{l^{2}}{4 \text{ Dt}}} \sum_{n=1,3,5,...}^{\infty} \exp\left[-\frac{-n^{2} l^{2}}{4 \text{ Dt}}\right]$$
 (32)

and simplified to

$$\frac{F_t}{F_t} = \phi = \frac{4}{\sqrt{\pi}} \sqrt{X} \exp(-X) \tag{33}$$

where ϕ is the flux ratio, which is achieved from t=0, up to the time the permeability rate is at steady state, and X = F/4Dt, In Eqn. 33, the diffusion coefficients, D, is assumed to be concentration and time independent. For each value of F_t/F_{∞} , a value of X can be calculated, and from a plot of 1/X versus t, the diffusion coefficient, D, can be determined from the slope of the straight line. The authors further described two dimensionless constants, k_1 and k_2 ;

$$k_1 = \frac{t_{1/4}}{t_{3/4}} = \frac{X_{1/4}}{X_{3/4}} = 0.4405$$
 (34)

$$k_2 = \frac{t_{1/4}}{t_{1/2}} = \frac{X_{1/4}}{X_{1/2}} = 0.6681$$
 (35)

where $X_{1/4}$, $X_{1/2}$ and $X_{3/4}$ denote the numerical values of X when the permeability experiment has reached values of 0.25, 0.5 and 0.75 respectively for F_t/F_{∞} , the transmission rate ratio.

The numerical values of the constants, k_1 and k_2 , as given in Eqn. 34 and 35, together with linear relationship of 1/X versus time (t), will provide the criteria to evaluate the consistency of the experimental data.

MATERIALS AND METHODS

Packaging Materials

Six commercial barrier film structures were evaluated in the present study. All six packaging films were coated with a 1/2' wide pattern cold seal(PCS) on one side of the film. The six polymer structures evaluated included:

- 1.3 mil printed oriented polypropylene (OPP)
- 1.0 mil Saran coated oriented polypropylene (Saran coated OPP)
- 1.5 mil high density polyethylene (HDPE)
- 1.2 mil Acrylic coated oriented polypropylene
 (Acrylic coated OPP)
- 1.2 mil white opaque Glassine (Glassine)
- 1.1 mil metallized polyethylene terephthalate (PET)/oriented polypropylene (Met PET/OPP)

Ethyl acetate, toluene, limonene, methyl ethyl ketone, and α -pinene were used as the organic penetrants. Acetonitrile, xylenes and dichrorobenzene were used as solvents to prepare standard solutions for developing the respective calibration curves for quantification.

Ethyl acetate (CH₃COOC₂H₅)

J. T. Baker Chemical Co. (Phillipsburg, NJ)

Analytical Reagent grade

88.11 Molecular weight

0.894 g/ml Density at 25°C 77.2 ± 0.5°C Boiling range

Purity 99.9%

Toluene (C₆H₅CH₃)

J. T. Baker Chemical Co. (Phillipsburg, NJ)

Analytical Reagent grade

92.14 Molecular weight

Density at 25°C 0.893 g/ml 110.4 ± 0.2 °C Boiling range 99.9ક

Purity

Methyl ethyl ketone (C.H.COCH.)

Sigma Chemical Co. (St. Louis, MO)

ASC Reagent

Molecular weight 72.11 Density at 25°C 0.81 g/mlBoiling range $80 \pm 0.1^{\circ}C$

99⁺ક Purity

α -pinene ($C_{10}H_{16}$)

Sigma Chemical Co. (St. Louis, MO)

GLC grade

136.24 Molecular weight 0.857 g/ml Density at 25°C

 $155.5 \pm 0.5^{\circ}C$ Boiling range

99⁺% Purity

Limonene $(C_{10}H_{16})$

Aldrich Chemical Co. (Milwaukee, WI)

Analytical Reagent grade

Molecular weight 136.24 Density at 25°C 0.84 g/ml 175.5 ± 0.25 °C Boiling range

978 Purity

Acetonitrile (CH₃CN)

EM Industries, Inc. (Gibbstown, NJ) HPLC grade Molecular weight 41.05 Density at 25°C 0.78 g/ml Boiling range 82.0 \pm 0.1°C Purity 99.8%

Xylenes ($C_6H_4(CH_3)_2$)

J. T. Baker Chemical Co. (Phillipsburg, NJ) Analytical Reagent grade Molecular weight 106.17 Density at 25°C 0.87 g/ml Boiling range 139 \pm 0.5°C Purity 99'%

O-Dichlorobenzene (C₆H₄Cl₂)

Aldrich Chemical Co. (Milwaukee, WI)

Analytical Reagent grade
Molecular weight 147
Density at 25°C 1.306 g/ml
Boiling range 179.5 \pm 0.5°C
Purity 99 $^{+}$ %

Permeability Test Methods

Quasi-isostatic procedure

The quasi-isostatic was carried out in a permeability cell according to Baner et al., 1986 and Hernandez et al., 1986. The cell was comprised of two cell chambers of 50 cm³ each and a hollow center chamber ring which allowed two film samples to be run simultaneously. Vapor of known penetrant

concentration was flowed continuously through the center chamber during permeability measurements. Prior to operation, two samples of test film were mounted in the permeation cell and bolted together tightly. The permeation cells were equipped with Viton O-rings to assure good seal integrity between the films and the surroundings. Permeation cell chambers on either side of the sample film were equipped with an injection port with septa for sampling. The surface area of the film exposed to the permeant was approximately 50 cm², determined by the center diameter of the O-ring.

The permeant vapor was produced by bubbling nitrogen gas through the liquid permeant. The nitrogen stream containing the organic vapor at its saturation vapor pressure was mixed with pure nitrogen gas to provide organic vapor of known penetrant concentrations. The nitrogen tank regulator was set at 5 psi. The vapor generator system consisted a Kontes Gas Washing Bottle, \$29/42, 250 ml (Fisher, Scientific, Pittsburgh, PA) with Nupro "M" series needle valves and rotameters used to obtain the desired penetrant concentration (Hernandez et al., 1986). The vapor generator system was maintained at a temperature of 24±1 °C. In order to maintain a constant temperature throughout the entire test period, the permeation cells were placed in a temperature controlled oven, maintained at 24±1 °C.

The permeant vapor which permeated into the lower concentration chambers with time, was quantified by gas chromatography with flame ionization detection. The total permeant quantity was plotted as a function of time. The slope of the liner portion of this curve is the transmission rate, from which the permeability coefficient was calculated. The sampling procedure was as follows: At predetermined time intervals, a 100 μ l sample of headspace was removed from the low concentration cell chambers with a 500 μ l gastight syringe (Hamilton No. 1750, side port type) and injected into the gas chromatograph. The permeant concentration supplied to the center ring was also measured via a sampling port.

Isostatic procedure

Permeability studies were also carried out by an isostatic procedure utilizing the MAS 2000 Organic Vapor Permeation Test System (Testing Machines Inc., Amityville, NY). The apparatus allowed for the continuous collection and measurement of the permeation rate of the organic vapor through a polymer membrane, from the initial time zero to steady state conditions. The apparatus incorporates a flame ionization detector (FID), precise temperature and flow rate control, and is interfaced to an IBM 486SX computer system. The activation and deactivation of the gas flow direction,

cell opening/closing, as well as display data on the screen were controlled through the computer. Permeation data can be stored in the computer hard drive or on a floppy disc, and LOTUS 1-2-3 used to recall the permeation data to calculate and print out the respective mass transfer parameters and the transmission rate profile curve.

For each run, a film sample was placed in the permeability cell, which exposed sample area of 0.0081 m². The film was mounted with the pattern cold seal facing away from the high permeant concentration stream. The permeability studies were carried out at three temperatures, and for each temperature, three vapor activity levels were evaluated.

A constant concentration of permeant vapor for delivery to the high concentration cell chamber was produced by bubbling nitrogen through the liquid permeant. The liquid permeant was contained in a vapor generator consisting of a Kontes Fritted Midget Bubbler, \$24/40, 25 ml(Fisher, Scientific, Pittsburgh, PA). The organic vapor stream was then mixed with another source of pure nitrogen. Rotameters were used to provided an indication of settings required for the desired vapor activities. The gas flows to the rotameters were regulated by Nupro "M" series needle valves.

Determining vapor activity

Prior to testing, flowmeter settings were determined to provide vapor activity(a) values of approximately 0.05, 0.1, 0.2 and 0.4. Because of the wide variation in the saturation vapor pressure of the various penetrants, at the respective temperatures of test, the partial pressure gradient for the permeability experiments was expressed as vapor activity. This allowed for barrier performance to be compared at a standard driving force for the five permeants evaluated. Vapor activity values were calculated by:

Vapor activity (a) =
$$\frac{p}{p_0}$$
 (36)

where p = partial vapor pressure

 p_0 = saturated vapor pressure

The saturation vapor pressure of the permeants was determined as following. Five ml of the test liquid permeant were placed into a septa seal vial equipped with a Teflon-faced silicone septum and aluminum crimp cap. The vial was sealed and allowed to equilibrate at 24 ± 1 °C for a period of 48 hours. Following equilibration, a 50 to 100 μ l sample was withdrawn from the headspace of the septa seal vial with

a 500 μ l gastight syringe (Hamilton Co., Reno, NV) and injected into the gas chromatograph for quantification.

The saturation vapor pressure values determined for ethyl acetate, toluene, methyl ethyl ketone, α -pinene and limonene were 88, 20.2, 77, 6, and 0.7 mmHg respectively. All vapor pressure values were determined at 24±1 °C.

Determining partial pressure

For the isostatic procedure utilizing the MAS 2000 Permeation Test System, the organic vapor was generated at 24 ± 1 °C (point A), while the permeability rate were evaluated with the test cell at point B. Cell temperatures ranged from 30 °C to 60 °C. The partial pressure (p₂) at the test temperature was determined from the Ideal Gas Law. The parameters of temperature, concentration, partial pressure and volume for the organic vapor generation and test conditions are denoted as T_1 and T_2 , C_1 and C_2 , C_1 and C_2 , and C_2 , respectively.

$$C = M/F$$

$$Q = (Au \times CF)$$

$$Sampling port test cell$$

$$M = 0 / time$$

where Au is GC's response reported in area unit.

CF is calibration factor in unit of GC unit over gram. F is flow rate, 30 ml/min.

M is mass flow (Q/min).

Q is the quantity.

$$M_1 = c_1 \times F_1$$

 F_1 is flow rate, 30 ml/min, at point A assume that mass flow is air and it behaves as Ideal Gas Law

therefore:

$$F_2 = F_1 \frac{T_2}{T_1}$$

concentration, at point A:

$$c_1 = M_1 / F_1$$

$$c_1 = c \frac{F}{F_1}$$

 $c_1 = c$, measured by injection

concentration, at point B:

$$c_2 = M_2 / F_2$$

$$c_2 = c_1 \frac{T_1}{T_2}$$

Expressing c or p by ideal gas law, at point A:

$$p = \frac{nRT}{v} = \frac{R}{MW} \cdot \frac{m}{v} \cdot T = \frac{R}{MW} \cdot c \cdot T$$

$$\frac{\mathbf{p}_2}{\mathbf{p}_1} = \frac{\mathbf{c}_2 \mathbf{T}_2}{\mathbf{c}_1 \mathbf{T}_1}$$

$$p_2 = p_1 \cdot \frac{1}{c_1 T_1} \cdot \frac{c_1 T_1}{T_2} \cdot T_2 = p_1$$

at point A and point B:

- 1. temperature are different
- 2. mass flow are equal
- 3. flow rate are different
- 4. partial pressure are equal
- 5. saturation vapor pressure are different
- 6. vapor activity are different

A sampling port was installed between the dispensing manifold and the test cell to provide an accurate measure of the permeant vapor concentration or activity. To determine the specific vapor concentration, a 50 or 100 µl sample was removed from the sampling port with a Hamilton 500 µl, 1750SN gastight syringe and the sample injected directly into the gas chromatograph (Model 5890A, Hewlett Packard, Avondale, PA) equipped with flamed ionization detector, and interfaced to a Hewlett-Packard integrator (Model 3395, Avondale, PA). A setting of 1 minute purge "on" was employed for all analyses. The gas chromatography conditions are presented as following:

column: Supelcowax 10

Fused silica capillary column polar bounded stationary phase 60 m length and 0.32 mm I.D. carrier gas: Helium at 1.5 ml/min

Attenuation: 0

Zero: same as the signal after ignition

Purge on: 1 min

Temperature cycle for ethyl acetate:

injection temp.	220	°C
initial temp.	40	°C
initial time	1	min
temp. rate	5	°C/min
final temp.	200	°C
final time	10	min
detector temp.	250	°C
range	2	

Temperature cycle for toluene:

range	2	
injection temp.	220	°C
initial temp.	60	°C
initial time	1	min
temp. rate	5	°C/min
final temp.	200	°C
final time	10	min
detector temp.	250	°C

Temperature cycle for limonene:

range		2	
injec	tion temp.	220	°C
initi	al temp.	60	°C
initi	al time	1	min
temp.	rate	5	°C/min
final	temp.	200	°C
final	time	10	min
detec	tor temp.	250	°C

column: Supelco SPB-5

Fused silica capillary column

non-polar bounded stationary phase

30 m length and 0.32 mm I.D.

carrier gas: Helium at 1.5 ml/min

Attenuation: 0

Zero: same as the signal after ignition

Purge on: 1 min

Temperature cycle for methyl ethyl ketone:

	_ 4	
range	4	
injection temp.	220	°C
initial temp.	50 '	°C

initial time	2	min
temp. rate	5	°C/min
final temp.	200	°C
final time	10	min
detector temp.	250	°C

Temperature cycle for α -pinene:

range	2	
injection t	emp. 220	°C
initial tem	p. 50	°C
initial tim	e 1	min
temp. rate	5	°C/min
final temp.	200	°C
final time	10	min
detector te	mp. 250	°C

Integrator setting (Model 3395):

Zero: 0,0

Attenuation: 6

Chart speed: 0.5 cm/min

Peak width: 0.04 Threshold: 0

Area rejection: 0

Retention time for ethyl acetate: 5.4 min

toluene: 7.9 min
limonene: 9.3 min

MEK: 2.0 min

 α -pinene: 6.8 min

For each permeant, a calibration curve of area response vs. permeant quantity was constructed from standard solutions of known concentration. Standard solutions were prepared by dissolution known quantities of ethyl acetate in acetonitrile, toluene in methanol, limonene in acetonitrile, methyl ethyl ketone in xylene and α -pinene in acetonitrile. Calibration data are shown in Appendix A.

Once the operational parameters of gas flow rates, temperature and signal base line have attained steady state, the MAS 2000 Permeation Test System was calibrated as follows: 100 μ l samples of ethyl acetate, toluene and limonene and 50 μ l samples of methyl ethyl ketone and α pinene vapor of known concentration was removed from the sampling port interfaced to the dispensing manifold of the vapor generator system and the gaseous sample conveyed directly to the flame ionization detector of the MAS 2000 Permeation Test System via the injection port incorporated on the instrument chassis. The detector response in picoamps was then related to the quantity in grams of permeant injected to determine a calibration factor which was calculated from the ideal Gas Law (PV = nRT). All operational parameters of the MAS 2000 Permeation System were as recommended by the manufacture in the operation manual. The specific temperatures (°C) selected for the permeability studies were based on the structure of the respective test films and are presented below:

	Ethyl Acetate Tol		luene Limo			onene				
OPP	30,	40,	50	30,	40,	50		40,	50,	60
HDPE	30,	40,	50	30,	40,	50		30,	40,	50
Glassine	23,	40,	50	30,	40,	50		30,	40,	50
Saran Opp	40,	50,	60	40,	50,	60		40,	50,	60

Acrylic OPP	50, 60, 70	50, 60, 70	40, 50, 60
Met PET/OPP	50, 60, 70	50, 60, 70	40, 50, 60
	MEK	<u>α-Pinene</u>	
OPP	30, 40, 50	40, 50, 60	
HDPE	30, 40, 50	30, 40, 50	
Glassine	30, 40, 50,	30, 40, 50	
Saran Opp	40, 50, 60	40, 50, 60	
Acrylic OPP	40, 50, 60	40, 50, 60	
Met PET/OPP	40, 50, 60	40, 50, 60	

RESULTS AND DISCUSSION

Permeability of Packaging Films by an Isostatic Procedure

Effect of vapor activity and temperature on the organic vapor permeability

Permeance and diffusion coefficient values determined by the isostatic procedure for the respective structures, as a function of vapor activity and temperature, are summarized in Tables 1 - 10, respectively. For the metallized polyethylene terephthalate/OPP laminate, no measurable rate of diffusion was detected, following continuous testing for 44 hours at 60°C and at the highest vapor activity evaluated for the respective penetrants. Since several films investigated in the present study were multilayer or coated structures, permeance values were calculated to describe the barrier properties of the total structure and the diffusion coefficient values reported were apparent diffusion coefficients, representative of the specific structures.

To better illustrate the effect of vapor activity on the permeance of the test films, the results are presented graphically in Figure 1 to 20, where log permeance (P) is plotted as a function of vapor activity, at constant temperature.

Table 1. Permeance constant of ethyl acetate through packaging films as a function of temperature and vapor activity $^{(1)}$

Vapor ⁽²⁾			$P \times 10^{-12} \left(\frac{\text{Kg}}{\text{m}^2 \cdot \text{sec. Pa}} \right)$					
	Temp (°C)	HDPE	OPP	Saran	Acrylic	Glassine		
				-OPP	-OPP			
	24					1.1 ± .07		
	30	$10.4 \pm .03$	$0.6 \pm .04$			1.9 ± 0.1		
0.095	40	17.9 ± 0.7	1.8 ±09	$0.1 \pm .001$		4.4 ± 0.3		
	50	28.3 ± 0.9	4.7 ± 0.4	$0.5 \pm .001$	$0.1 \pm .007$			
	60			$1.7 \pm .005$	$0.6 \pm .001$			
	70				$1.5 \pm .004$			
	24					2.2 ± .007		
	30	24.5 ± 1.1	$0.7 \pm .06$			3.0 ± 0.3		
0.21	40	29.5 ± 0.6	$2.1 \pm .04$	$0.2 \pm .007$		5.5 ± 0.2		
	50	36.7 ± 0.4	4.8 ± 0.1	$0.6 \pm .04$	$0.2 \pm .01$			
	60			$1.7 \pm .02$	$1.3 \pm .03$			
	70				$3.7\pm.05$			
	30	29.6 ± .04	$0.9 \pm .02$					
0.41	40	39.0 ± 2.1	2.2 ± 0.1	$0.3 \pm .0007$				
	50	52.2 ± 2.0	5.2 ± 0.1	$0.9 \pm .03$	$0.4 \pm .01$			
	60	-	· · · · · · · · · · · · · · · · · · ·	$0.3 \pm .04$	$1.4 \pm .04$			
	70				$3.9 \pm .04$			

 $^{^{(1)}}$ The reported results are the average of duplicate analyses \pm average of the absolute deviations from their mean.

Vapor activity values were determined at ambient temperature (24°C) .

Table 2. Diffusion coefficient of ethyl acetate through packaging films as a function of temperature and vapor activity(1)

			$D \times 10^{-13} (m^2/sec)$						
Vapor activity	Temp (°C)	HDPE	OPP	Saran ⁽²⁾	Acrylic ⁽²⁾	Glassine ⁽²⁾			
	24				·	15.1 ± 0.1			
	30	$0.4 \pm .004$	$0.3 \pm .003$			17.5 ± 0.9			
0.095	40	$1.5 \pm .011$	$1.1 \pm .008$	$.09 \pm .002$		18.1 ± 2.3			
	50	5.5 ± 0.3	4.1 ± 0.2	$0.5 \pm .006$	$.08 \pm .003$				
	60			$2.1 \pm .07$	$0.4 \pm .013$				
	70				$1.4 \pm .001$				
	24					23.5 ± 1.0			
	30	5.3 ± 0.4	$0.3 \pm .008$			21.8 ± 0.8			
0.21	40	10.7 ± 0.3	$1.2 \pm .05$	$0.1 \pm .007$		17.4 ± 1.0			
	50	18.5 ± 0.2	$4.4 \pm .01$	$0.6 \pm .02$	$.09 \pm .003$				
	60			$2.1 \pm .06$	$0.4 \pm .006$				
	70				$1.6 \pm .09$				
	30	4.7 ± .06	$0.3 \pm .001$						
0.41	40	10.3 ± 0.5	$1.1 \pm .09$	$0.1 \pm .009$					
	50	17.9 ± 0.4	$4.0 \pm .12$	$0.7 \pm .06$	$0.1 \pm .004$				
	60			$2.1 \pm .01$	$0.4 \pm .001$				
	70				$1.4 \pm .01$				

 $^{^{(1)}}$ The reported results are the average of duplicate analyses \pm average of the absolute deviations from their mean.

(2) Values reported are apparent diffusion coefficients,

representative of the structure.

Table 3. Permeance constant of toluene through packaging films as a function of temperature and vapor activity $^{(1)}$

Vapor (°C) HDPE OPP Saran Acrylic Glassin -OPP -OPP

Vapor (2)	Temp	•	<u> </u>			
activity	(°C)	HDPE	OPP	Saran -OPP	Acrylic -OPP	Glassine
	30	23.7 ± 1.6	5.4 ± 0.2			3.1 ± .07
0.067	40	38.0 ± 3.1	12.8 ±. 0.9	$0.1 \pm .01$		4.4 ± 0.6
	50	65.6 ± 3.6	20.5 ± 1.2	$0.7 \pm .06$		$6.0 \pm .08$
	60			$2.7 \pm .09$		
	70				N/A ⁽³⁾	
	30	44.9 ± 0.3	8.4 ± 0.1			4.0 ± 0.4
0.22	40	63.8 ± 3.5	16.6 ± 0.9	$0.3 \pm .01$		6.1 ± 0.2
	50	96.1 ± 0.1	32.0 ± 1.0	1.2 ± 0.1		7.9 ± 0.4
	60			3.1 ± 0.1		
	70				N/A ⁽³⁾	
	30	85.4 ± 2.4	15.6 ± 0.4			4.6 ± 0.4
0.44	40	99.6 ± 1.2	22.6 ± 0.2	$0.4 \pm .005$		6.4 ± 0.4
	50	110.4 ± 4.3	36.6 ± 0.3	$1.6 \pm .04$	$.08 \pm .007$	8.1 ± 0.2
	60			3.5 ± 0.1	$0.4 \pm .01$	
	7 0				$1.8 \pm .0.5$	

 $^{^{(1)}}$ The reported results are the average of duplicate analyses \pm average of the absolute deviations from their mean.

⁽²⁾ Vapor activity values were determined at ambient temperature (24°C) .

No measurable level of permeation detected, run for 44 hr.

Table 4. Diffusion coefficient of toluene through packaging films as a function of temperature and vapor activity(1)

		D x10 ⁻¹³ (m ² /sec)						
Temp	=							
(°C)	HDPE	OPP	Saran ⁽²⁾ -OPP	Acrylic ⁽²⁾ -OPP	Glassine (2)			
30	1.6 ± 0.2	0.1 ± .005			13.2 ± 0.3			
40	3.8 ± 0.2	$0.6 \pm .007$	$.02 \pm .002$		13.3 ± 0.6			
50	$8.8 \pm .04$	1.9 ± 0.05	$0.2 \pm .003$		8.0 ± 0.3			
60			$1.2 \pm .02$					
70				N/A ⁽³⁾				
30	1.6 ± 0.1	.08 ± .006			10.8 ± 0.3			
40	3.7 ± 0	$0.7 \pm .02$	$.05 \pm .005$		15.1 ± 0.4			
50	8.3 ± 0.3	2.2 ± 0.1	$0.3 \pm .01$		17.8 ± 2.0			
60			$1.3 \pm .04$					
70				N/A ⁽³⁾				
30	2.6 ± .01	$0.3 \pm .004$			7.6 ± 0.3			
40	4.9 ± 0.3	$0.8 \pm .05$	$0.4 \pm .07$		11.2 ± 0.3			
50	9.1 ± 0.1	$2.0 \pm .02$	$0.3 \pm .002$	$.01 \pm 0$	15.7 ± 0.1			
60			$1.3 \pm .02$	$.06 \pm .003$				
70				$0.2 \pm .001$				
	30 40 50 60 70 30 40 50 60 70	30 1.6 ± 0.2 40 3.8 ± 0.2 50 8.8 ± .04 60 70 30 1.6 ± 0.1 40 3.7 ± 0 50 8.3 ± 0.3 60 70 30 2.6 ± .01 40 4.9 ± 0.3 50 9.1 ± 0.1 60	(°C) HDPE OPP $ \begin{array}{c ccccccccccccccccccccccccccccccccccc$	(°C) HDPE OPP Saran ⁽²⁾ -OPP $ \begin{array}{cccccccccccccccccccccccccccccccccc$	(°C) HDPE OPP Saran ⁽²⁾ Acrylic ⁽²⁾ -OPP OPP $ \begin{array}{cccccccccccccccccccccccccccccccccc$			

The reported results are the average of duplicate analyses \pm average of the absolute deviations from their mean.

Values reported are apparent diffusion coefficients representative of the structure.

representative of the structure.

(3) No measurable level of permeation detected, run for 44 hr.

Table 5. Permeance constant of limonene through packaging films as a function of temperature and vapor activity (1) (4)

			$P \times 10^{-12} \left(\frac{\text{Kg}}{\text{m}^2 \cdot \text{sec. Pa}} \right)$						
Vapor ⁽²⁾	Temp (°C)	HDPE	OPP	Saran -OPP	Glassine				
	30	10.5 ± 0.9			14.6 ± .07				
0.1	40	30.1 ± 0.5	6.6 ± 3.6		17.0 ± 0.7				
	50	67.7 ± 8.7	18.1 ± 0.7	$N/A^{(3)}$	$22.3 \pm .01$				
	60		37.2 ± 4.0	3.3 ± 0.2					
	30	21.4 ± 1.3			15.4 ± 0.7				
0.2	40	48.0 ± 0.7	32.1 ± 2.8		17.4 ± 1.0				
	50	83.7 ± 9.3	79.0 ± 1.7	$N/A^{(3)}$	24.6 ± 1.0				
	60		141.4 ± 2.5	3.3 ± 0.3					
	30	62.5 ± 6.6			16.2 ± 0.6				
0.4	40	97.2 ± 3.7	49.7 ± 0.4	$N/A^{(3)}$	19.3 ± 1.2				
	50	171.7 ± 8.3	100.9 ± 10.7	$0.9 \pm .09$	29.7 ± 1.6				
	60		173.9 ± 17.2	3.3 ± 0.3					

 $^{^{(1)}}$ The reported results are the average of duplicate analyses \pm average of the absolute deviations from their mean.

Vapor activity values were determined at ambient temperature $(24\pm1~^\circ\text{C})$.

No measurable level of permeation detected, run for 44 hr.

No measurable level of permeation was detected for the Acrylic coated oriented polypropylene, under the conditions of test.

Table 6. Diffusion coefficient of limonene through packaging films as a function of temperature and vapor activity $^{\scriptscriptstyle{(1)}}$

Vapor activity			D x10) ⁻¹³ (m ² /sec)	
	Temp (°C)	HDPE	OPP	Saran ⁽²⁾	Glassine ⁽²⁾
	30	0.3 ± .008			3.2 ± 0.3
0.1	40	$0.6 \pm .06$	$.08 \pm .006$		5.8 ± 0.4
	50	$1.6 \pm .04$	$0.2 \pm .008$	$N/A^{(3)}$	9.0 ± 0.4
	60		$1.0 \pm .03$	$.03 \pm .0009$	
	30	0.3 ± .01			2.8 ± .001
0.2	40	$0.6 \pm .006$	$.07 \pm .002$		4.2 ± 0.4
	50	$1.2 \pm .02$	$0.3 \pm .01$	$N/A^{(3)}$	7.6 ± 0.3
	60		$1.0 \pm .05$	$0.2 \pm .003$	
	30	0.3 ± .01			$2.0 \pm .06$
0.4	40	$0.6 \pm .05$	$.08 \pm .007$	$N/A^{(3)}$	$3.2 \pm .03$
	50	1.4 ± 0.1	$0.3 \pm .004$.03 ± .0007	6.3 ± 0.5
	60	23.0 ± 0.3	$1.2 \pm .002$	$0.2 \pm .006$	

 $[\]overline{}^{(1)}$ The reported results are the average of duplicate analyses \pm average of the absolute deviations from their mean.

⁽²⁾ Values reported are apparent diffusion coefficients

representative of the structure.

(3) No measurable level of permeation detected, run for 44 hr.

(4) No measurable level of diffusion coefficient was detected for the Acrylic coated oriented polypropylene, under the conditions of test.

Table 7. Permeance constant of methyl ethyl ketone through packaging films as a function of temperature and vapor activity $^{(1)}$

		$P \times 10^{-12} \left(\frac{\text{Kg}}{\text{m}^2 \cdot \text{sec. Pa}} \right)$						
Vapor (2) activity	Temp (°C)	HDPE	OPP	Saran -OPP	Acrylic -OPP	Glassine		
	30	5.4 ± 0.1	1.4 ± 0.1			$0.7 \pm .02$		
0.05	40	8.6 ± 0.6	3.5 ± 0.3	$0.1 \pm .002$	$.05 \pm .0009$	$1.7 \pm .06$		
	50	10.7 ± 0.3	5.6 ± 0.2	$0.5 \pm .01$	$0.2 \pm .02$	2.0 ± 0.2		
	60			$1.3 \pm .03$	$0.8 \pm .03$			
	30	6.4 ± 0.4	1.6 ± .05			$0.7 \pm .03$		
0.1	40	9.1 ± 0.3	3.7 ± 0.3	$0.1 \pm .01$	$.06 \pm .003$	$1.8 \pm .04$		
	50	12.9 ± 0.7	6.4 ± 0.4	$0.5 \pm .02$	$0.2 \pm .005$	2.4 ± 0.2		
	60			$1.5 \pm .03$	$0.9 \pm .02$			
	30	7.0 ± .08	1.6 ± 0.1			0.9 ± .03		
0.2	40	10.2 ± 0.2	$3.7 \pm .09$	$0.3 \pm .02$	$0.2 \pm .0002$	$2.1 \pm .03$		
	50	13.4 ± 0.2	8.0 ± 0.2	$0.7 \pm .05$	$0.4 \pm .0009$	$3.3 \pm .003$		
	60			$1.9 \pm .05$	$1.2 \pm .07$			

 $^{^{(1)}}$ The reported results are the average of duplicate analyses \pm average of the absolute deviations from their mean.

Vapor activity values were determined at ambient temperature (24°C).

Table 8. Diffusion coefficient of methyl ethyl ketone through packaging films as a function of temperature and vapor activity(1)

			D	x10⁻¹³ (m ² /	sec)	
Vapor	Temp			(2)		
activity	(°C)	HDPE	OPP	Saran ⁽²⁾ -OPP	Acrylic ⁽²⁾ -OPP	Glassine ⁽²⁾
	30	4.2 ± .08	$0.4 \pm .03$			17.7 ± 0.3
0.05	40	7.7 ± 0.5	1.5 ± 0.2	$.09 \pm .004$	$.03 \pm .001$	17.5 ± 0.3
	50	$15.2 \pm .03$	3.2 ± 0.4	$0.5 \pm .007$	$0.1 \pm .003$	18.3 ± 1.2
	60			1.7 ± 0.2	$0.5 \pm .02$	
	30	4.7 ± .07	0.4 ± .007			17.9 ± 2.2
0.1	40	8.6 ± 0.4	$1.3 \pm .05$	$.08 \pm .009$	$.04 \pm .007$	$20.2 \pm .07$
	50	14.3 ± 0.3	3.7 ± 0.1	$0.4 \pm .006$	$0.1 \pm .005$	18.4 ± 2.2
	60			1.7 ± 0.3	$0.5 \pm .02$	
	30	5.0 ± .01	$0.3 \pm .009$			9.7 ± 1.4
0.2	40	9.2 ± 0.7	1.1 ± 0.2	$0.1 \pm .09$	$.04 \pm .001$	18.1 ± 0.7
	50	14.7 ± 0.5	$2.9 \pm .09$	$0.5 \pm .02$	$0.1 \pm .02$	14.5 ± 0.5
	60			$1.7 \pm .01$	$0.6 \pm .004$	

The reported results are the average of duplicate analyses ± average of the absolute deviations from their mean.

Values reported are apparent diffusion coefficients representative of the structure.

Table 9. Permeance constant of $\alpha\text{-pinene}$ through packaging films as a function of temperature and vapor activity $^{\text{(1)}\;(4)}$

Vapor ⁽²⁾ activity					
	Temp (°C)	HDPE	OPP	Saran -OPP	Glassine
	30	$0.6 \pm .05$	74	<u> </u>	4.4 ± 0.1
0.1	40	3.7 ± 0.1	N/A ⁽³⁾		5.4 ± 0.2
	50	7.1 ± 0.7	4.2 ± 0.2		6.2 ± 0.3
	60	25.3 ± 1.4	11.9 ± 0.8	N/A ⁽³⁾	
	30	1.7 ± 0.2			$5.6 \pm .06$
0.2	40	4.4 ± 0.1	$1.7 \pm .07$		5.8 ± 0.3
	50	11.1 ± 0.4	6.1 ± 0.6	$N/A^{(3)}$	7.4 ± 0.3
	60	28.6 ± 2.9	12.2 ± 0.6	$0.1 \pm .01$	
	30	3.2 ± .08			6.6 ± 0.6
0.4	40	5.3 ± 0.4	2.6 ± 0.2		9.3 ± 0.3
	50	$12.1 \pm .06$	6.2 ± 0.6	N/A ⁽³⁾	9.1 ± 0.1
	60		14.9 ± 1.0	0.1 ± .006	

The reported results are the average of duplicate analyses ± average of the absolute deviations from their mean.

⁽²⁾ Values reported are apparent diffusion coefficients representative of the structure.

No measurable level of permeation detected, run for 44 hr.

⁽⁴⁾ No measurable level of diffusion coefficient was detected for the Acrylic coated oriented polypropylene, under the conditions of test.

Table 10. Diffusion coefficient of α -pinene through packaging films as a function of temperature and vapor activity(1)(4)

Vapor activity			D x10⁻¹³ (m ² /sec)					
	Temp (°C)	HDPE	OPP	Saran ⁽²⁾	Glassine ⁽²			
				-OPP				
	30	.07 ± .008			3.1 ± 0.3			
0.1	40	$0.2 \pm .02$	N/A		7.2 ± 1.0			
	50	$0.5 \pm .03$	$.06 \pm .004$		$11.0 \pm .08$			
	60	$0.9 \pm .02$	$0.3 \pm .006$	N/A ⁽³⁾				
	30	.06 ± .006			0.7 ± 0.1			
0.2	40	$0.2 \pm .006$	$.02 \pm .002$		4.3 ± 1.2			
	50	$0.5 \pm .007$	$.07 \pm .006$	$N/A^{(3)}$	$11.5 \pm .05$			
	60	$1.4 \pm .009$	$0.3 \pm .003$	$.03 \pm .004$				
	30	.08 ± .003			$0.3 \pm .05$			
0.4	40	$0.2 \pm .02$	$.02 \pm .002$		$8.1 \pm .03$			
	50	$0.5 \pm .08$	$.06 \pm .006$	N/A	$11.9 \pm .02$			
	60		$0.2 \pm .002$	$.04 \pm .002$				

The reported results are the average of duplicate analyses \pm average of the absolute deviations from their mean.

⁽²⁾ Values reported are apparent diffusion coefficients

representative of the structure.

(3) No measurable level of permeation detected, run for 44 hr.

(4) No measurable level of diffusion coefficient was detected for the Acrylic coated oriented polypropylene, under the conditions of test.

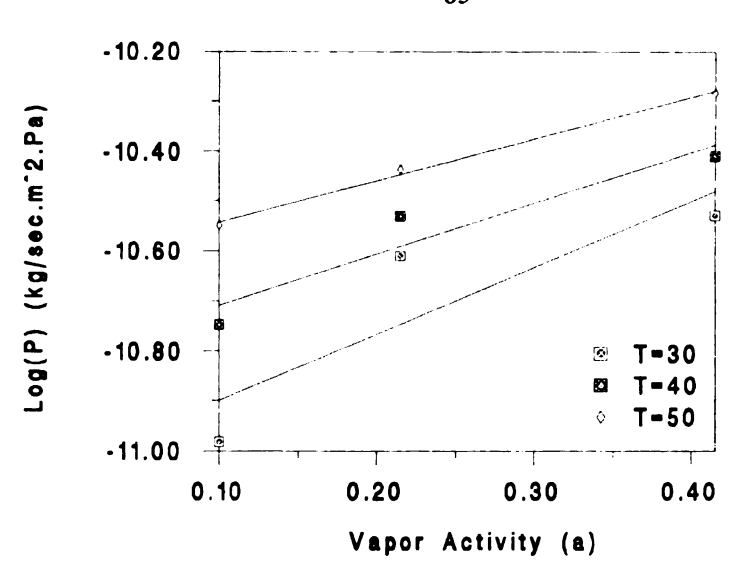


Figure 1. The effect of ethyl acetate vapor activity on permeance for high density polyethylene

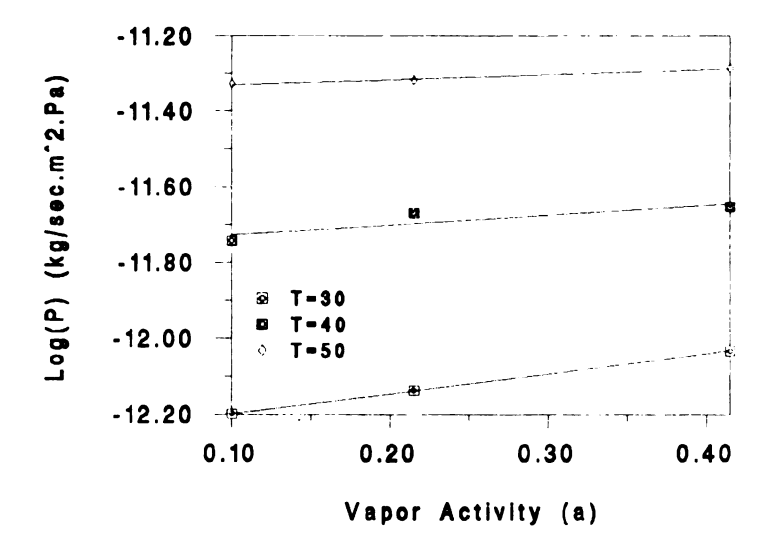


Figure 2. The effect of ethyl acetate vapor activity on permeance for oriented polypropylene

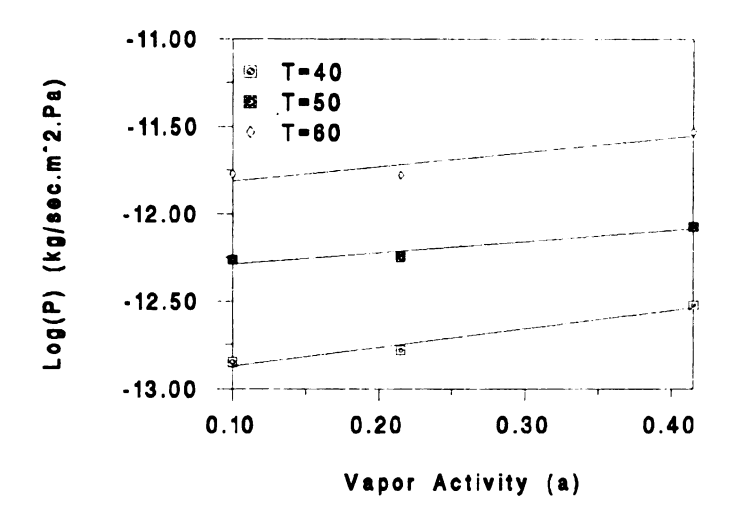


Figure 3. The effect of ethyl acetate vapor activity on permeance for Saran coated OPP

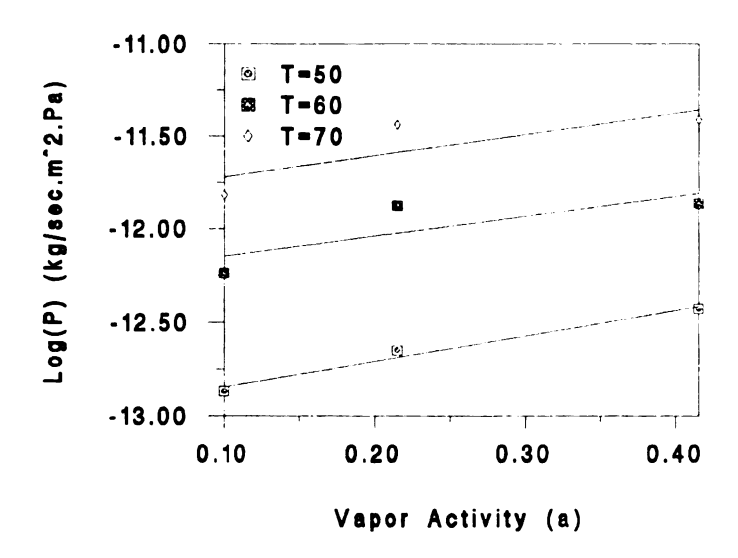


Figure 4. The effect of ethyl acetate vapor activity on permeance for Acrylic coated OPP

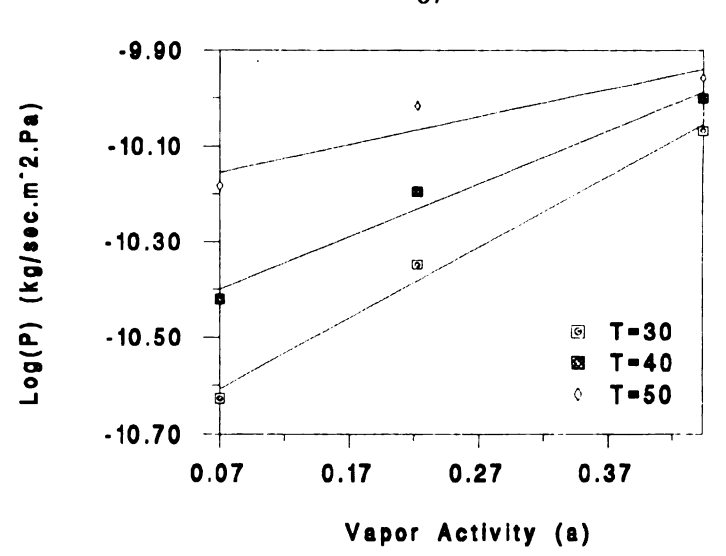


Figure 5. The effect of toluene vapor activity on permeance for high density polyethylene

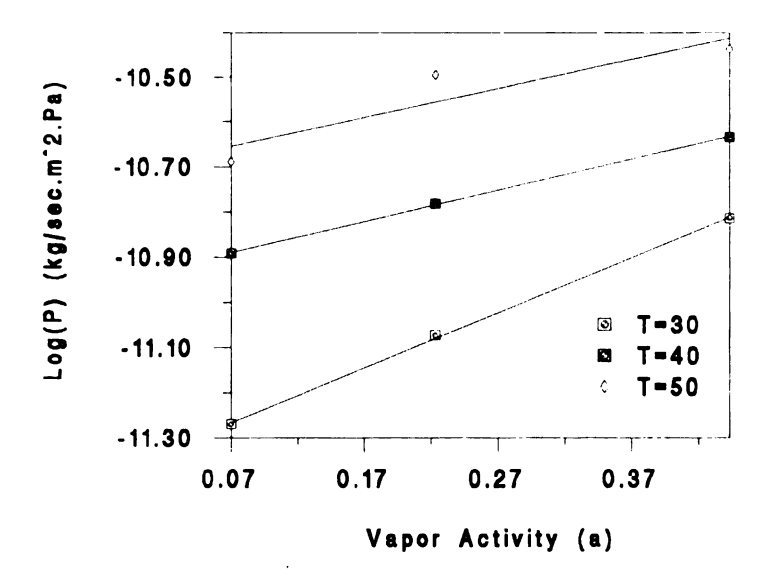


Figure 6. The effect of toluene vapor activity on permeance for oriented polypropylene

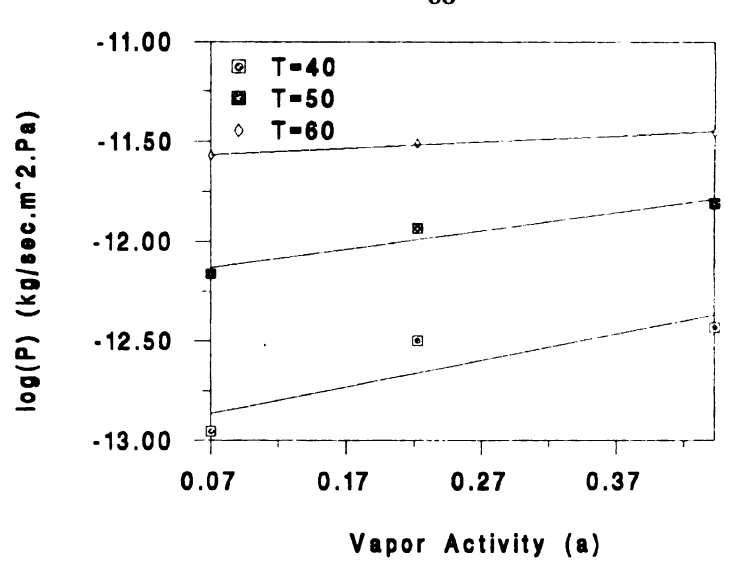


Figure 7. The effect of toluene vapor activity on permeance for Saran coated OPP

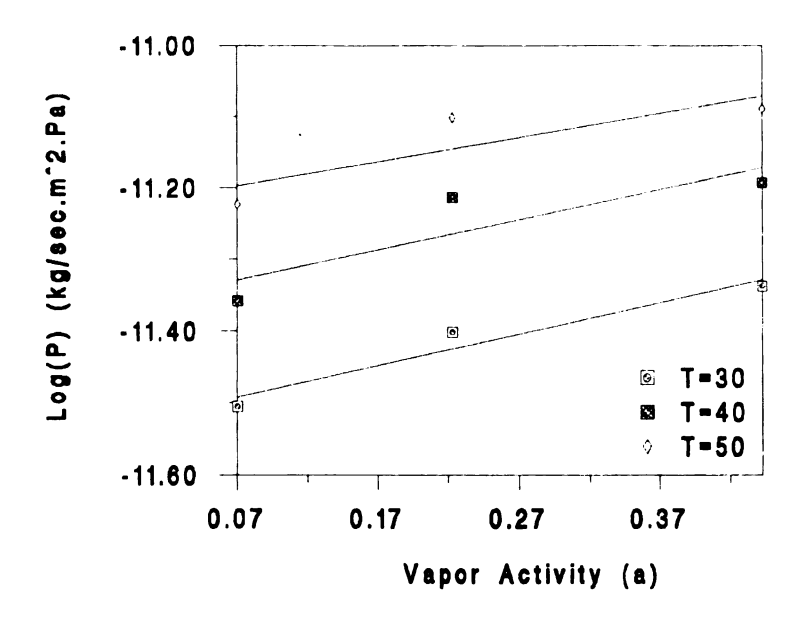


Figure 8. The effect of toluene vapor activity on permeance for Glassine

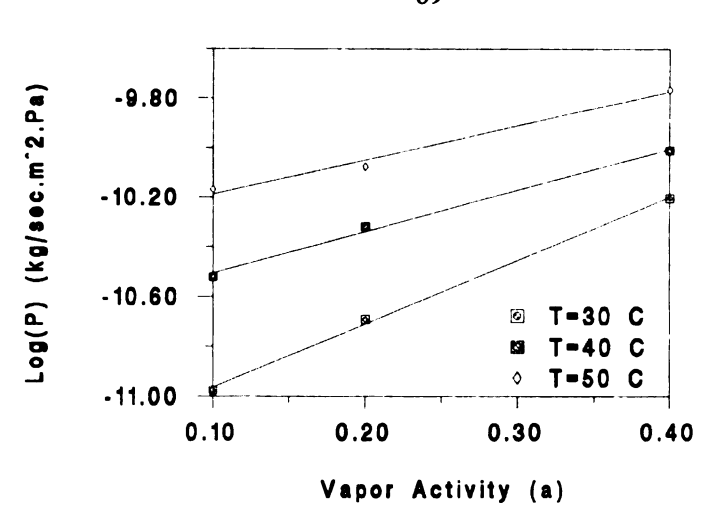


Figure 9. The effect of limonene vapor activity on permeance for high density polyethylene

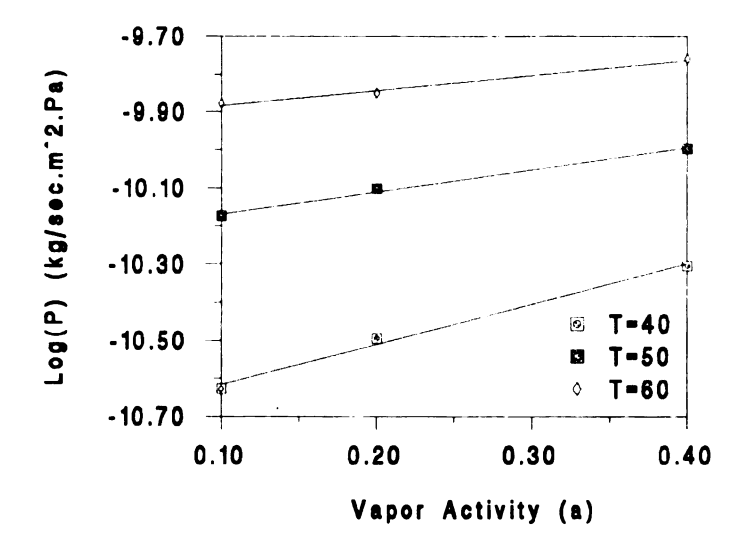


Figure 10. The effect of limonene vapor activity on permeance for oriented polypropylene

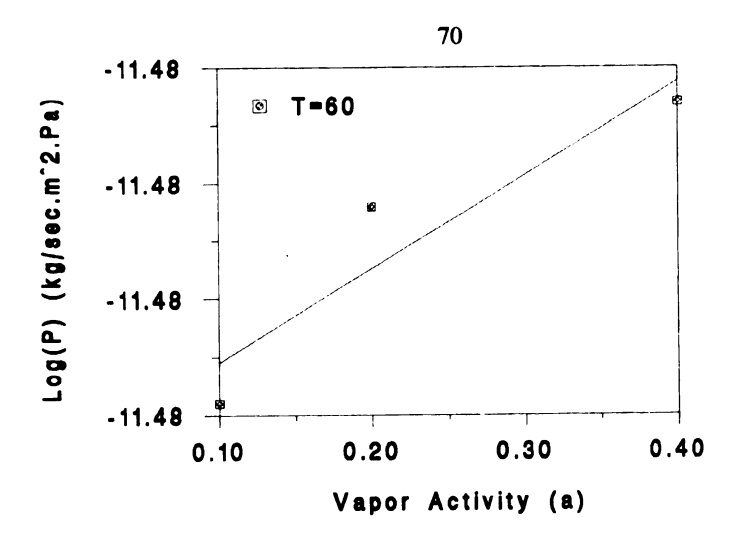


Figure 11. The effect of limonene vapor activity on permeance for Saran coated OPP

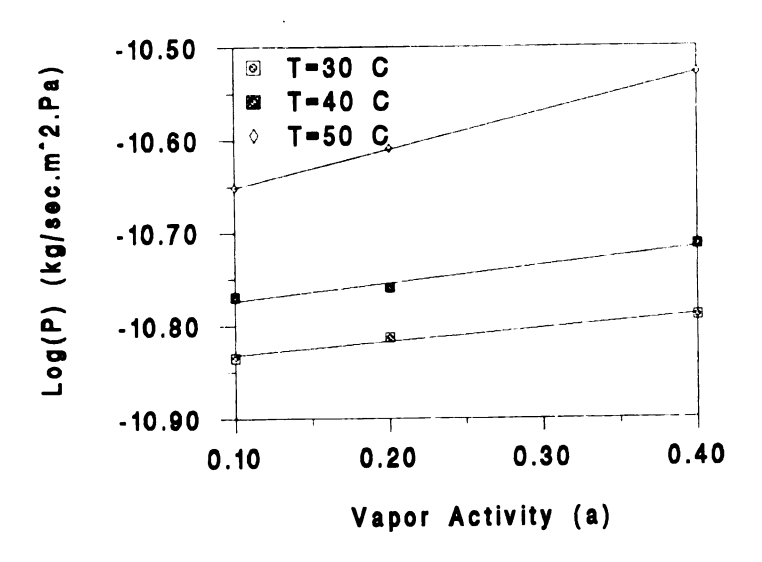


Figure 12. The effect of limonene vapor activity on permeance for Glassine

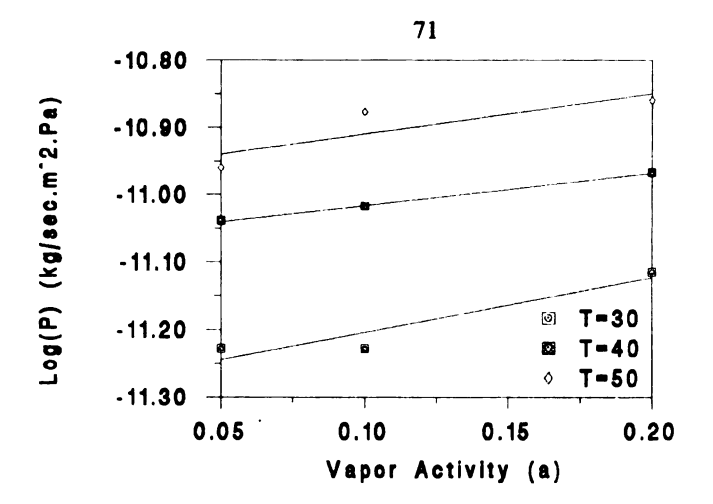


Figure 13. The effect of methyl ethyl ketone vapor activity on permeance for high density polyethylene

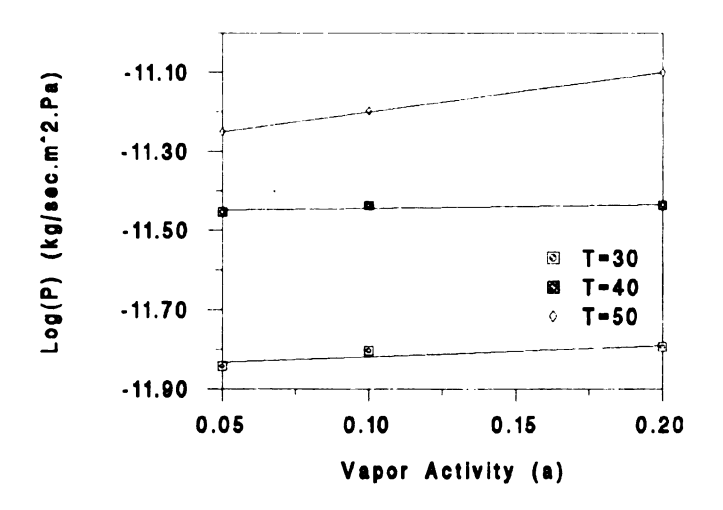


Figure 14. The effect of methyl ethyl ketone vapor activity on permeance for oriented polypropylene



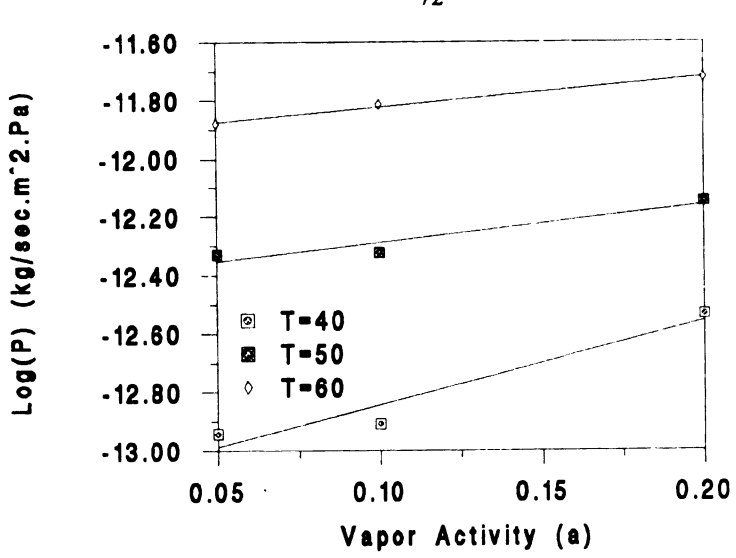


Figure 15. The effect of methyl ethyl ketone vapor activity on permeance for Saran coated OPP

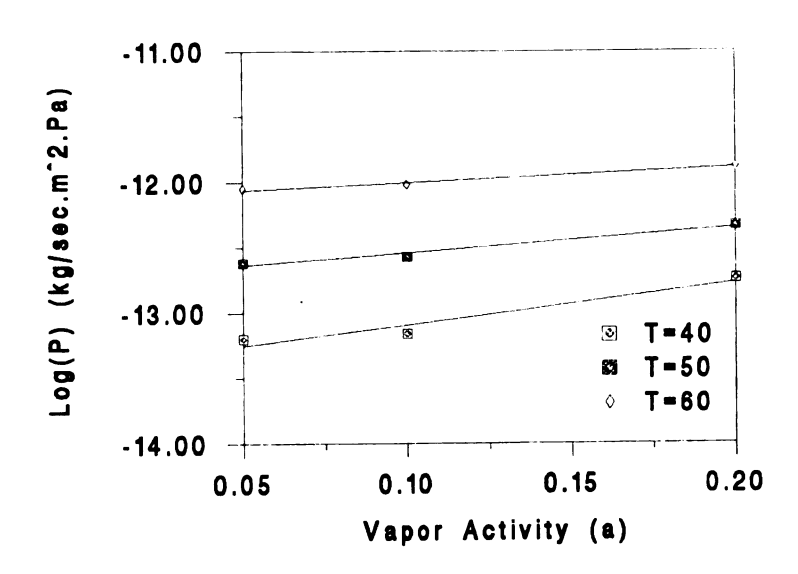


Figure 16. The effect of methyl ethyl ketone vapor activity on permeance for Acrylic coated OPP

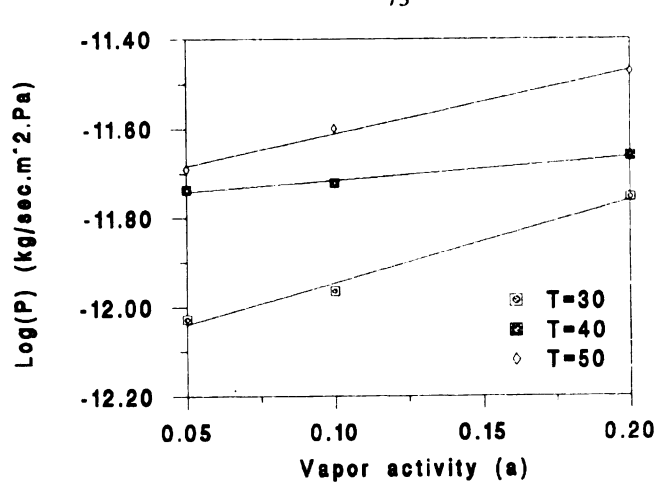


Figure 17. The effect of methyl ethyl ketone vapor activity on permeance for Glassine

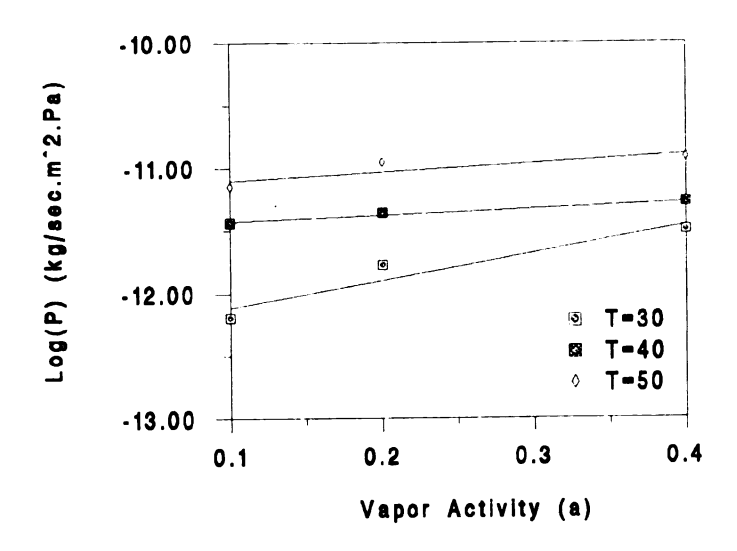


Figure 18. The effect of pinene vapor activity on permeance for high density polyethylene

		Fi
	·	
		F

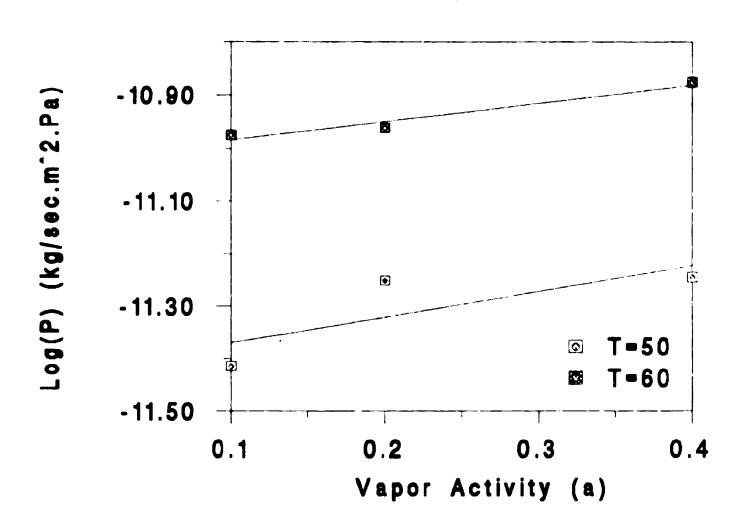


Figure 19. The effect of pinene vapor activity on permeance for oriented polypropylene

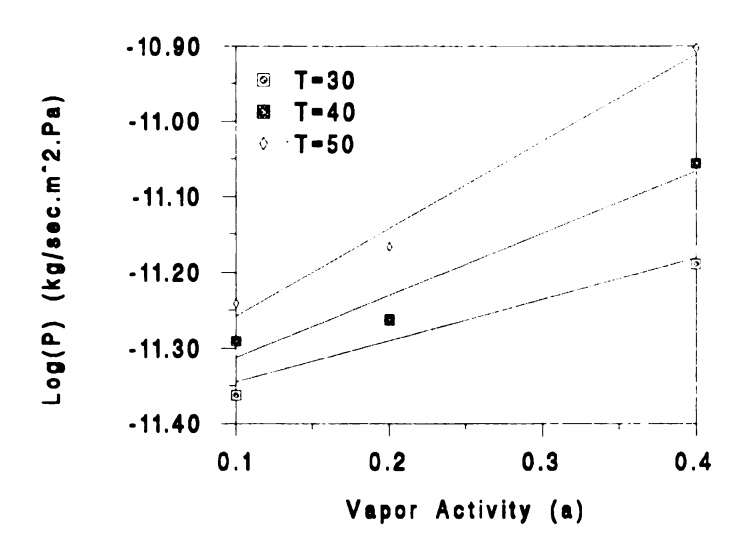


Figure 20. The effect of pinene vapor activity on permeance for Glassine

From a least squares fit, the following expressions were derived to describe the relationship between the permeance constant of the test films and vapor activity. The correlation coefficient values (r^2) are also presented. For the permeability of ethyl acetate vapor through the test polymer structures, the relationship between the permeance value(P) and vapor activity(a) was found to be:

HDPE	log(P) _(30°C)	-11.024 + 1.326×	(a) $r^2 = 0.764$
	log(P) _(40°C)	-10.805 + 1.020×	(a) $r^2 = 0.903$
	log(P) _(50°C)	-10.622 + 0.837×	(a) $r^2 = 0.996$
OPP	log(P) _(30°C)	-12.248 + 0.529×	(a) $r^2 = 1.000$
	log(P) _(40°C)	-11.751 + 0.258×	(a) $r^2 = 0.763$
	log(P) _(50°C)	-11.343 + 0.138×	(a) $r^2 = 0.970$
Saran- OPP	log(P) _(40°C)	-12.969 + 1.060×	(a) $r^2 = 0.969$
Off	log(P) _(50°C)	-12.347 + 0.639×	(a) $r^2 = 0.919$
	log(P) _(60°C)	-11.889 + 0.826×	(a) $r^2 = 0.856$
Acrylic-	log(P) _(50°C)	-12.974 + 1.366×	(a) $r^2 = 0.978$
OFF	log(P) _(60°C)	-12.244 + 1.059×	(a) $r^2 = 0.680$
	log(P) _(70°C)	-11.830 + 1.155×	(a) $r^2 = 0.660$

For the permeability of toluene vapor through the test polymer structures, the relationship between the permeance value(P) and vapor activity(a) was found to be:

HDPE
$$\log(P)_{(30^{\circ}C)} = -10.706 + 1.479 \times (a)$$
 $r^2 = 0.990$ $\log(P)_{(40^{\circ}C)} = -10.747 + 1.106 \times (a)$ $r^2 = 0.979$ $\log(P)_{(50^{\circ}C)} = -10.193 + 0.581 \times (a)$ $r^2 = 0.871$

OPP
$$\log(P)_{(30^{\circ}C)} = -11.348 + 1.219 \times (a)$$
 $r^2 = 0.999$ $\log(P)_{(40^{\circ}C)} = -10.936 + 0.687 \times (a)$ $r^2 = 0.999$ $\log(P)_{(50^{\circ}C)} = -10.697 + 0.646 \times (a)$ $r^2 = 0.847$ Saran- $\log(P)_{(40^{\circ}C)} = -12.952 + 1.334 \times (a)$ $r^2 = 0.788$ $\log(P)_{(50^{\circ}C)} = -12.190 + 0.918 \times (a)$ $r^2 = 0.929$ $\log(P)_{(60^{\circ}C)} = -11.587 + 0.312 \times (a)$ $r^2 = 0.988$ Glassine $\log(P)_{(30^{\circ}C)} = -11.521 + 0.437 \times (a)$ $r^2 = 0.948$ $\log(P)_{(40^{\circ}C)} = -11.356 + 0.417 \times (a)$ $r^2 = 0.759$ $\log(P)_{(50^{\circ}C)} = -10.220 + 0.337 \times (a)$ $r^2 = 0.734$

For the permeability of limonene vapor the test polymer structures, the relationship between the permeance value(P) and vapor activity(a) was found to be:

HDPE
$$\log(P)_{(30^{\circ}C)} = -11.220 + 2.555 \times (a)$$
 $r^2 = 0.998$ $\log(P)_{(40^{\circ}C)} = -10.675 + 1.675 \times (a)$ $r^2 = 0.995$ $\log(P)_{(50^{\circ}C)} = -10.325 + 1.377 \times (a)$ $r^2 = 0.987$ OPP $\log(P)_{(40^{\circ}C)} = -10.723 + 1.061 \times (a)$ $r^2 = 0.992$ $\log(P)_{(50^{\circ}C)} = -10.226 + 0.582 \times (a)$ $r^2 = 0.994$ $\log(P)_{(60^{\circ}C)} = -9.922 + 0.399 \times (a)$ $r^2 = 0.989$ Saran-OPP $\log(P)_{(60^{\circ}C)} = -11.484 + 0.008 \times (a)$ $r^2 = 0.872$ Glassine $\log(P)_{(30^{\circ}C)} = -10.846 + 0.142 \times (a)$ $r^2 = 0.967$ $\log(P)_{(40^{\circ}C)} = -11.792 + 0.192 \times (a)$ $r^2 = 0.970$ $\log(P)_{(50^{\circ}C)} = -10.692 + 0.411 \times (a)$ $r^2 = 1.000$

For the permeability of methyl ethyl ketone vapor through the test polymer structures, the relationship between the permeance value(P) and vapor activity(a) was found to be:

HDPE	log(P) _(30°C)	=	-11.286	+	0.698×(a)	$r^2 = 0$	0.867
	log(P) _(40°C)	=	-11.089	+	0.482×(a)	$r^2 = 0$	0.999
	log(P) _(50°C)	=	-10.980	+	0.594×(a)	$r^2 = 0$	0.772
OPP	log(P) _(30°C)	=	-11.847	+	0.285×(a)	$r^2 = 0$	0.720
	log(P) _(40°C)	=	-11.453	+	0.092×(a)	$r^2 = 0$	0.645
	log(P) _(50°C)	=	-11.300	+	1.009×(a)	$r^2 = 2$	1.000
Saran- OPP	log(P) _(40°C)	=	-13.139	+	2.630×(a)	$r^2 = 0$	0.939
OFF	log(P) _(50°C)	=	-12.428	+	1.296×(a)	$r^2 = 0$	0.909
	log(P) _(60°C)	=	-11.923	+	1.020×(a)	$r^2 = 0$	0.993
Acrylic- OPP	log(P) _(40°C)	=	-13.484	+	3.221×(a)	$r^2 = 0$	0.934
OFF	log(P) _(50°C)	=	-12.794	+	1.955×(a)	$r^2 = 0$	0.971
	log(P) _(€0°C)	=	-12.165	+	1.143×(a)	$r^2 = 0$	0.971
Glassine	log(P) _(30°C)	=	-12.223	+	0.773×(a)	$r^2 = 0$	0.985
	log(P) _(40°C)	=	-11.793	+	0.522×(a)	$r^2 = 0$	0.983
	log(P) _(50°C)	=	-11.766	+	1.427×(a)	$r^2 = 0$	0.990

For the permeability of α -pinene vapor through the test polymer structures, the relationship between the permeance value(P) and vapor activity(a) was found to be:

HDPE
$$\log(P)_{(40^{\circ}C)} = -12.335 + 2.202 \times (a)$$
 $r^2 = 0.907$ $\log(P)_{(50^{\circ}C)} = -11.475 + 0.511 \times (a)$ $r^2 = 0.960$

$$\log(P)_{(60^{\circ}C)} = -11.165 + 0.687 \times (a) \qquad r^{2} = 0.720$$
OPP
$$\log(P)_{(50^{\circ}C)} = -11.381 + 0.491 \times (a) \qquad r^{2} = 0.666$$

$$\log(P)_{(60^{\circ}C)} = -10.968 + 0.346 \times (a) \qquad r^{2} = 0.958$$
Glassine
$$\log(P)_{(30^{\circ}C)} = -11.391 + 0.548 \times (a) \qquad r^{2} = 0.927$$

$$\log(P)_{(40^{\circ}C)} = -11.370 + 0.817 \times (a) \qquad r^{2} = 0.953$$

$$\log(P)_{(50^{\circ}C)} = -11.257 + 0.590 \times (a) \qquad r^{2} = 0.992$$

From the permeance data presented it becomes evident that the permeance constant is dependent on vapor activity, with the permeance values increasing with and increase in vapor activity level. However, the relationship was not linear in all cases, as shown by the range of correlation coefficient values, $r^2 = 0.66$ to 0.99. The log(P) vs. (a) plot exhibited varying concentration dependency characteristics, depending on the nature of both the polymer structure and permeant. For example, the Saran coated OPP and Acrylic coated OPP structures displayed convex shaped curves to the activity axis. Polypropylene, had a higher overall permeance value than Saran coated OPP, and was much more concentration dependent. For the HDPE, OPP, and Saran coated OPP, at the higher permeant concentration levels, these films approached a similar permeance value. These results are quite similar to the results reported by Hagenbaugh (1987). Rogers (1964) described the variation of the permeability coefficient with organic permeant vapor

activity as an exponential function of vapor activity, where the log of P becomes progressively non-linear at higher vapor activities. Cutler et al., (1951) also pointed out that at very low vapor activities, the permeability can be reduced to a linear dependence on vapor pressure.

The (apparent) diffusion coefficient values, for the respective polymer film-organic vapor permeant combination, did not show a clear vapor concentration dependence (see Tables 2, 4, 6, 8, 10). While not fully understood, two possible explanations for the diffusion coefficient values showing less dependency on the contacting vapor concentration may be as following: First, the changing permeant concentration gradient in the polymer during the transient period. The half-time diffusion method, as applied in the present study, assumes the diffusion coefficient is a constant with vapor concentration level (D = $I^2/7.2t_{1/2}$). Secondly, according to Fick's second law equation $([\partial c/\partial t] =$ $D[\partial^2 c/\partial x^2]$), the diffusion coefficient is a constant independent of concentration, space coordinate, and time in an isotropic continuum. However, for many penetrant-polymer systems, D is not a constant but rather is a function of concentration, or in some cases spatial coordinates and or/ the lapsed time since diffusion started (Rogers, 1985).

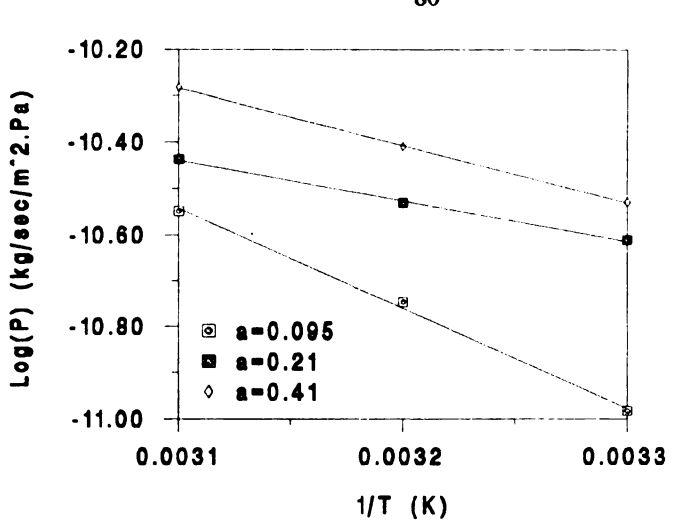


Figure 21. Temperature dependence of permeance for ethylacetate in high density polyethylene

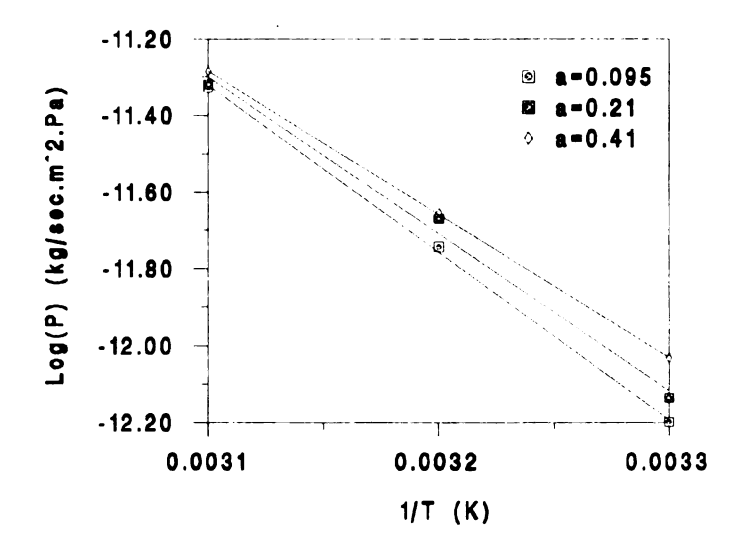


Figure 22. Temperature dependence of permeance for ethyl acetate in oriented polypropylene

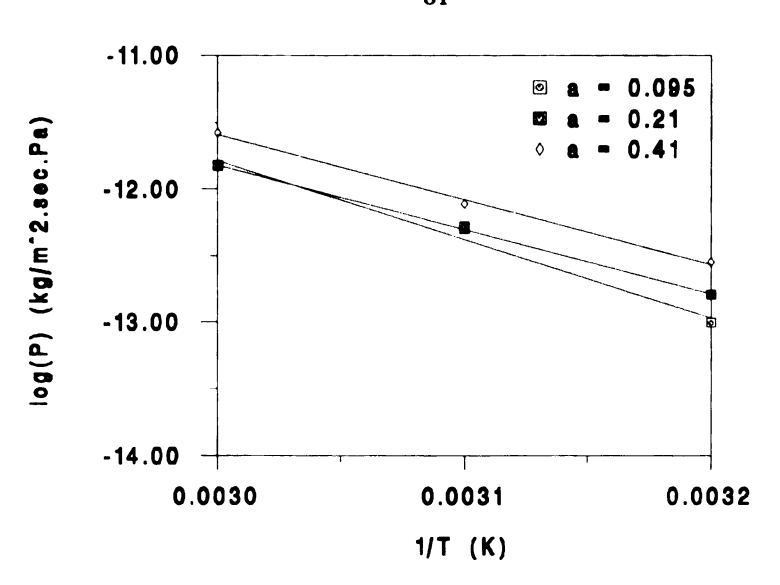


Figure 23. Temperature dependence of permeance for ethyl acetate in Saran coated OPP

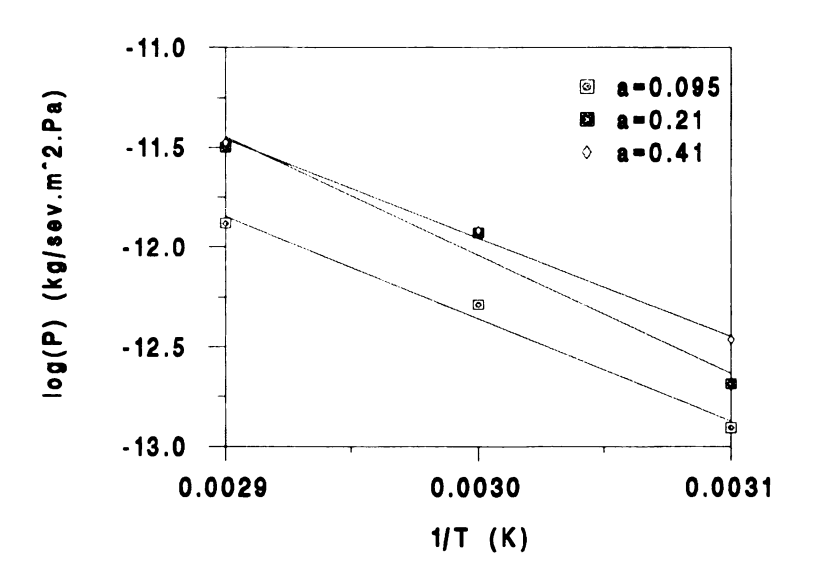


Figure 24. Temperature dependence of permeance for ethyl acetate in Acrylic coated OPP

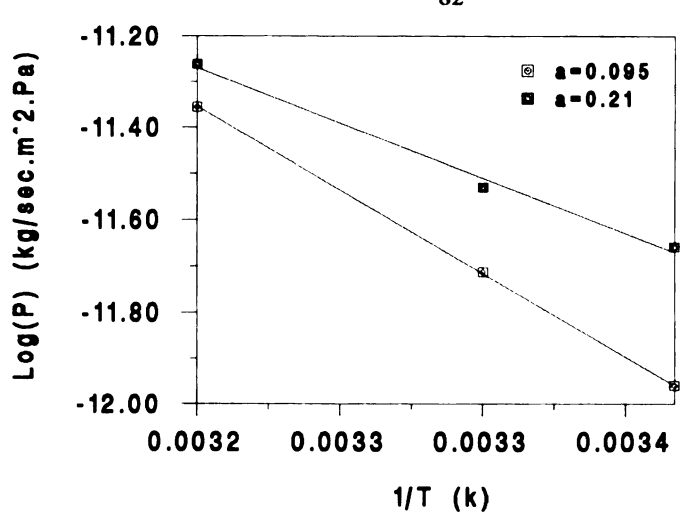


Figure 25. Temperature dependence of permeance for ethyl acetate in Glassine

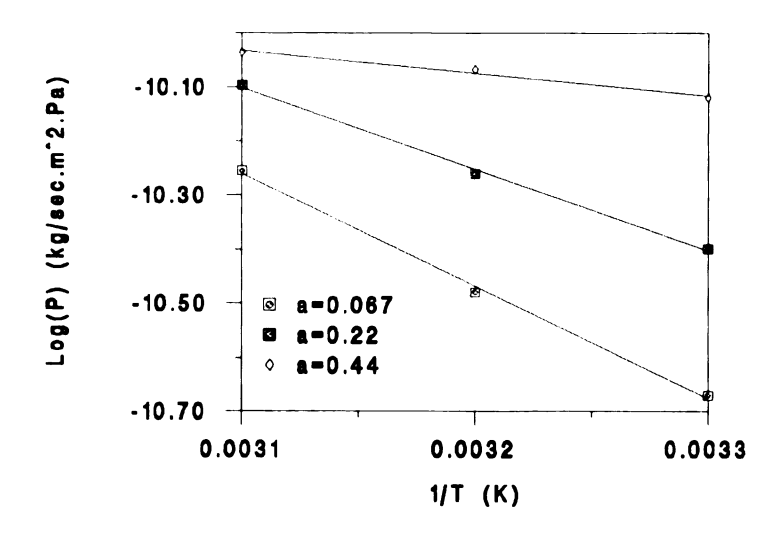


Figure 26. Temperature dependence of permeance for toluene in high density polyethylene

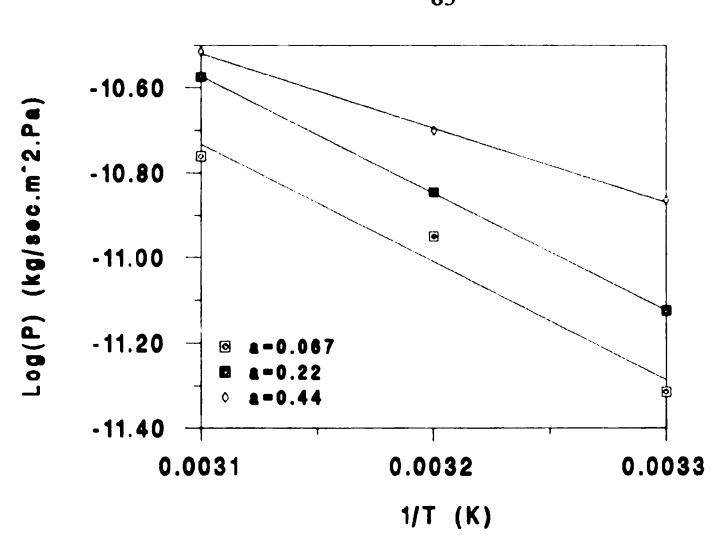


Figure 27. Temperature dependence of permeance for toluene in oriented polypropylene

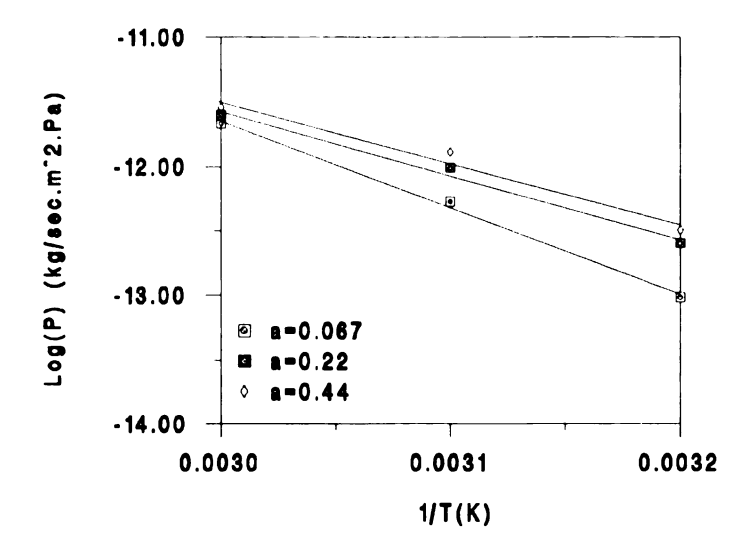


Figure 28. Temperatured dependence of permeance for toluene in Saran coated OPP

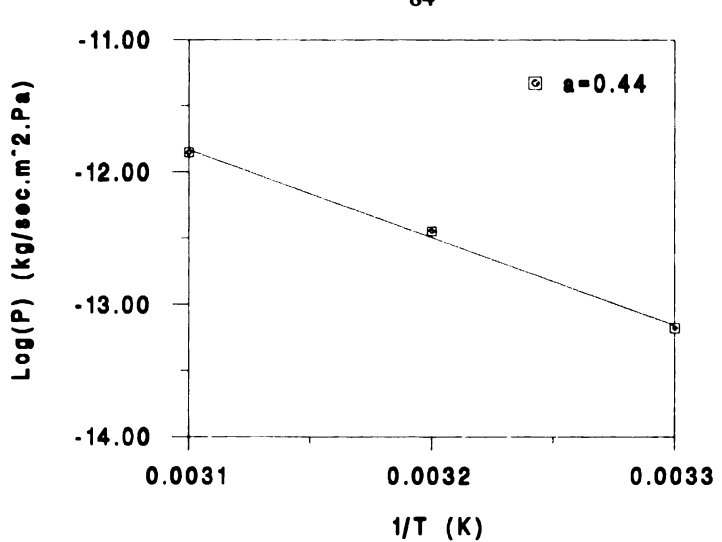


Figure 29. Temperature dependence of permeance for toluene in Acrylic coated OPP

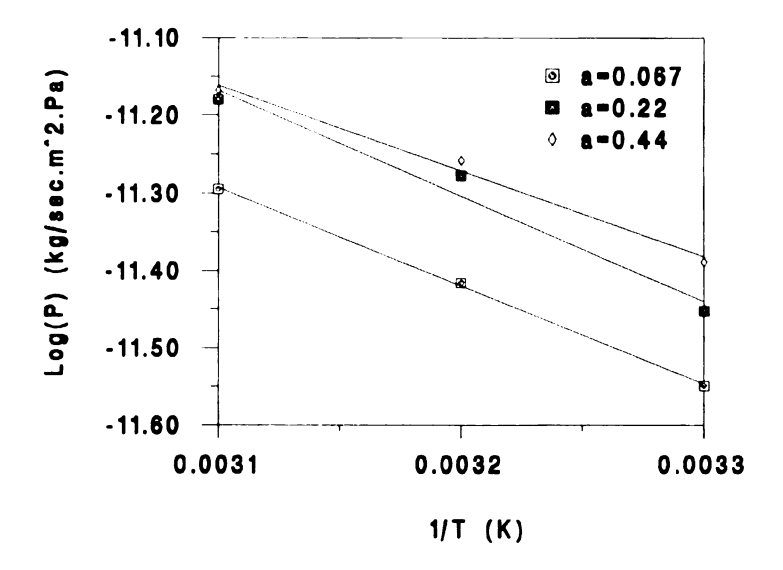


Figure 30. Temperature dependence of Permeance for toluene in Glassine

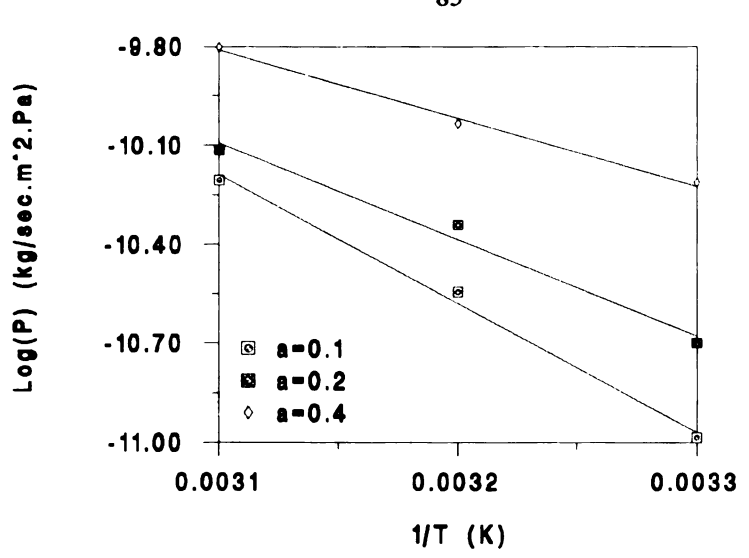


Figure 31. Temperature dependence of permeance for limonene in high density polyethylene

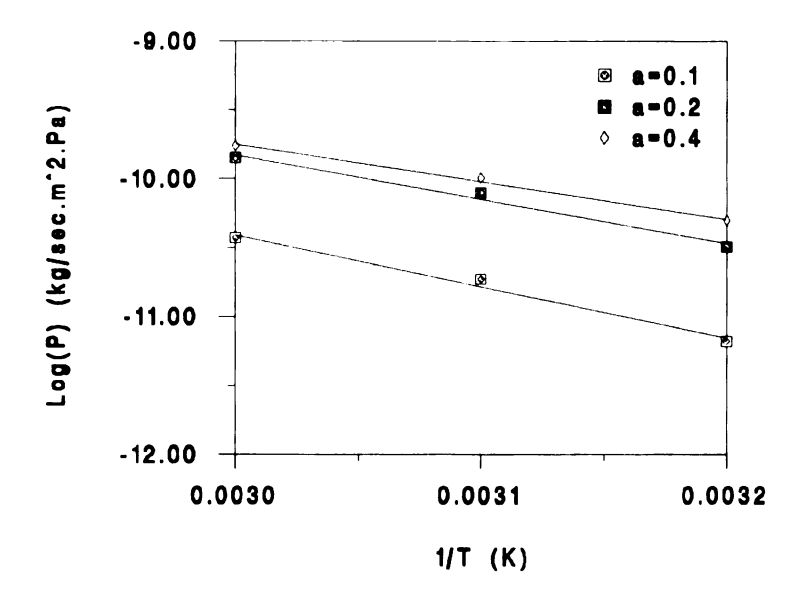


Figure 32. Temperature dependence of permeance for limonene in oriented polypropylene

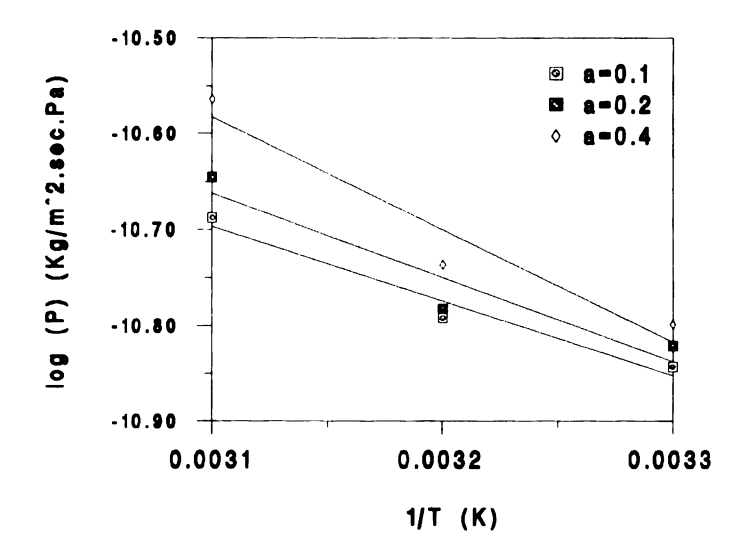


Figure 33. Temperature dependence of permeance for limonene in Glassine

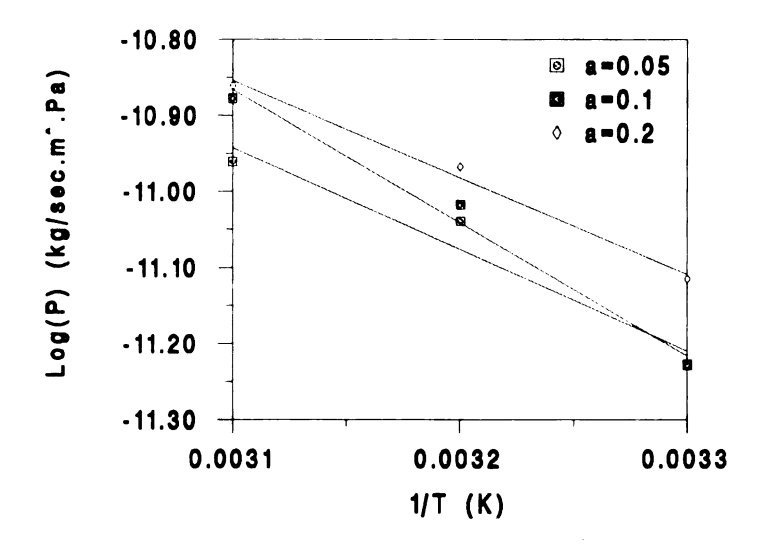


Figure 34. Temperature dependence of permeance for methyl ethyl ketone in high density polyethylene

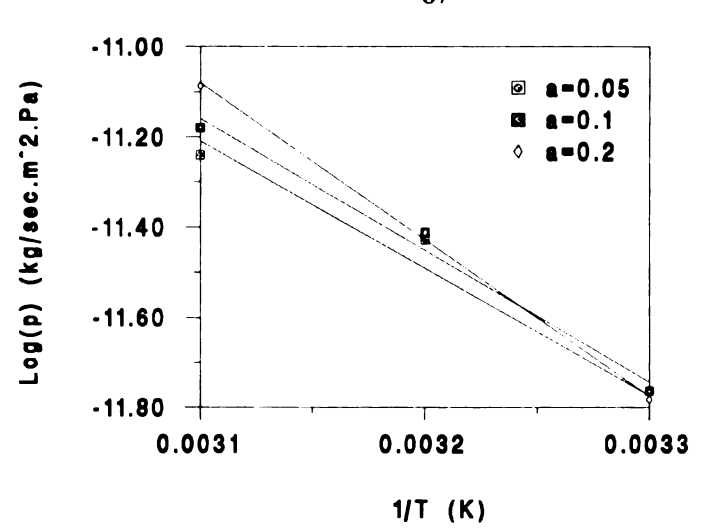


Figure 35. Temperature dependence of permeance for methyl ethyl ketone in oriented polypropylene

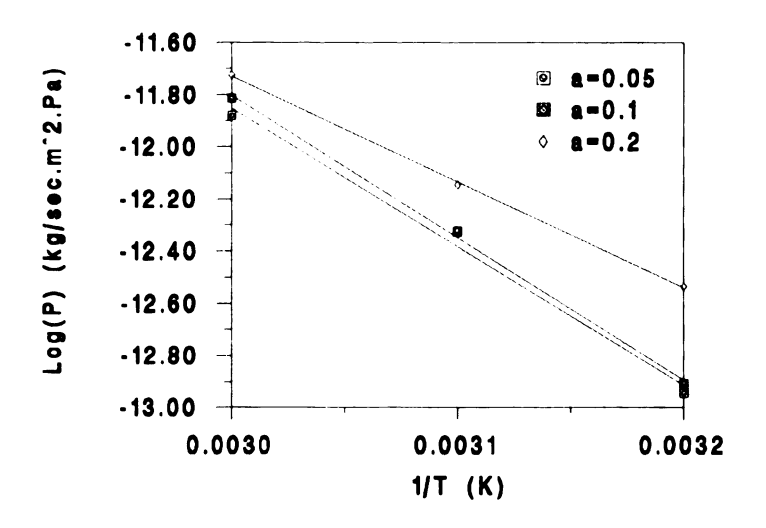


Figure 36. Temperature dependence of permeance for methyl ethyl ketone in Saran coated OPP

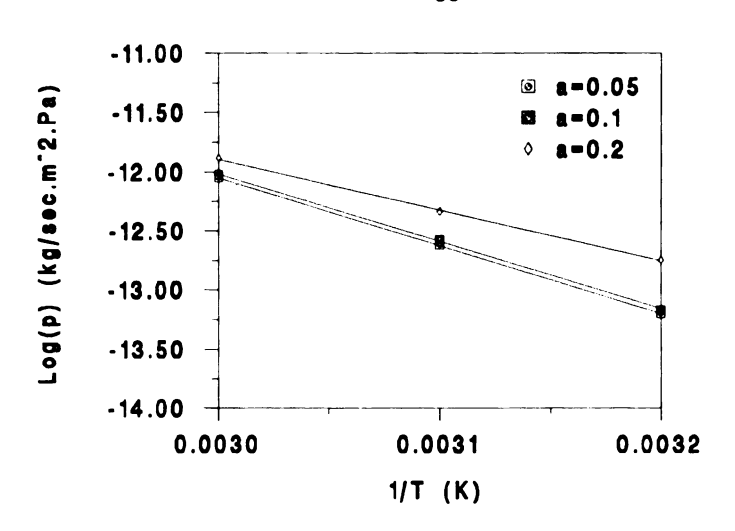


Figure 37. Temperature dependence of permeance for methyl ethyl ketone in Acrylic coated OPP

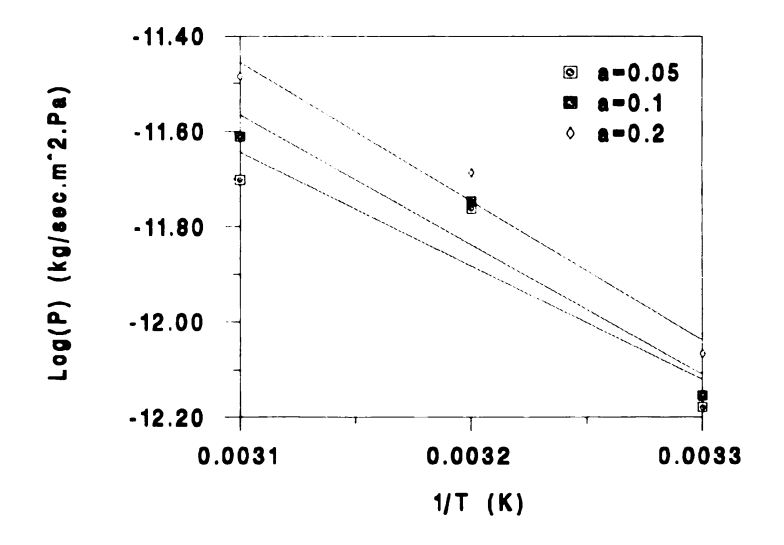


Figure 38. Temperature dependence of permeance for methyl ethyl ketone in Glassine



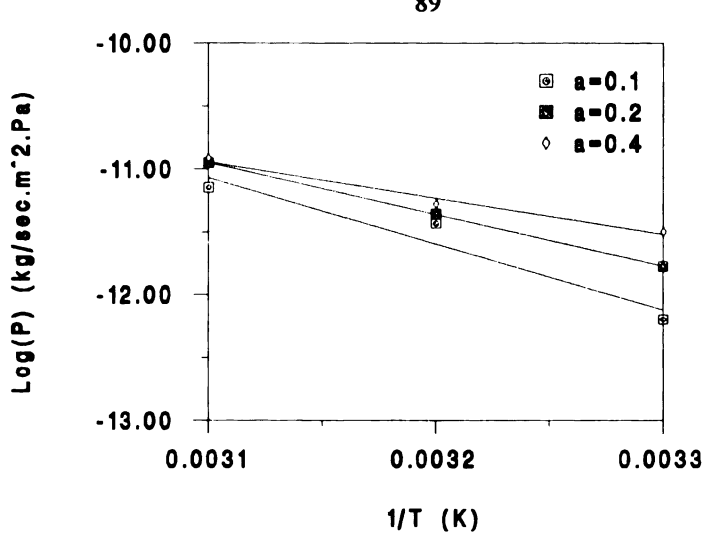


Figure 39. Temperature dependence of permeance for pinene in high density polyethylene

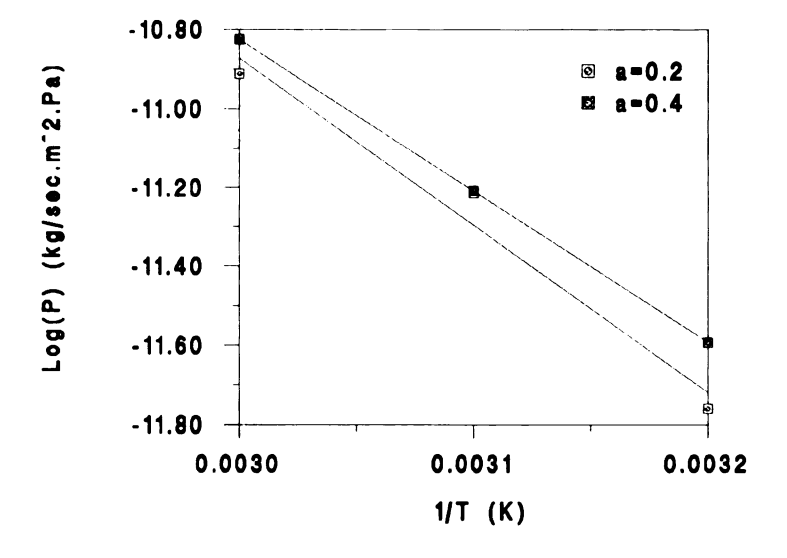


Figure 40. Temperature dependence of permeance for pinene in oriented polypropylene

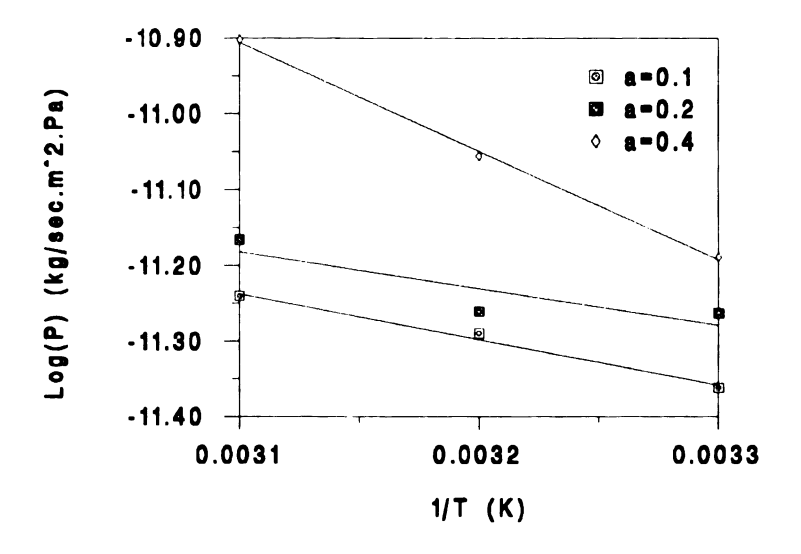


Figure 41. Temperature dependence of permeance for pinene in Glassine

From the permeability parameters values summarized in Tables 1 to 10, it becomes evident that permeance and diffusion coefficient values are highly dependent on temperature, at a constant vapor activity level. The temperature dependence of the permeance values is illustrated in Figures 23 - 44, where the log of the permeance constant is plotted as a function of the reciprocal of absolute temperature (°K), for studies carried out on the test films and the respective penetrant vapors. The following expressions were derived using a least squares fit and were found to be:

For the permeability of ethyl acetate vapor through the test polymer structures, the relationship between the permeance values (P) and temperature (1/T) was found to be:

HDPE	log(P) _(a=0.095)	= -	$-3.814 - 2170 \times (1/T)$	$\mathbf{r}^2 = 0$	0.998
	log(P) _(a=0.21)	=	-7.723 - 876×(1/T)	r ² =	0.998
	log(P) _(a=0.41)	=	-6.461 - 1233×(1/5	$r^2 =$	0.999
OPP	log(P) _(a=0.095)	=	2.194 - 4360×(1/T	$r^2 = 0$	0.998
	log(P) _(a=0.21)	=	1.375 - 4088×(1/5	$r^2 =$	0.994
	log(P) _(a=0.41)	=	2.980 - 3736×(1/5	$r^2 =$	1.000
Saran- OPP	log(P) _(a=0.095)	=	4.378 - 5378×(1/T	$r^2 = 0$	0.998
Off	log(P) _(a=0.31)	=	3.296 - 5021×(1/5	$r^2 =$	0.999
	log(P) _(a=0.41)	=	3.379 - 4970×(1/5	$r^2 =$	0.999
Acrylic-	log(P) _(a=0.095)	=	3.470 - 5259×(1/T	$r^2 = 0$	0.987

$$\log(P)_{(a=0.21)} = 6.229 - 6072 \times (1/T) \qquad r^2 = 0.975$$

$$\log(P)_{(a=0.41)} = 3.343 - 5028 \times (1/T) \qquad r^2 = 0.996$$
Glassine
$$\log(P)_{(a=0.095)} = 0.223 - 3618 \times (1/T) \qquad r^2 = 1.000$$

$$\log(P)_{(a=0.21)} = -3.598 - 2397 \times (1/T) \qquad r^2 = 0.993$$

For the permeability of toluene vapor through the test polymer structures, the relationship between the permeance value(P) and reciprocal temperature(1/T) was found to be:

HDPE
$$\log(P)_{(a=0.067)} = -3.320 - 2216 \times (1/T)$$
 $r^2 = 0.998$ $\log(P)_{(a=0.22)} = -4.896 - 1654 \times (1/T)$ $r^2 = 0.998$ $\log(P)_{(a=0.44)} = -8.233 - 555 \times (1/T)$ $r^2 = 0.986$ OPP $\log(P)_{(a=0.067)} = -1.635 - 2911 \times (1/T)$ $r^2 = 0.971$ $\log(P)_{(a=0.22)} = -1.534 - 2891 \times (1/T)$ $r^2 = 1.000$ $\log(P)_{(a=0.44)} = -4.584 - 1889 \times (1/T)$ $r^2 = 0.999$ Saran-OPP $\log(P)_{(a=0.22)} = 3.346 - 4944 \times (1/T)$ $r^2 = 0.993$ $\log(P)_{(a=0.44)} = 3.253 - 4887 \times (1/T)$ $r^2 = 0.993$ $\log(P)_{(a=0.44)} = 3.253 - 4887 \times (1/T)$ $r^2 = 0.978$ Acrylic- $\log(P)_{(a=0.44)} = 8.118 - 6838 \times (1/T)$ $r^2 = 0.997$ Glassine $\log(P)_{(a=0.44)} = -6.854 - 1409 \times (1/T)$ $r^2 = 0.999$ $\log(P)_{(a=0.44)} = -6.854 - 1501 \times (1/T)$ $r^2 = 0.999$ $\log(P)_{(a=0.44)} = -7.234 - 1242 \times (1/T)$ $r^2 = 0.999$

For the permeability of limonene vapor through the test polymer structures, the relationship between the permeance value(P) and reciprocal temperature(1/T) was found to be:

HDPE
$$log(P)_{(a=0.1)} = 2.367 - 4039 \times (1/T)$$
 $r^2 = 0.995$

$$\log(P)_{(a=0.2)} = -0.543 - 3069 \times (1/T) \qquad r^2 = 0.985$$

$$\log(P)_{(a=0.4)} = -2.968 - 2196 \times (1/T) \qquad r^2 = 0.995$$

$$\log(P)_{(a=0.1)} = 0.862 - 3756 \times (1/T) \qquad r^2 = 0.985$$

$$\log(P)_{(a=0.2)} = -0.165 - 3221 \times (1/T) \qquad r^2 = 0.985$$

$$\log(P)_{(a=0.4)} = -1.583 - 2732 \times (1/T) \qquad r^2 = 0.994$$

$$Glassine \qquad \log(P)_{(a=0.1)} = -7.820 - 916 \times (1/T) \qquad r^2 = 0.973$$

$$\log(P)_{(a=0.2)} = -7.470 - 1018 \times (1/T) \qquad r^2 = 0.929$$

$$\log(P)_{(a=0.4)} = -6.476 - 1313 \times (1/T) \qquad r^2 = 0.945$$

For the permeability of methyl ethyl ketone vapor through the test polymer structures, the relationship between the permeance value(P) and reciprocal temperature(1/T) was found to be:

HDPE
$$\log(P)_{(a=0.05)} = -6.376 - 1477 \times (1/T)$$
 $r^2 = 0.958$ $\log(P)_{(a=0.1)} = -6.177 - 1520 \times (1/T)$ $r^2 = 1.000$ $\log(P)_{(a=0.2)} = -6.486 - 1413 \times (1/T)$ $r^2 = 0.993$ OPP $\log(P)_{(a=0.05)} = -2.045 - 2960 \times (1/T)$ $r^2 = 0.968$ $\log(P)_{(a=0.1)} = -1.799 - 3025 \times (1/T)$ $r^2 = 0.987$ $\log(P)_{(a=0.2)} = -0.309 - 3480 \times (1/T)$ $r^2 = 1.000$ Saran- $\log(P)_{(a=0.05)} = 4.522 - 5457 \times (1/T)$ $r^2 = 0.992$ $\log(P)_{(a=0.1)} = 5.003 - 5601 \times (1/T)$ $r^2 = 0.998$ $\log(P)_{(a=0.2)} = 1.354 - 4359 \times (1/T)$ $r^2 = 1.000$ Acrylic- $\log(P)_{(a=0.05)} = 5.583 - 5886 \times (1/T)$ $r^2 = 1.000$ $\log(P)_{(a=0.1)} = 5.457 - 5839 \times (1/T)$ $r^2 = 0.999$

$$\log(P)_{(a=0.2)} = 1.327 - 4422 \times (1/T) \qquad r^2 = 0.999$$
Glassine
$$\log(P)_{(a=0.05)} = -4.259 - 2382 \times (1/T) \qquad r^2 = 0.843$$

$$\log(P)_{(a=0.1)} = -3.146 - 2716 \times (1/T) \qquad r^2 = 0.923$$

$$\log(P)_{(a=0.2)} = -2.445 - 2907 \times (1/T) \qquad r^2 = 0.970$$

For the permeability of α -pinene vapor through the test polymer structures, the relationship between the permeance value(P) and reciprocal temperature(1/T) was found to be:

HDPE
$$\log(P)_{(a=0.1)} = 5.210 - 5251 \times (1/T)$$
 $r^2 = 0.937$ $\log(P)_{(a=0.2)} = 1.769 - 4099 \times (1/T)$ $r^2 = 0.999$ $\log(P)_{(a=0.4)} = -1.956 - 2900 \times (1/T)$ $r^2 = 0.981$ OPP $\log(P)_{(a=0.2)} = 1.833 - 4235 \times (1/T)$ $r^2 = 0.974$ $\log(P)_{(a=0.4)} = 0.677 - 3834 \times (1/T)$ $r^2 = 1.000$ Glassine $\log(P)_{(a=0.1)} = -8.888 - 747 \times (1/T)$ $r^2 = 0.992$ $\log(P)_{(a=0.2)} = -9.214 - 623 \times (1/T)$ $r^2 = 0.845$ $\log(P)_{(a=0.4)} = -8.580 - 781 \times (1/T)$ $r^2 = 0.792$

As can be seen, the temperature dependency of the transport process associated with the respective barrier membranes, over the temperature range studied, follows well the Van't Hoff-Arrhenius relationship as given by

$$P = P_0 \exp\left(-\frac{E_p}{RT}\right)$$
 (23)

From the general Arrhenius equation :

$$P = P_0 \exp \left(-\frac{E_p}{RT} \right)$$

$$log(P) = -\frac{E_p}{2.3 R} \times \frac{1}{T} + log(P_0)$$
 (37)

$$slope = \frac{E_p}{2.3 R}$$
 (38)

From the slope of the Arrhenius plots, the activation energy for the permeation process (E_p) was determined for the respective film samples, as a function of vapor activity. The determined activation energy values are summarized in Tables 11 - 15.

Table 11. Activation energy values for the permeation of ethyl acetate through polymer membranes

	E (Kj/mole)		
Polymer Membranes	a=0.095	a=0.21	a=0.41
HDPE	41.50	35.87	23.59
OPP	83.38	78.18	71.44
Saran OPP	102.84	96.02	95.04
Acrylic OPP	100.57	116.11	97.18
Glassine	69.19	45.84	M ⁽²⁾
Met PET/OPP	N/A ⁽¹⁾	N/A ⁽¹⁾	N/A ⁽¹⁾

⁽¹⁾ N/A denotes not available

⁽²⁾ Missing data

Table 12. Activation energy values for the permeation of toluene through polymer membranes

	E (Kj/mole)			
Polymer Membranes	a=0.067	a=0.22	a=0.44	
HDPE	42.38	31.63	10.62	
OPP	55.67	55.28	36.12	
Saran OPP	132.50	94.54	93.45	
Acrylic OPP	N/A ⁽¹⁾	N/A ⁽¹⁾	130.76	
Glassine	26.94	28.70	23.75	
Met PET/OPP	N/A ⁽¹⁾	N/A ⁽¹⁾	N/A ⁽¹⁾	

⁽¹⁾ N/A denotes not available.

Table 13. Activation energy values for the permeation of limonene through polymer membranes

	E (Kj/mole)			
Polymer Membranes	a=0.1	a=0.2	a=0.4	
HDPE	77.24	58.69	41.99	
OPP	71.83	61.60	52.24	
Saran OPP	N/A ⁽¹⁾	N/A ⁽¹⁾	N/A ⁽¹⁾	
Acrylic OPP	N/A ⁽¹⁾	N/A ⁽¹⁾	N/A ⁽¹⁾	
Glassine	17.52	19.47	25.11	
Met PET/OPP	N/A ⁽¹⁾	N/A ⁽¹⁾	N/A ⁽¹⁾	

⁽I) N/A denotes not available.

Table 14. Activation energy values for the permeation of methyl ethyl ketone through polymer membranes

	E (Kj/mole)			
Polymer Membranes	a=0.05	a=0.1	a=0.2	
HDPE	27.67	29.07	27.02	
OPP	56.60	57.85	66.55	
Saran OPP	104.35	107.11	83.36	
Acrylic OPP	112.56	111.66	84.56	
Glassine	45.56	51.94	55.59	
Met PET/OPP	N/A ⁽¹⁾	N/A ⁽¹⁾	N/A ⁽¹⁾	

N/A denotes not available.

Table 15. Activation energy values for the permeation of $\alpha\text{-pinene}$ through polymer membranes

	E (Kj/mole)			
Polymer Membranes	a=0.1	a=0.2	a=0.4	
HDPE	100.42	78.39	55.46	
OPP	N/A ⁽¹	80.99	73.32	
Saran OPP	N/A ⁽¹⁾	N/A ⁽¹⁾	N/A ⁽¹⁾	
Acrylic OPP	N/A ⁽¹⁾	N/A ⁽¹⁾	N/A ⁽¹⁾	
Glassine	14.27	11.91	14.26	
Met PET/OPP	N/A ⁽¹⁾	N/A ⁽¹⁾	N/A ⁽¹⁾	

⁽¹⁾ N/A denotes not available.

The results described above for the respective organic penetrants studied show that the temperature dependency of the transport process associated with the barrier membranes evaluated, was described by the Arrhenius expression.

The Arrhenius expression used to describe the permeance as a function of temperature is typically applied over a temperature range either above or below the glass transition temperature (T_q) of the polymer membrane, but not within a temperature range which includes T_q. DeLassus et al., (1988) and Begley et al., (1990) indicated that a straight line extrapolation typically cannot be made through T_q and a graphical analysis is expected to show a change in slope at the T_{α} . Since the glass transition temperatures of polyethylene ($T_g = -125$ °C), polypropylene ($T_g = -19$ °C), and Saran ($T_q = -18$ °C) (Polymer Hanhbook) are below the minimum temperature evaluated, and the $T_{\rm q}$ value of PET ($T_{\rm q}=$ 81°C) is above the maximum temperature evaluated in the present study, the T_q of the respective test structures was therefore assumed not to be of concern and the Arrhenius analysis is expected to be linear.

Activation energy values for the respective test structure/permeant vapor combinations indicated that for both oriented polypropylene and high density polyethylene, activation energy values decreased with an increase in vapor

activity, while the activation energy values for the Saran and Acrylic coated polypropylene structures were not greatly affected by permeant vapor activity levels. The activation energy values for Glassine appeared to be unaffected by vapor concentration levels for the organic permeants, toluene and α -pinene, but were found to increase with vapor concentration level increases for the permeants, limonene and methyl ethyl ketone.

While not fully understood, the concentration dependency of the activation energy for the polyolefins may be due in part to penetrant-induced relaxation effects occurring within the polymer matrix. Such relaxation effects would be most favorable above the glass transition temperature (T_{σ}) of the polymer membrane, which is the case for PE and OPP. The absorption of organic vapors can result in polymer swelling and thus change the conformation of the polymer chain. These conformational changes are not instantaneous, but are controlled by the retardation time of polymer chains. If these time is long, stresses may be set up which relax slowly. Thus the absorption and diffusion of organic vapors can be accompanied by concentration as well as timedependent processes within the polymer bulk phase, which are slower than the micro-Brownian motion of polymer chain segments which promote diffusion (Mears, 1965).

There is precedence in the literature in support of such long period relaxation effects occurring in polymer films above their glass transition temperature (Berens, 1977 and Blackadder and Keniry, 1937). Thus there may be concentration dependent relaxation effects occurring during the diffusion of organic penetrants through the polyolefin films investigated. Such relaxation processes which occur over a longer time-scale than diffusion may be related to a structural reordering of the free volume elements in the polymer. Thus, providing additional sites of appropriate size and frequency of formation, which promote diffusion and may account for the observed decrease in activation energy with an increase in vapor activity.

Moisan (1985) has suggested that the activation energy can be considered as the energy required to loosen the molecular chain for a given distance. This involves the cohesive energy of the chain segment which, like the heat of vaporization is dependent on the temperature. That is why an increase in temperature provides energy to increase segmental mobility which results in an increase in penetrant diffusion rate. Prager (1951) proposed that, when the chemical nature of both the penetrant and polymer are not too different, the fraction of penetrant-polymer contacts should be proportional to concentration. If these contacts are weaker than polymer-polymer contacts, the energy

required for a diffusive jump should decrease linearly with increasing concentration. This might explain the observed decrease in the activation energy, with an increase in the penetrant concentration level, for ethyl acetate, toluene and limonene through high density polyethylene and oriented polypropylene.

From this study, the metallized PET/OPP based structure was found to have the best organic vapor barrier property among the six polymer films evaluated.

Estimation of permeance values at vapor activity levels impractical to measure experimentally

Knowledge of the temperature and concentration dependence of the mass transfer process provides a means of estimating the permeance of the barrier membranes, at organic vapor concentration levels below which it would be impractical to measure experimentally. As discussed above, by application of the Arrhenius equation, expressions describing the relationship between permeance and temperature were derived for the respective penetrant vapor activity levels evaluated. The permeability data obtained for limonene vapor, serves to illustrate how permeance values can be estimated at vapor concentration levels not measurable experimentally.

Based on the linear Arrhenius expressions derived, permeance values at ambient temperature (24°C) were estimated for each individual vapor activity. Table 16 summarizes the calculated permeance values at 24°C, for the respective packaging structures evaluated, at three vapor activity levels. Permeance values varied as a function of the vapor activity levels.

Table 16. Estimated permeance values of test packaging structures for limonene at 24°C (based on Arrhenius Equation)

-		$P(\frac{Kg}{m^2.sec.Pa})$)
Vapor activity	HDPE	OPP	Glassine
0.1	5.86 × 10-12	1.64 × 10-12	1.25 × 10-11
0.2	1.33 × 10-11	9.77×10^{-12}	1.26×10^{-11}
0.4	4.35×10^{-11}	1.65×10^{-11}	1.27×10^{-11}

The concentration dependency of the permeance values for the respective test structures at 24°C, is presented graphically in Figure 45, where the permeance values are plotted as a function of vapor activity. The relationship between the permeance constants and vapor activity, for the

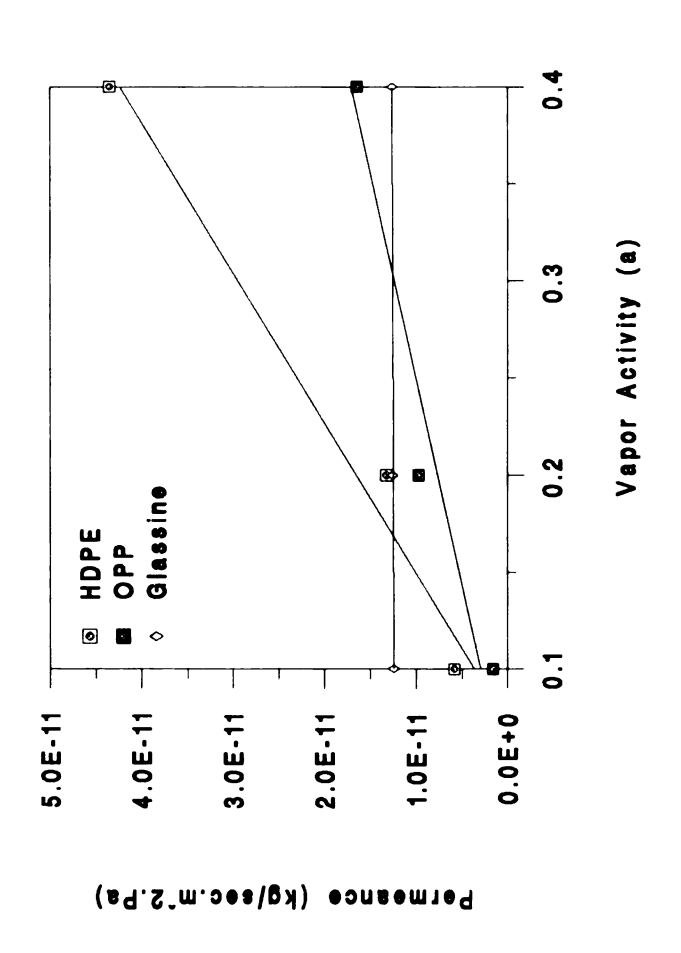


Figure 42. The effect of limonene vapor activity on permeance for different polymer structures at $24\ \text{C}$

respective films evaluated at 24°C, can be described by the following expressions, derived from a least squares fit.

HDPE
$$P = -9.24 \times 10^{-12} + 1.29 \times 10^{-10} (a)$$
 $r^2 = 0.979$

OPP
$$P = -1.72 \times 10^{-12} + 4.73 \times 10^{-11} (a)$$
 $r^2 = 0.941$

Glassine
$$P = 1.25 \times 10^{-11} + 6.43 \times 10^{-13} (a)$$
 $r^2 = 0.964$

Assuming these expressions are valid over a broad range of vapor activity levels, permeance values at limonene vapor concentrations, not measurable experimentally, can be readily estimated by substitution into the appropriate equation.

Permeation Study of Packaging Films by a Quasi-isostatic Procedure

A limited number of penetrant/polymer film combinations were studied using the quasi-isostatic procedure and test apparatus described in the Materials and Methods Section.

Studies were carried out at 24±1°C and at one vapor activity level per permeant vapor. Vapor activity levels ranged from 0.05 to 0.4 depending upon the specific penetrant.

Representative transmission rate profile curves for high density polyethylene, oriented polypropylene, Saran-coated OPP, Acrylic coated OPP and Glassine are presented in Figures 43 - 47, where the total quantity permeated is plotted as a function of time.

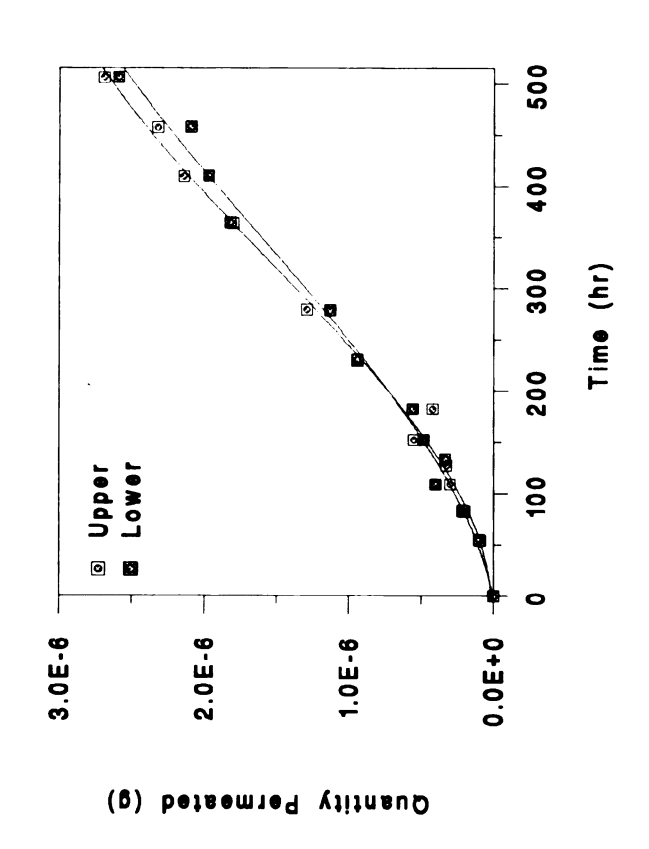


Figure 43. Permeation rate curve of limenene through Saran coated OPP at a=0.4

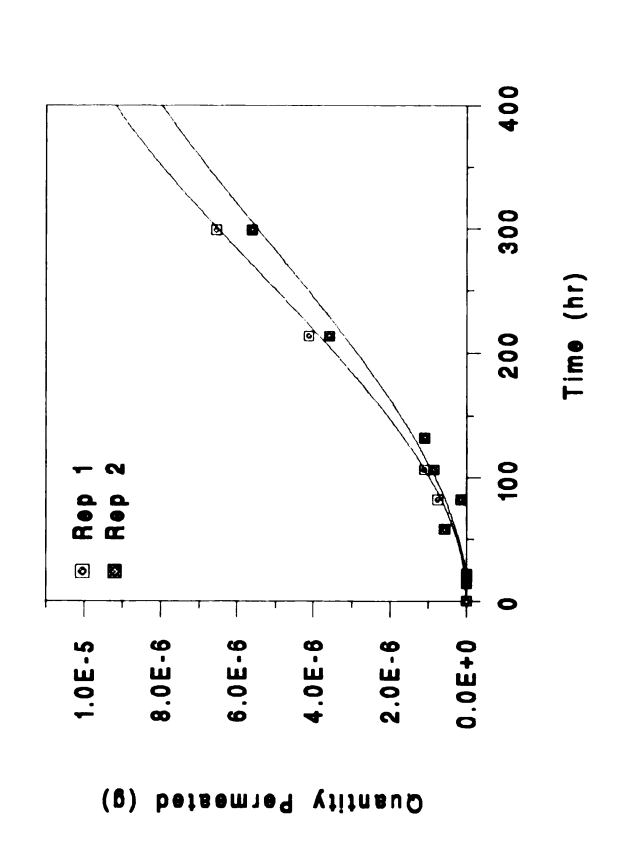


Figure 44. Permeation rate curve of pinene through Acrylic coated OPP at a=0.4

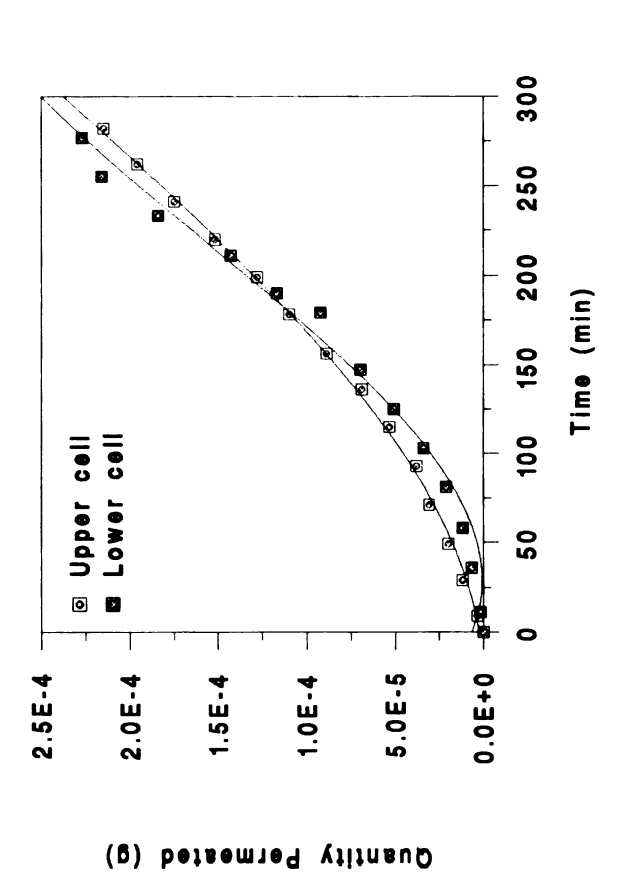


Figure 45. Permeation rate curve of ethyl acetate through Glassine at a=0.05

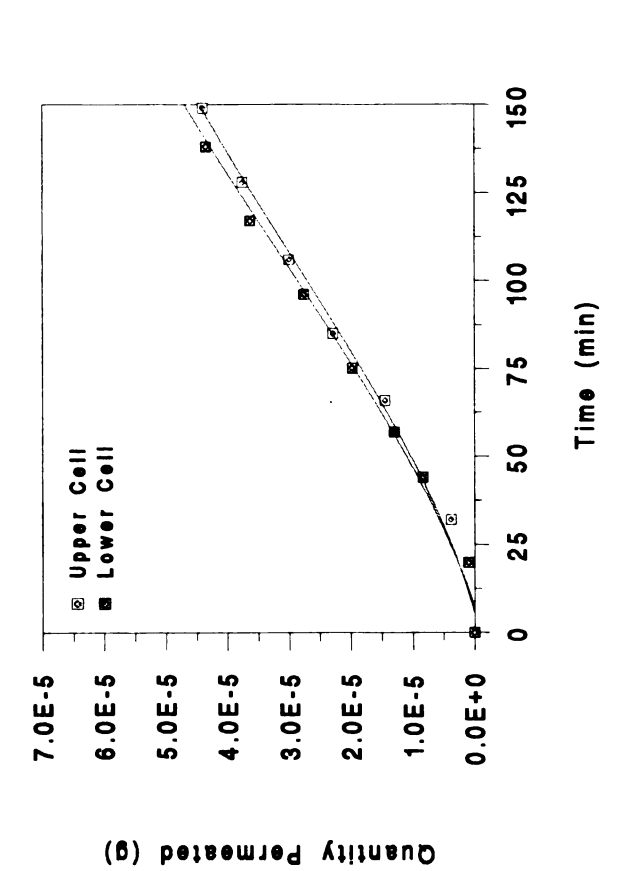


Figure 46. Permeation rate curve of toluene through high density polyethylene at a=0.05

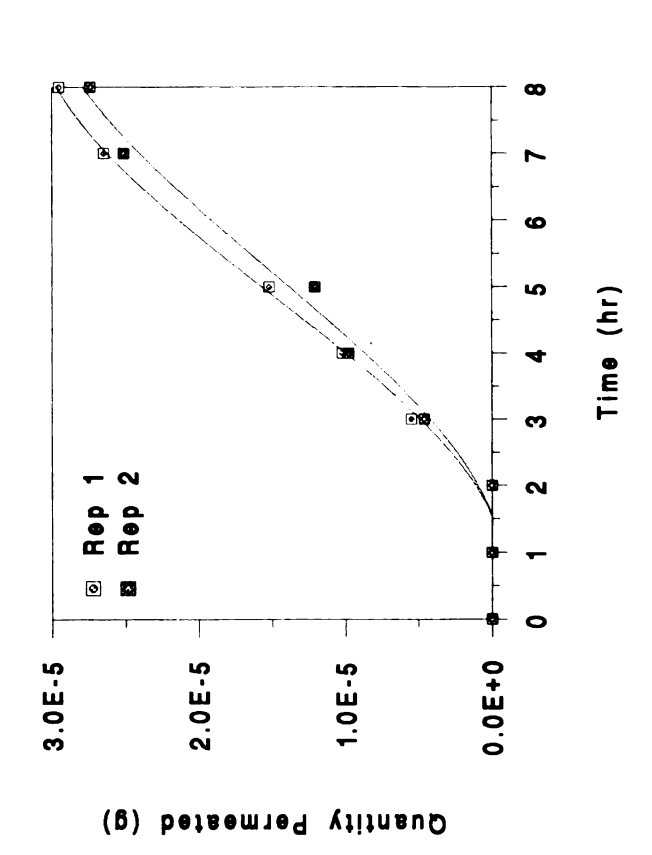


Figure 47. Permeation rate curve of methyl ethyl ketone through oriented polypropylene at a=0.05 $\,$

As shown, the permeation behavior of the respective films had, as predicted by theory, an initial induction period, followed by a non-steady state rate of diffusion, which preceded a steady state transmission rate. This characteristic transmission rate profile was observed for all of the penetrant/polymer combinations evaluated. For the low penetrant concentrations used in these studies, it was considered appropriate to assume that the diffusion process was Fickian.

Since several of the packaging films evaluated are laminate or coated structures, which have different layer thickness and combinations of layers, the results were expressed as permeance values, kg/(sec.m².Pa). The permeability tests were terminated when the penetrant concentration levels in the down stream cell chamber was approximately 2% of the driving force concentration in the up stream cell chamber, for activity levels above a=0.1. For driving force concentration levels below a=0.1, the down stream vapor concentration level did not exceed 5% of the up stream concentration at the time the test was terminated.

Expressions describing the steady state transmission rate were derived using a least square fit and applying experimental data and are summarized in Appendix C. The permeability parameters calculated from these data are summarized in Tables 17 - 21, respectively.

Table 17. Permeability parameters for high density polyethylene by quasi-isostatic procedure at 24° C

Permeant	Vapor Activity	Transmission Rate (g/min)	Permeance ^(a) (kg/m².sec.Pa)
Ethyl Acetate	0.05	1.4×10 ⁻⁶	7.4×10 ⁻¹²
		1.2×10 ⁻⁶	$(\pm 1.1 \times 10^{-14})$
Toluene	0.05	4.4×10 ⁻⁷	1.1×10 ⁻¹¹
		4.4×10^{-7}	$(\pm 4.6 \times 10^{-14})$
Limonene	0.1	3.8×10 ⁻⁹	1.3×10 ⁻¹²
		3.7×10^{-9}	$(\pm 6.0 \times 10^{-15})$
Methyl Ethyl	0.05	6.0×10 ⁻⁷	3.9×10 ⁻¹²
Ketone		5.9×10 ⁻⁷	$(\pm 4.2 \times 10^{-14})$
α- Pinene	0.1	4.0×10 ⁻⁹	1.5×10 ⁻¹³
		3.4×10^{-9}	$(\pm 1.2 \times 10^{-14})$

⁽a) Data reported as average ± average of absolute deviations from their mean.

Table 18. Permeability parameters for oriented polypropylene by quasi-isostatic procedure at 24° C

Permeant	Vapor Activity	Transmission Rate (g/hr)	Permeance ^(a) (kg/m².sec.Pa)
Ethyl Acetate	0.08	3.4×10 ⁻⁶	2.5×10 ⁻¹³
		4.9×10^{-6}	$(\pm 4.4 \times 10^{-14})$
Toluene	0.05	6.6×10 ⁻⁷	2.8×10 ⁻¹³
		6.8×10^{-7}	$(\pm 3.9 \times 10^{-14})$
Limonene	0.1	1.2×10 ⁻⁷	8.8×10 ⁻¹³
		1.8×10 ⁻⁷	$(\pm 1.8 \times 10^{-13})$
Methyl Ethyl	0.05	5.0×10 ⁻⁶	5.3×10 ⁻¹³
Ketone		4.8×10 ⁻⁶	$(\pm 1.1 \times 10^{-14})$
α-Pinene	0.2	6.8×10 ⁻⁷	2.4×10 ⁻¹³
		7.2×10^{-7}	$(\pm 6.2 \times 10^{-15})$

⁽a) Data reported as (average ± average of absolute deviations from their mean.

Table 19. Permeability parameters for Saran coated OPP by quasi-isostatic procedure at 24° C

Permeant	Vapor Activity	Transmission Rate (g/hr)	Permeance (a) (kg/m².sec.Pa)
Ethyl Acetate	0.2	6.2×10 ⁻⁷ 4.6×10 ⁻⁷	1.3×10^{-14} (± 1.9×10^{-15})
Toluene	0.2	9.9×10 ⁻⁸ 10.2×10 ⁻⁸	1.0×10 ⁻¹⁴ (± 1.8×10 ⁻¹⁶)
Limonene	0.4	6.0×10 ⁻⁹ 5.1×10 ⁻⁹	8.3×10^{-15} (± 6.5×10^{-16})
Methyl Ethyl Ketone	0.2	1.4×10 ⁻⁶ 1.9×10 ⁻⁶	4.5×10^{-14} (± 6.2×10^{-15})
α-Pinene	0.4	2.1×10 ⁻⁷ 2.0×10 ⁻⁷	3.6×10^{-14} (± 4.3×10^{-16})

 $^{^{(}a)}$ Data reported as average \pm average of absolute deviations from their mean.

Table 20. Permeability parameters for Acrylic coated OPP by quasi-isostatic procedure at 24° C

Permeant	Vapor Activity	Transmission Rate (g/hr)	Permeance (a) (kg/m².sec.Pa)
Ethyl Acetate	0.2	4.3×10 ⁻⁷	1.3×10 ⁻¹⁴
		6.5×10^{-7}	$(\pm 2.5 \times 10^{-15})$
Toluene	0.2	7.3×10 ⁻⁸	7.5×10 ⁻¹⁵
		7.3×10^{-8}	$(\pm 2.1 \times 10^{-17})$
Limonene	0.4	5.6×10 ⁻⁹	7.2×10 ⁻¹⁵
		4.1×10 ⁻⁹	$(\pm 1.1 \times 10^{-15})$
Methyl Ethyl	0.2	3.7×10 ⁻⁷	1.1×10 ⁻¹⁴
Ketone		4.2×10^{-7}	$(\pm 7.2 \times 10^{-16})$
α- Pinene	0.4	2.6×10 ⁻⁸	4.0×10 ⁻¹⁵
		2.1×10 ⁻⁸	$(\pm 4.5 \times 10^{-16})$

 $^{^{(}a)}$ Data reported as average \pm average of absolute deviations from their mean.

Table 21. Permeability parameters for Glassine by quasiisostatic procedure at 24° C

Permeant	Vapor Activity	Transmission Rate (g/min)	Permeance ^(a) (kg/m².sec.Pa)
Ethyl Acetate	0.05	1.0×10 ⁻⁶	6.0×10 ⁻¹²
		1.1×10 ⁻⁶	$(\pm 2.8 \times 10^{-13})$
Toluene	0.05	0.8×10^{-7}	2.5×10 ⁻¹²
		1.2×10 ⁻⁷	$(\pm 4.2 \times 10^{-13})$
Limonene	0.1	2.1×10 ⁻⁸	6.1×10^{-12}
		1.3×10 ⁻⁸	$(\pm 1.4 \times 10^{-12})$
Methyl Ethyl	0.05	1.4×10 ⁻⁷	7.9×10 ⁻¹³
Ketone		1.0×10 ⁻⁷	$(\pm 1.2 \times 10^{-13})$
α-Pinene	0.1	5.6×10 ⁻⁸	2.0×10 ⁻¹²
		4.0×10^{-8}	$(\pm 3.4 \times 10^{-13})$

⁽a) Data reported as average ± average of absolute deviations from their mean.

A Comparison of Organic Vapor Permeance Values by Isostatic and Quasi-isostatic Procedures

A comparison of the permeance values determined by the quasi-isostatic and isostatic test methods for ethyl acetate, toluene, limonene, methyl ethyl ketone, and α -pinene at 24°C is shown in Tables 22 - 26, respectively. For the high barrier Saran and Acrylic coated OPP structures, permeance values at ambient temperature (24°C) were estimated from the derived Arrhenius expressions. As shown by the overall consistency of the permeability data, an acceptable agreement was obtained between the permeance

values determined by the isostatic and quasi-isostatic procedures, for a broad range of barrier structures.

Table 22. A comparison of permeance values determined by isostatic and quasi-isostatic procedures for ethyl acetate at 24°C [Unit: kg/(m².sec.Pa)]

Film	Quasi-isostatic	Isostatic	Arrhenius	
	Method	Method	Estimation	
HDPE	7.4×10^{-12} (a=0.08)	7.5x 10 ⁻¹² (a=0.095)	7.6×10^{-12} (a=0.095)	
Oriented polypropylene	2.5×10^{-13} (a=0.08)	4.9×10^{-13} (a=0.095)	3.5×10^{-13} (a=0.095)	
Saran coated OPP	1.3×10^{-14} (a=0.2)	N/A ⁽¹⁾	2.5×10^{-14} (a=0.21)	
Acrylic coated OPP	1.3×10^{-14} (a=0.2)	N/A ⁽¹⁾	1.7 x 10 ⁻¹⁴ (a=0.21)	
Glassine	6.0×10^{-12} (a=0.05)	1.1×10^{-12} (a=0.095)	1.1 x 10 ⁻¹² (a=0.095)	

⁽¹⁾ No measurable level of permeation detected, run for 44 hr.

Table 23. A comparison of permeance values determined by isostatic and quasi-isostatic procedures for toluene at 24°C [Unit: kg/(m².sec.Pa)]

Film	Quasi-isostatic	Isostatic	Arrhenius
	Method	Method	Estimation
HDPE	1.1×10^{-11} (a=0.05)	1.6×10^{-11} (a=0.067)	1.7 x 10 ⁻¹¹ (a=0.067)
Oriented polypropylene	2.8×10^{-13} (a=0.05)	3.1×10^{-12} (a=0.067)	3.7×10^{-12} (a=0.067)
Saran coated OPP	1.0×10^{-14} (a=0.2)	N/A ⁽¹⁾	5.0×10^{-14} (a=0.22)
Acrylic coated OPP	7.5×10^{-15} (a=0.2)	N/A ⁽¹⁾	1.2×10^{-15} (a=0.44)
Glassine	2.5 x 10 ⁻¹² (a=0.05)	1.7×10^{-12} (a=0.067)	2.5×10^{-12} (a=0.067)

⁽¹⁾ No measurable level of permeation detected, run for 44 hr.

Table 24. A comparison of permeance values determined by isostatic and quasi-isostatic procedures for limonene at 24°C [Unit: kg/(m².sec.Pa)]

Film	Quasi-isostatic	Isostatic	Arrhenius
	Method	Method	Estimation
HDPE	1.3×10^{-12} (a=0.1)	6.9×10^{-12} (a=0.1)	5.9×10^{-12} (a=0.1)
Oriented polypropylene	8.8×10^{-13} (a=0.1)	N/A ⁽¹⁾	16.4×10^{-13} (a=0.1)
Saran coated OPP	8.3×10^{-15} (a=0.4)	N/A ⁽¹⁾	N/A ⁽¹⁾
Acrylic coated OPP	7.2×10^{-15} (a=0.4)	N/A ⁽¹⁾	N/A ⁽¹⁾
Glassine	6.2×10^{-12} (a=0.1)	13.0×10^{-12} (a=0.1)	12.4×10^{-12} (a=0.1)

⁽¹⁾ No measurable level of permeation detected, run for 44 hr.

Table 25. A comparison of permeance values determined by isostatic and quasi-isostatic procedures for methyl ethyl ketone at 24°C [Unit: kg/(m².sec.Pa)]

Film	Quasi-isostatic	Isostatic	Arrhenius
	Method	Method	Estimation
HDPE	3.9×10^{-12} (a=0.05)	3.7x 10 ⁻¹² (a=0.05)	4.5×10^{-12} (a=0.05)
Oriented polypropylene	5.3 x 10 ⁻¹³ (a=0.05)	6.9×10^{-13} (a=0.05)	9.7 x 10 ⁻¹³ (a=0.05)
Saran coated OPP	4.5×10^{-14} (a=0.2)	N/A ⁽¹⁾	4.8 x 10 ⁻¹⁴ (a=0.2)
Acrylic coated OPP	1.1×10^{-14} (a=0.2)	N/A ⁽¹⁾	2.7×10^{-14} (a=0.2)
Glassine	7.9×10^{-13} (a=0.05)	6.6×10^{-13} (a=0.05)	5.3 x 10 ⁻¹³ (a=0.05)

⁽¹⁾ No measurable level of permeation detected, run for 44 hr.

Table 26. A comparison of permeance values determined by isostatic and quasi-isostatic procedures for α -pinene at 24°C [Unit: kg/(m².sec.Pa)]

Film	Quasi-isostatic	Isostatic	Arrhenius
	Method	Method	Estimation
HDPE	1.5×10^{-13} (a=0.05)	N/A ⁽¹⁾	3.4×10^{-13} (a=0.05)
Oriented polypropylene	2.4×10^{-13} (a=0.2)	N/A ⁽¹⁾	3.8×10^{-13} (a=0.2)
Saran coated OPP	3.6×10^{-14} (a=0.2)	N/A ⁽¹⁾	N/A ⁽¹⁾
Acrylic coated OPP	4.0×10^{-15} (a=0.2)	N/A ⁽¹⁾	N/A ⁽¹⁾
Glassine	2.0×10^{-12} (a=0.05)	7.0×10^{-13} (a=0.05)	4.0×10^{-12} (a=0.05)

(1) No measurable level of permeation detected, run for 44 hr.

Evaluation of The Consistency of The Continuous Flow Permeability Data

The consistency of the results obtained for selected transmission rate data for limonene and α -pinene through OPP and HDPE was evaluated by the procedure of Gavara and Hernandez (1993). The constants K_1 and K_2 , calculated from the experimental data, are presented in Table 27 and were found to be within 7% of the theoretical values given in Eqn. 34 and 35. As previously described, the value of the permeation rate at any time (F_t) , during the unsteady state portion of the permeability experiment, varies from zero, at time equal to zero, up to the transmission rate value (F_{∞})

reached at the steady state. This is described by the following expression (Pasternak et al., 1970)

$$\frac{F_{t}}{F_{\infty}} = \phi = (\frac{4}{\sqrt{\pi}}) \left(\sqrt{\frac{l^{2}}{4 \text{ Dt}}} \right) \sum_{n=1,3,5...}^{\infty} \exp\left(\frac{-n^{2} l^{2}}{4 \text{ Dt}} \right)$$
 (32)

which can be simplified to

$$\frac{F_{r}}{F_{\infty}} = \phi = (\frac{4}{\sqrt{\pi}}) X^{1/2} \exp(-X)$$
 (33)

For the values of X (X = $I^2/4Dt$) in Eqn. 33, D is assumed to be concentration and time independent. By using a bisection method, values of X were calculated as a function of time, for ϕ = 0.1 to ϕ = 0.9. It was found that the maximum ϕ value was equal 0.968, and each X (when X < X_{0.968}) has two roots (far root and near root). However, only the far root of each X value could be fit to the transmission curve. The values of X determined are as follows: X_{0.1} = 3.7815, X_{0.2} = 2.9672, X_{0.25} = 2.6961, X_{0.3} = 2.4700, X_{0.4} = 2.1015, X_{0.5} = 1.8013, X_{0.6} = 1.5410, X_{0.7} = 1.3029, X_{0.75} = 1.1877, X_{0.8} = 1.0717, X_{0.9} = 0.8202.

Plots of 1/X as a function of time are shown in Figures 48, 50, 52, and 54 for the systems, limonene/HDPE, limonene/OPP, α -pinene/HDPE and α -pinene/OPP, respectively. The linear relationship between 1/X and time obtained for

		+
		·
		-
		a
		<u>.</u>
		5
		v
		:
		,
		,
		,

the respective penetrant/polymer membrane system indicated that the experimental data obtained are consistent with the assumptions of an ideal system and well controlled temperature and vapor concentration parameters. From the slope of the plots of 1/X versus time, values of $D_{0.1}$ to $D_{0.9}$ were determined, and an average diffusion coefficient value D (Dave) calculated. The resultant diffusion coefficient values (Dave) are summarized in Table 27. A parameter estimation procedure was also applied to determine the best estimated D value (Desti), which was based on a sum of squares technique. Figure 49, 51, 53, and 55 show the results of plots of sum of squares as a function of estimated D, for the test systems, limonene/HDPE, limonene/OPP, α -pinene/HDPE and α -pinene/OPP. The minimum value of D on the convex curve is assumed to be the best estimated D value (D_{esti}) . The estimated and the average diffusion coefficient values obtained for the respective penetrant/polymer membrane systems are presented in Table 27, and show the excellent agreement obtained. From the consistency analysis of the continuous flow permeability data, it can be concluded that the diffusion processes were Fickian and the parameters of the experiment were under control.

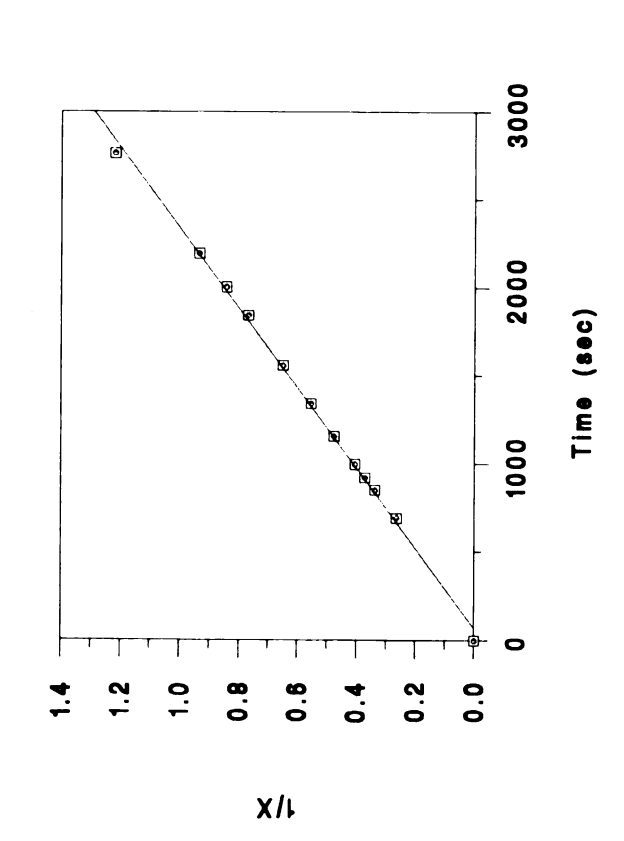
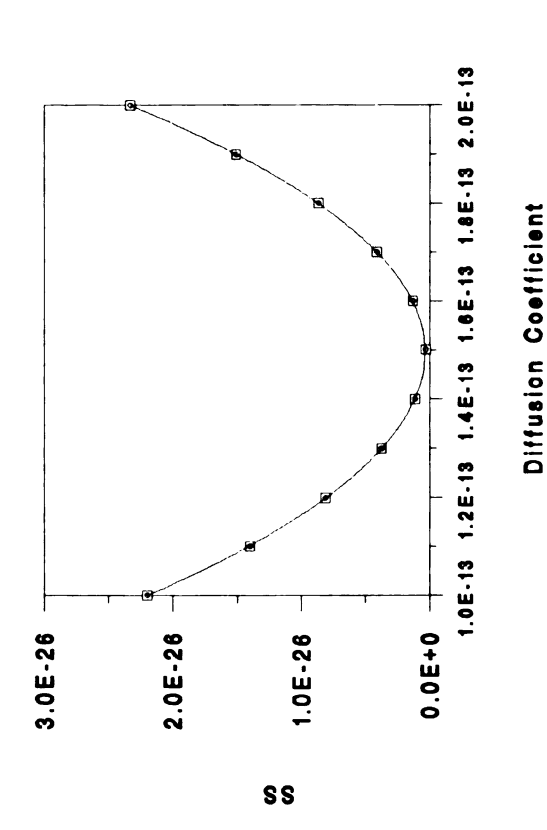


Figure 48. 1/X as a function of time for HDPE/limonene at a-0.4, T-50 C



Best estimation for diffusion coefficient as a function of sum of squared estimated D for HDPE/limonene system at a=0.4, $T=50\ C$ Figure 49.

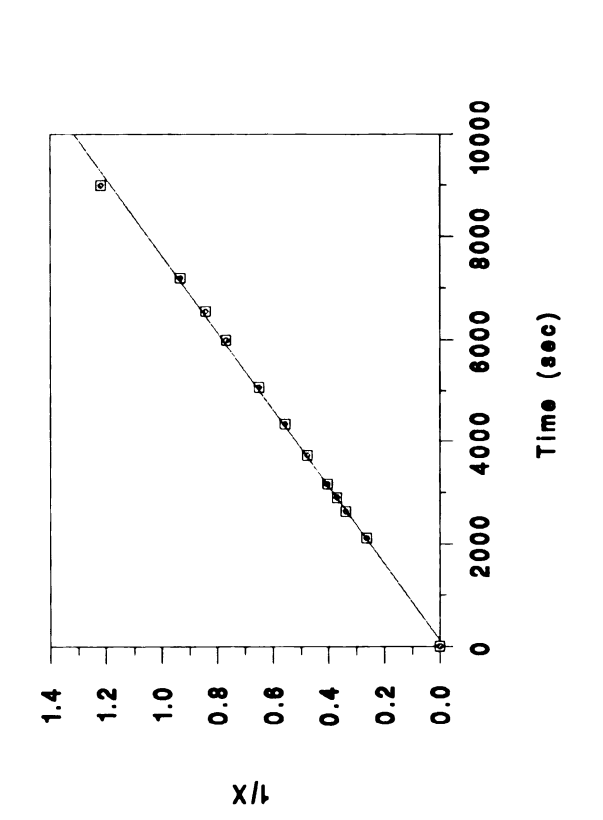


Figure 50. 1/X as a function of time for system OPP/limonene at a=0.4, T=50 C

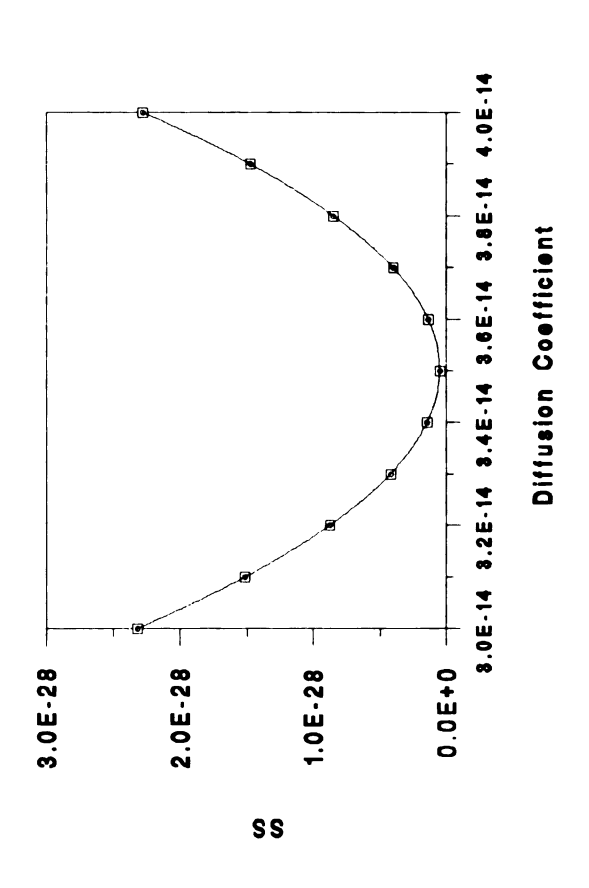


Figure 51. BEst estimateion for diffusion coefficient as a function of sum of squared estimated D for OPP/limonene system at a=0.4, T=50 C

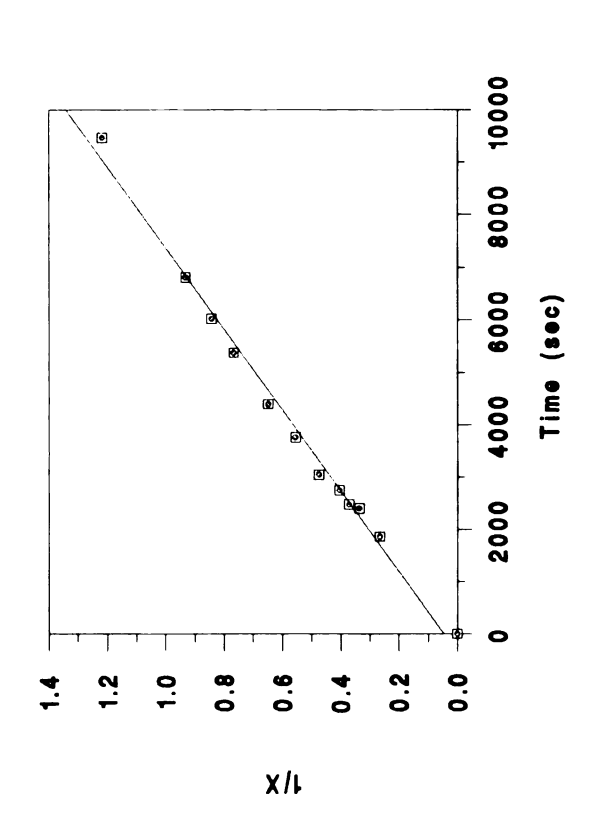


Figure 52. 1/X as a function of time for system HDPE/pinene at a=0.4, T=50 C

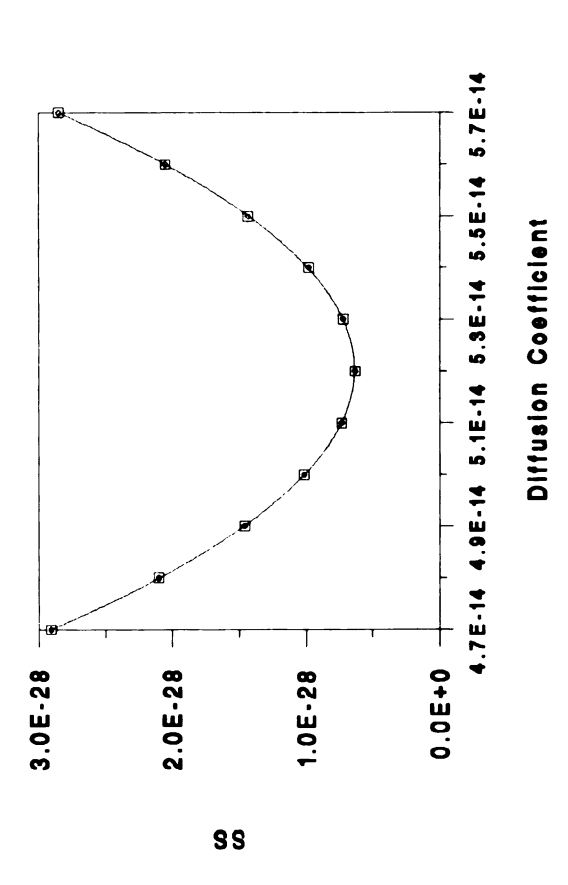


Figure 53. Best estimation for diffusion coefficient as a function of sum of squared of estimated D for HDPE/pinene system at a=0.4, T=50 C

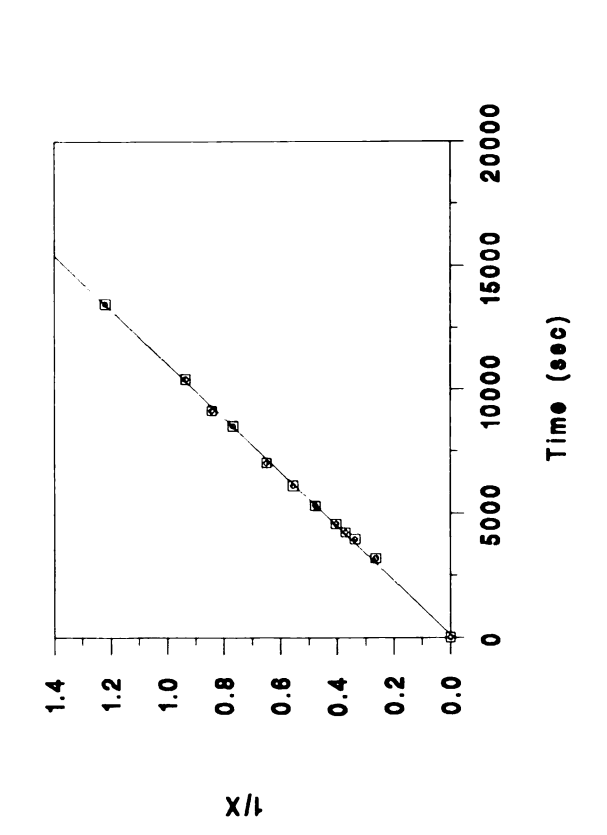
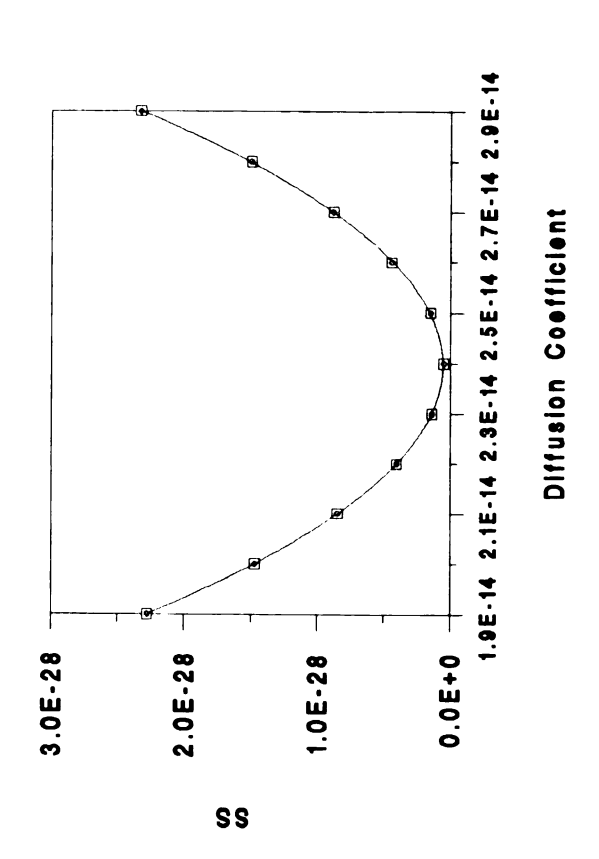


Figure 54. 1/X as a function of time for system OPP/pinene at a=0.4, T=60 C



Best estimation for diffusion coefficient as a function of sum of squared of estimated D for OPP/pinene system a=0.4, T=60 C Figure 55.

Table 27. Experimental data for limonene and α -pinene in high density polyethylene and oriented polypropylene structures at a=0.4, T=50°C

Parameters	Limonene		α-Pinene	
	HDPE	OPP	HDPE	OPP
t _{1/4} (sec)	921	2907	2467	4240
t _{1/2} (sec)	1341	4344	3758	6128
t _{3/4} (sec)	2004	6540	6012	9143
K ₁	0.4600	0.4445	0.4103	0.4637
K ₂	0.6868	0.6692	0.6565	0.6919
D_{ave} $(m^2/sec 10^{-14})$	14.9 ± .6	3.51 ± .2	5.2 ± .3	2.42 ± .2
$\begin{array}{c} \mathbf{D_{esti}} \\ (\text{m}^2/\text{sec } 10^{-14}) \end{array}$	15.0	3.50	5.20	2.42

Evaluation The Applicability of MAS 2000 Organic Vapor Permeation Test System

The lower limit of detectability for the system was found to be approximately 0.2 to 0.4 mg/hr, with a running time of 44 hr. A recent system upgrade allows for a run time greater than 44 hr. If the MAS 2000 permeability unit is modified with a device for dynamic trapping of permeated vapor, the dynamic purge and trap/thermal desorption system, the system sensitivity can be increased by three or four order of magnitude over the continuous flow isostatic procedure (Chang, 1996).

Software developed for the MAS 2000 permeation Test

System, for determining the permeability constant and

diffusion coefficient, is based on the assumption that the

diffusion process can be described as Fickian. The

application of the consistency test to the experimental data

showed that for the penetrant/polymer systems evaluated,

that the diffusion process was Fickian and the experimental

parameters of temperature and vapor concentration were well

controlled.

To eliminate "dead time", the cycle time entered should be close to the total length of time it takes the computer to cycle through all required functions, which represents a total time of about 3.52 seconds. The typical cycle time for the system is 5 seconds.

ERROR ANALYSIS

The error associated with gas or vapor permeation measurements which involves gas headspace sampling and injection will be highly dependent upon the operators skill in handling the gas or vapor samples and in recognizing sampling problems. If we assume that the gas sampling syringe is working properly and there is no operator error, the total estimated error in a single headspace syringe sample measurement is 7%, which includes 2% syringe volume accuracy, 1% GC's detector accuracy, 2% sampling volume error from leaking septa, and 2% decreased permeant due to sample removal or mixing problem. The relative error is the percent error where the amount of variation or uncertainty in a measurement is divided by the best estimate of the true value for the parameter which is an average of several experimental values (Taylor, 1982).

Other sources of error include temperature fluctuations in the environment, which will effect the permeant vapor concentration. Increases in temperature will raise the permeant concentration by increasing the saturation vapor pressure of the permeant in the carrier gas. The following error analysis describes the error in this particular procedure and makes estimations of the magnitude of these errors and their effect on experimental results.

Isostatic procedure:

For the permeability parameters determined by the MAS 2000 Organic Vapor Permeation Test System, the errors and uncertainties in the steady state permeation come from: (i) individual measurement error and variability; and (ii) fundamental error of initial baseline. In general, steady state transmission rate values showed a variation at about 3%, based on the last 10 permeation readings from the system. The error associated with the baseline is within 3%. Based on duplicate analyses, the precision of the instrument was ±10% of the mean. A variation of 5% in film thickness, and 5% syringe error related to the determining of the calibration factor for the MAS 2000 Permeability unit also to the error. The errors for permeability can be combined by the following equation (Taylor, 1982) and gives an estimate of the uncertainty of permeance values of approximatly 13% error.

$$\sqrt{3^2 + 3^2 + 10^2 + 5^2 + 5^2} = 13\%$$

Quasi-isostatic procedure:

In addition to sampling error, as described above, another major source of error in the quasi-isostatic procedure is determining the straight line describing the steady state transmission rate. The errors and uncertainties

in the steady state permeation come from (i)individual measurement error and variability; and (ii)determination of the transmission rate from the linear portion of the transmission rate curve. The estimated uncertainties for this calculated parameter are associated with 5% syringe measurement error, 5% polymer films surface and thickness error, 5% permeant concentration uncertainty, and 12% permeation rate error for duplication. The total error estimation was 16%.

SUMMARY AND CONCLUSIONS

For a series of organic vapor/polymer membrane combinations, permeance values were obtained from permeability studies based on an isostatic procedure utilizing the MAS Technology Model 2000 Permeation Test System and a quasi-isostatic procedure. For each temperature three vapor activity levels were evaluated. The specific activity levels varied as a function of both the specific polymer and temperature of test. Permeability studies were carried out at three temperatures to allow evaluation of the Arrhenius relationship.

From the results presented in the previous sections, the following are the conclusions of this study:

- 1. Temperature strongly affects the permeability and diffusivity of flavor and aroma compounds in barrier structures. Over the temperature range studied, the relationship between permeance and temperature followed well the Arrhenius expression. Concentration levels greatly affected the permeance values but not the diffusion coefficients of flavor and aroma compounds in the barrier films.
- 2. The agreement between the permeance values determined by the isostatic and quasi-isostatic procedures was quite satisfactory.

- 3. The experimental data evaluated by the consistency test showed that two the constants $(K_1 \text{ and } K_2)$, calculated from the experimental data, were about 7% different from the theoretical values. This test also showed that the diffusion process was Fickian and the experimental parameters of temperature and vapor concentration were well controlled.
- 4. The barrier properties of the six polymer structures evaluated, in order of decreasing barrier performance, are as following: Metallized PET/OPP, Acrylic coated OPP, Saran coated OPP, OPP, HDPE and Glassine.
- 5. The results of the studies described illustrate the general utility of the MAS Technologies Inc. Model 2000 Organic Vapor Permeation Test System for evaluating the organic vapor barrier properties of polymer membranes. With the low limit of detectability ranging between 0.4 mg/hr for toluene permeability to 0.2 mg/hr for the permeability of ethyl acetate for continuous running 44 hours.

Appendix A

Table 28. Calibration data for ethyl acetate in acetonitrile with a 1 μ l injection volume

Solution Con.	Total Quantity	Area Response
(ppm)	(g)	(Au)
0	0	0
10	8.94×10 ⁻⁹	5746
20	17.88×10 ⁻⁹	14157
40	35.76×10 ⁻⁹	35158

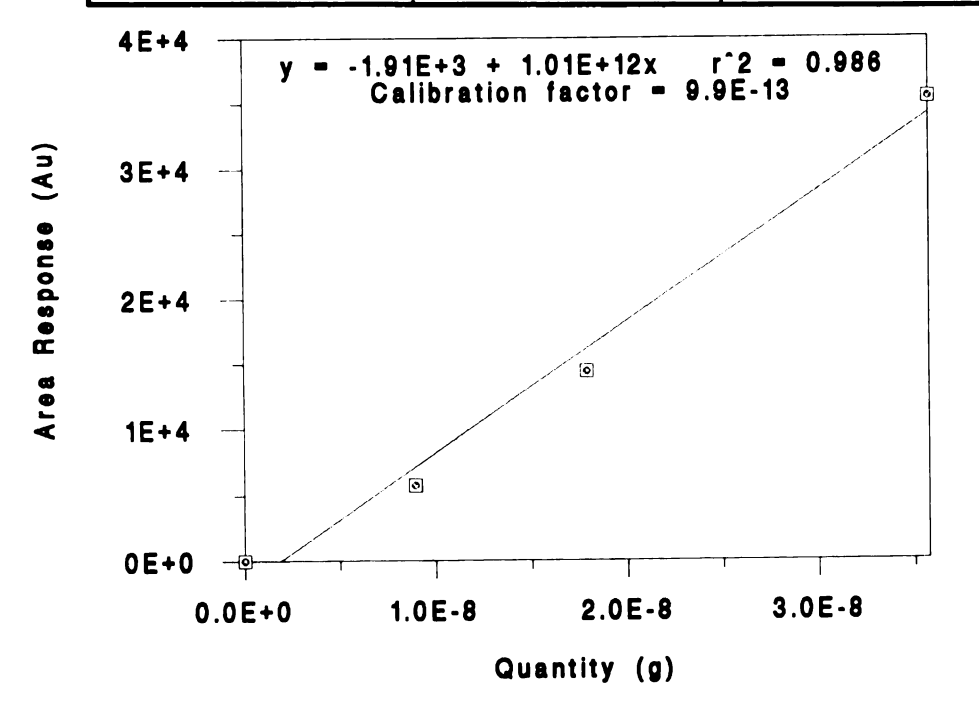


Figure 56. Calibration curve for ethyl acetate by GC-FID

Table 29. Calibration data for toluene in ortho- dichlorobenzen with a 1 μ l injection volume

Solution Con.	Total Quantity	Area Response
(ppm)	(g)	(Au)
0	0	0
5	4.35×10 ⁻⁹	2885
10	8.70×10 ⁻⁹	5898
20	1.74×10 ⁻⁸	12370
40	3.48×10 ⁻⁸	24637

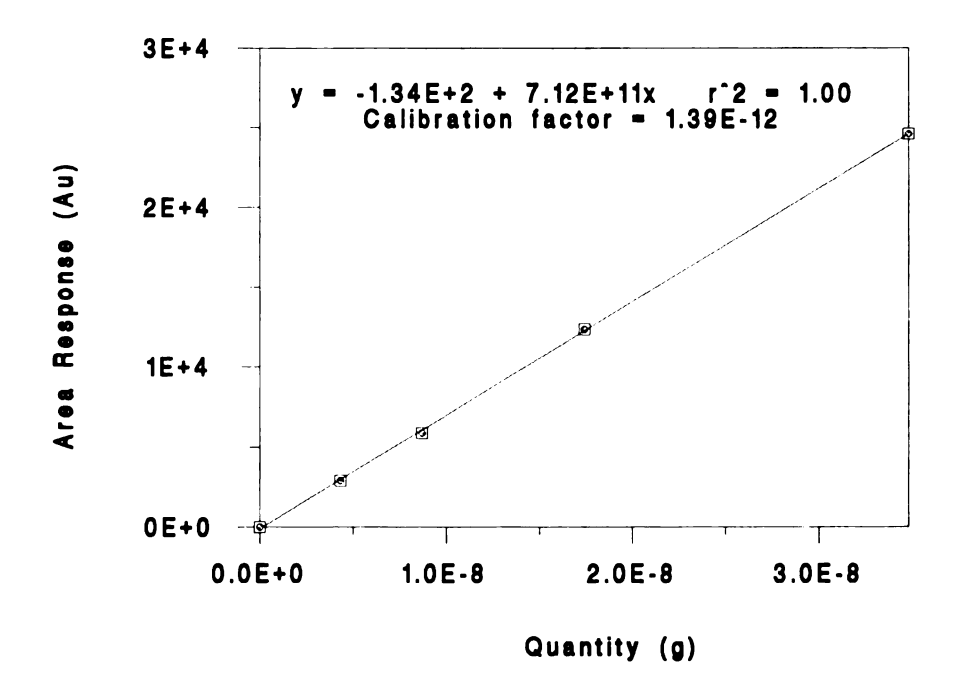


Figure 57. Calibration curve of toluene by GC-FID

Table 30. Calibration data for limonene in acetonitrile with a 1 μ l injection volume

Solution Con.	Total Quantity	Area Response
(ppm)	(g)	(Au)
0	0	0
6	5.04×10 ⁻⁹	29443
10	8.40×10 ⁻⁹	50562
20	1.68×10 ⁻⁸	101811
40	3.36×10 ⁻⁸	191058

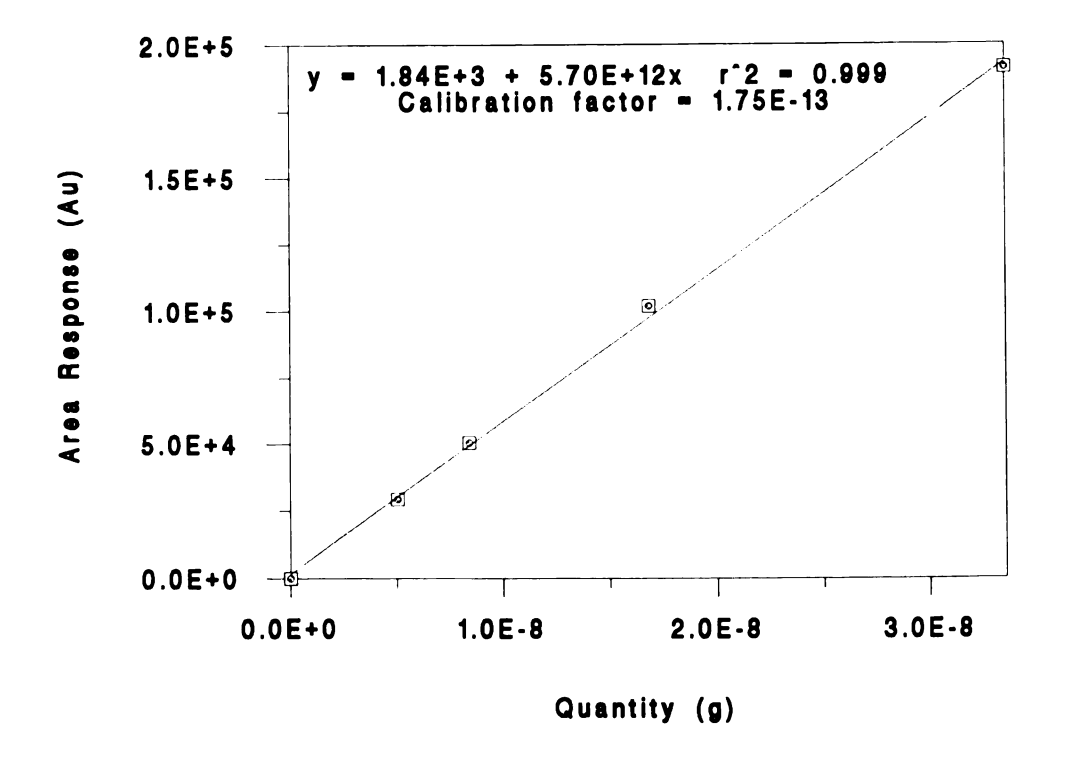


Figure 58. Calibration curve for limonene by GC-FID

Table 31. Calibration data for methyl ethyl ketone in xylenes with a 1 μ l injection volume

Solution Con.	Total Quantity	Area Response
(ppm)	(g)	(Au)
0	0	0
6	5.04×10 ⁻⁹	49273
10	8.40×10 ⁻⁹	83810
20	1.68×10 ⁻⁸	126900
40	3.36×10 ⁻⁸	240959

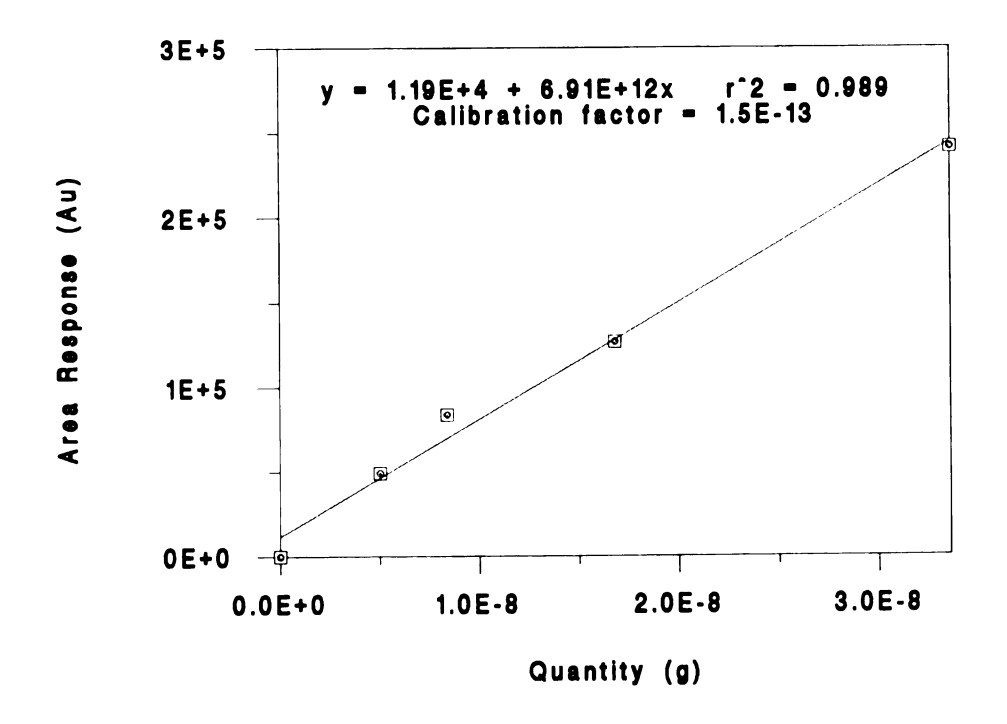


Figure 59. Calibration curve for methyl ethyl ketone by GC-FID

Table 32. Calibration data for $\alpha\text{-pinene}$ in acetonitrile with a 1 μl injection volume

Solution Con.	Total Quantity	Area Response
(ppm)	(g)	(Au)
0	0	0
5	4.29×10 ⁻⁹	112558
10	8.58×10 ⁻⁹	220965
20	1.72×10 ⁻⁸	467515
40	3.43×10 ⁻⁸	868631

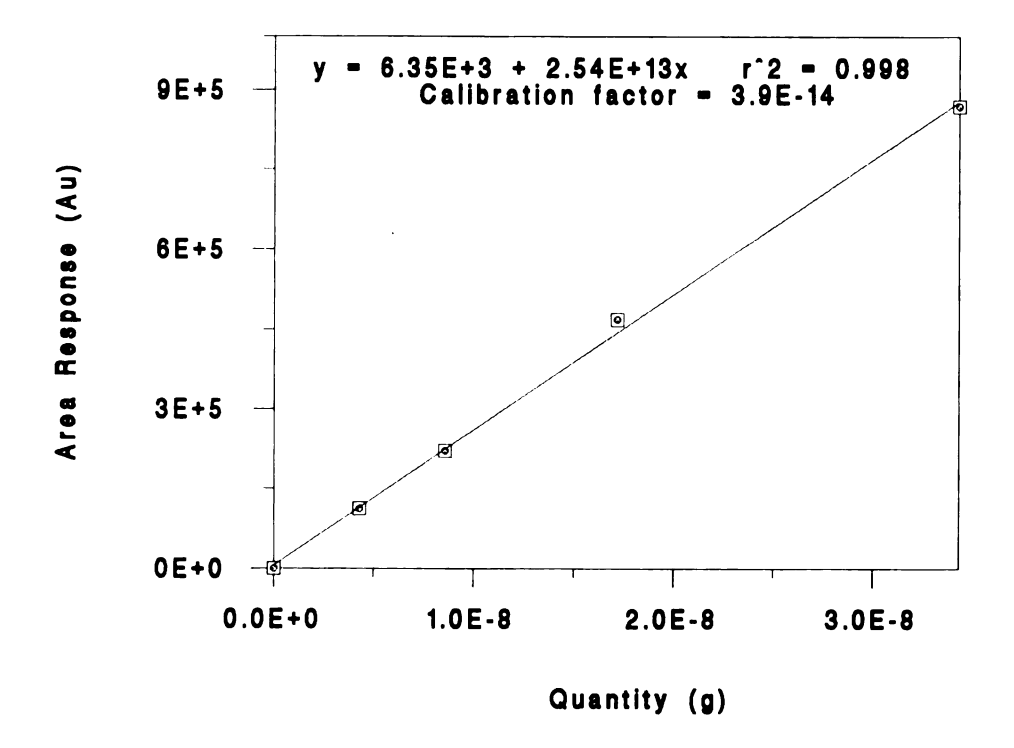


Figure 60. Calibration curve for pinene by GC-FID

Appendix B

For the permeant of ethyl acetate, the permeation rate of a series packaging films were as following:

HDPE (a=0.05)
$$P = -5.70 \times 10^{-6} + 1.41 \times 10^{-6} \text{ (min)}$$
 ($r^2 = 0.994$)

 $P = -6.64 \times 10^{-7} + 1.18 \times 10^{-6} \text{ (min)}$ ($r^2 = 0.991$)

OPP (a=0.08) $P = -1.29 \times 10^{-5} + 3.43 \times 10^{-6} \text{ (hr)}$ ($r^2 = 0.994$)

 $P = -1.89 \times 10^{-5} + 4.91 \times 10^{-6} \text{ (hr)}$ ($r^2 = 0.993$)

Saran OPP (a=0.2) $P = -2.38 \times 10^{-6} + 6.24 \times 10^{-7} \text{ (hr)}$ ($r^2 = 0.999$)

 $P = -1.93 \times 10^{-6} + 4.64 \times 10^{-7} \text{ (hr)}$ ($r^2 = 0.993$)

Acrylic OPP (a=0.2) $P = -4.75 \times 10^{-6} + 4.34 \times 10^{-7} \text{ (hr)}$ ($r^2 = 0.971$)

 $P = -2.94 \times 10^{-7} + 6.45 \times 10^{-7} \text{ (hr)}$ ($r^2 = 0.974$)

Glassine (a=0.05) $P = -7.13 \times 10^{-5} + 1.01 \times 10^{-6} \text{ (min)}$ ($r^2 = 0.991$)

 $P = -9.08 \times 10^{-5} + 1.11 \times 10^{-6} \text{ (min)}$ ($r^2 = 0.994$)

For the permeant of toluene, the permeation rate of a series packaging films were as following:

HDPE (a=0.05)
$$P = -7.87 \times 10^{-6} + 4.38 \times 10^{-7} \text{ (min)}$$
 $(r^2 = 0.996)$
 $P = -6.15 \times 10^{-6} + 4.41 \times 10^{-7} \text{ (min)}$ $(r^2 = 0.991)$
OPP (a=0.05) $P = -2.38 \times 10^{-6} + 6.59 \times 10^{-7} \text{ (hr)}$ $(r^2 = 0.984)$
 $P = -5.06 \times 10^{-6} + 6.78 \times 10^{-7} \text{ (hr)}$ $(r^2 = 1.000)$
Saran OPP (a=0.2) $P = -3.25 \times 10^{-7} + 9.85 \times 10^{-8} \text{ (hr)}$ $(r^2 = 0.997)$
 $P = -3.62 \times 10^{-6} + 1.02 \times 10^{-7} \text{ (hr)}$ $(r^2 = 1.000)$
Acrylic OPP (a=0.2) $P = -4.05 \times 10^{-7} + 7.33 \times 10^{-8} \text{ (hr)}$ $(r^2 = 0.998)$
 $P = -4.79 \times 10^{-7} + 7.29 \times 10^{-8} \text{ (hr)}$ $(r^2 = 0.994)$
Glassine (a=0.05) $P = -6.02 \times 10^{-6} + 8.29 \times 10^{-8} \text{ (min)}$ $(r^2 = 0.992)$

$$P = -4.64 \times 10^{-6} + 1.17 \times 10^{-7} \text{ (min)} \quad (r^2 = 0.996)$$

For the permeant of limonene, the permeation rate of a series packaging films were as following:

HDPE (a=0.1)
$$P = -2.06 \times 10^{-7} + 2.22 \times 10^{-7} (hr)$$
 $(r^2 = 0.994)$ $P = -4.99 \times 10^{-7} + 2.20 \times 10^{-7} (hr)$ $(r^2 = 0.994)$ OPP (a=0.1) $P = -1.64 \times 10^{-6} + 1.17 \times 10^{-7} (hr)$ $(r^2 = 0.986)$ $P = -2.82 \times 10^{-6} + 1.77 \times 10^{-7} (hr)$ $(r^2 = 0.990)$ Saran OPP (a=0.4) $P = -3.72 \times 10^{-7} + 6.01 \times 10^{-9} (hr)$ $(r^2 = 0.985)$ $P = -1.14 \times 10^{-7} + 5.14 \times 10^{-9} (hr)$ $(r^2 = 0.891)$ Acrylic OPP (a=0.4) $P = -9.23 \times 10^{-7} + 5.55 \times 10^{-9} (hr)$ $(r^2 = 0.967)$ $P = -5.30 \times 10^{-7} + 4.07 \times 10^{-9} (hr)$ $(r^2 = 0.934)$ Glassine (a=0.1) $P = -1.30 \times 10^{-6} + 2.11 \times 10^{-6} (min)$ $(r^2 = 0.993)$ $P = -1.2710^{-6} + 1.33 \times 10^{-8} (min)$ $(r^2 = 0.995)$

For the permeant of methyl ethyl ketone, the permeation rate of a series packaging films were as following:

HDPE (a=0.05)
$$P = -1.39 \times 10^{-5} + 6.00 \times 10^{-7} \text{ (min)}$$
 ($r^2 = 0.992$)
 $P = -1.18 \times 10^{-5} + 5.87 \times 10^{-7} \text{ (min)}$ ($r^2 = 0.999$)
OPP (a=0.05) $P = -9.49 \times 10^{-6} + 4.97 \times 10^{-6} \text{ (hr)}$ ($r^2 = 0.995$)
 $P = -9.88 \times 10^{-6} + 4.76 \times 10^{-6} \text{ (hr)}$ ($r^2 = 0.982$)
Saran OPP (a=0.2) $P = -4.16 \times 10^{-5} + 1.43 \times 10^{-6} \text{ (hr)}$ ($r^2 = 0.975$)
 $P = -9.32 \times 10^{-5} + 1.89 \times 10^{-6} \text{ (hr)}$ ($r^2 = 0.915$)
Acrylic OPP (a=0.2) $P = -1.39 \times 10^{-5} + 3.65 \times 10^{-7} \text{ (hr)}$ ($r^2 = 0.997$)
 $P = -1.65 \times 10^{-5} + 4.18 \times 10^{-7} \text{ (hr)}$ ($r^2 = 0.904$)
Glassine (a=0.05) $P = 1.67 \times 10^{-6} + 1.40 \times 10^{-7} \text{ (min)}$ ($r^2 = 0.961$)
 $P = 3.81 \times 10^{-7} + 1.04 \times 10^{-7} \text{ (min)}$ ($r^2 = 0.931$)

For the permeant of $\alpha\text{-pinene,}$ the permeation rate of a series packaging films were as following:

HDPE (a=0.1)
$$P = -3.45 \times 10^{-6} + 2.38 \times 10^{-7} (hr)$$
 $(r^2 = 0.993)$ $P = -2.64 \times 10^{-6} + 2.03 \times 10^{-7} (hr)$ $(r^2 = 0.991)$ OPP (a=0.2) $P = -2.11 \times 10^{-5} + 6.84 \times 10^{-7} (hr)$ $(r^2 = 0.948)$ $P = -4.39 \times 10^{-6} + 7.20 \times 10^{-7} (hr)$ $(r^2 = 0.987)$ Saran OPP (a=0.4) $P = -6.62 \times 10^{-6} + 2.08 \times 10^{-7} (hr)$ $(r^2 = 0.979)$ $P = -5.01 \times 10^{-6} + 2.03 \times 10^{-7} (hr)$ $(r^2 = 0.984)$ Acrylic OPP (a=0.4) $P = -1.32 \times 10^{-6} + 2.58 \times 10^{-8} (hr)$ $(r^2 = 0.999)$ $P = -6.29 \times 10^{-7} + 2.06 \times 10^{-8} (hr)$ $(r^2 = 0.998)$ Glassine (a=0.1) $P = -2.18 \times 10^{-6} + 5.64 \times 10^{-8} (min)$ $(r^2 = 0.954)$

 $P = -9.25 \times 10^{-7} + 4.03 \times 10^{-8} \text{ (min)} \quad (r^2 = 0.948)$

BIBLIOGRAPHY

- Anon. 1989. The aroma protection of sensitive food products barrier properties of coated Opp film. Packaging Production International, no. 3/4: 58-59.
- Apostolopoulos, D.; and Winters, N. 1991. Measurement of permeability for packaging films to d-limonene vapour at low levels. Packaging Technol. & Sci., 4(3): 131-138.
- Baner, A. L. 1987. The measurement and analysis of the diffusion of toluene in polymeric films. Master Thesis. Michigan State University, East Lansing, MI.
- Baner, A. L.; Hernandez, R. J.; Jayaraman, K.; and Giacin, J. R. 1986. Isostatic and quasi-isostatic methods for determining the permeability of organic vapors through barrier membranes. Current Technologies in Flexible Packaging, ASTM STP 912: 49-62. American Society for Testing and Materials, Philadelphia.
- Barrer, R. M., 1939, Trans. Faraday Society, 35: 628
- Begley T. H.; and Hollifield H. C. 1990. Evaluation polyethylene terephthalate cyclic trimer migration from microwave food packaging using temperature time profiles. Food Additives and Contaminants, 7(3): 339-346.
- Blakesley, G. N. 1974. Kinetic considerations of the permeation of organic vapours through a flexible packaging film. J. of Food Sci., vol 9: 285-296.
- Blakesley, G. N. 1974. Technical note: organic vapour permeation through packaging films. J. of Food Technol., vol 10: 365-367.
- Briston, J. H.; 1970. Plastic in packaging part III permeability of plastics. Flavor Industry, vol 11: 779-783.
- Comyn, J. 1985. Introduction to polymer permeability and the mathematics of diffusion. in "Polymer Permeability".

 Comyn, J. (ed), 1-10. Elsevier Applied Science

 Publishers, New York, N. Y.
- Comyn, J.; Cope, B. C.; and Werrett, M. R. 1990.

 Permeation of water through the polymeric components of boil-in-bag laminates. Food and Additives and

- Contaminants, 7(3): 347-356.
- Crank, J. and Park, G. S. 1968. "Diffusion in polymers", Academic Press, N. Y.
- Crank, J. 1975. "The Mathematical of Diffusion", 2nd ed., Clarendon Press, Oxford, England.
- Cutler, J. A., Kaplan, E., Mclaren, A. D. and Mark, H. 1951. The permeation of vapors through polyethylene. TAPPI. 34(9): 404.
- Demorest, R. L. 1992. Recent developments in testing the permeability of good barriers. J. of Plastic Film & Sheeting, vol 8: 109-123.
- DeLassus, P. T. 1993. Permeation of flavors and aromas through glassy polymers. Polymers, Laminations & Coatings Conference, no. 1: 263-266.
- DeLassus, P. T.; Strandburg, G.; and Howell, B. A. 1988. flavor and aroma permeation in barrier film: the effects of high temperature and high humidity. Tappi Journal, Nov.: 177-181.
- DeLassus, P. T.; Tou, J. C.; Babined, M. A.; Rulf, D. C.; Karp, B. K.; and Howell, B.? A. 19 Transport of apple aromas in polymer films. American Chemical Society Symposium Series, 365: 11-27.
- DeLassus, P. T.; and Marcus, S. A. 1987. Diffusion and sorption of organic molecules by polymer films. Activities Report of the R & D Association, San Antonio, TX, vol 39: 91-97.
- Felder, R. M.; Spence, R. D.; and Ferrell, J. K. 1975. Permeation of sulfur dioxide through polymer. J. of Chemical and Engineering, 20(3): 235-242.
- Fishman, D. 1995. Barrier structures for food packaging. Plastic World. vol 55: 66-67.
- Franz, R. 1993. Permeation of volatile organic compounds across polymer films part I: development of a sensitive test method suitable for high-barrier packaging films at very low permeant vapour pressures. Packaging Technol. & Sci., vol 6: 91-102.
- Fujita, H. 1961. Diffusion in polymer-diluent systems. Fortschr. Hochpolym.-Forsh. 3(9): 1.

- Fujita, H. 1968. Organic vapors above the glass transition temperature. ch. 3. in "Diffusion in polymers", Crank, J. and Park, G. S. (eds). Academic Press, N. Y.
- Gavara, R.; Hernandez, R. J. 1993. Consistency test for continuous flow permeability experimental data. J. of Plastic Film & Sheeting, 9(4): 126-138.
- Gavara, R.; Hernandez, R. J. 1993. The effect of water on the transport of oxygen through nylon-6 films. J. of Polymer Sci. Part B: Polymer physics, vol 32, 2375-2382.
- Gillette, P.C. 1988. Measurement of organic vapor migration in thin films. Advancing Coating & Packaging Technol. 4 (1): 193-198.
- Goldade, V. A.; Aleshkevich, E. N.; Bezrukov, S. S.; Pinchuk, L. S.; Reshits, G. V.; and Kestelman, V. N. 1995. Polymeric packaging film for food products. Packaging Technol. & Sci., vol 8: 149-158.
- Hatzidimitriu, E.; Gilbert, S. G.; Loukakis, G.; and Paik, S. 1987. Permeation studies of model flavor compounds in nylon 6 film. Frontiers of Flavor, Proceedings of the 5th International Flavor Conference. Elsevire Science Publishers B.V., 297-305.
- Hatzidimitriu, E.; Gilbert, S. G.; and Loukakis, G. 1987. Odor barrier properties of multi-layer packaging film at different relative humilities. J. of Food Sci., 52(2): 472-474.
- Hernandez, R. J.; Giacin, J. R.; and Baner, A. L. 1986. The evaluation of the aroma barrier properties of polymer films. J. of Plastic Film & Sheeting, vol. 2: 187-211.
- Hertlein, V. J.; Franz, L.; and Weisser, H. 1992.

 Measurement of gas permeability of packaging materials and packages comparison the precision of two test arrangements. Verpackungs-Rundschau. 43(4): 25-29.
- Hotchkiss, J. H. 1987. Plastic packaging can cause aroma sorption. Food Engineering, April, 39-42.
- Johansson, F.; and Leufven A. 1994. Food packaging polymer films as aroma vapor barrier at different relative humilities. J of Food Sci., 59(6): 1328-1331.

- Keller, L. E. 1992. Innovative BOPP packaging films for flexible packaging. ANTEC 50th Conference, Technical papers: 1853-1861.
- Lee, W. M. 1978. Selection of barrier materials from molecular structure. Org. Coating and Plast. Chem., vol. 39: 341-346.
- Letinski, J.; and Halek, G. W. 1992. Interactions of citrus flavor compounds with polypropylene films of varying crystallinities. J of Food Sci., 57(2): 481-484.
- Liang, B.; Fields, R. J.; and King, C. J. 1990. The mechanisms of transport of water and n-propanol through pulp and paper. Drying Technol. 8(4): 641-665.
- Lin, C. H. 1995. Permeability of organic vapors through a packaged confectionery product with a cold seal closure: theoretical and practical consideration. Master Thesis. Michigan State University, East Lansing, MI.
- Liu, K. J.; Hernandez, R. J.; and Giacin, J. R. 1991. The effect of water activity and penetrant vapor activity on the permeation of toluene vapor through a two-side PVDC coated opaque oriented polypropylene film. J. of Plastic Film & Sheeting, 7(1): 56-67.
- Mason, R. C.; Delassus, P. T.; Strandburg, G.; and Howell, B. A. 1991. Diffusion of flavors in polymers: effect of permeant size and shape. Polymers, Laminations & Coatings Conference, 629-635.
- Meares, P. 1958a. Diffusion of allyl chloride in PVA. Part I. The steady state of permeation. J. Polymer Sci. 27: 391.
- Miltz, J.; Passy, N.; and Mannheim, C. H. 1992. Mass transfer from and through packaging materials. Packaging Technol. & Sci., vol 5: 49-56.
- Nielsent, T. J.; and Giacin, J. R. 1994. The sorption of limonene/ethyl acetate binary vapour mixtures by a biaxially oriented polypropylene film. Packaging Technol. & Sci., 7(5): 247-258.
- Pascat, B. 1985. Study of some factors affecting permeation. in "Food Packaging and Preservation". Mathlouthi, M. (ed.), 7-23. Elsevier Applied Science Publishers, New York, N.Y.

- Peppas, N. A.; and Sekhon, G. S. 1980. Mathematical analysis of transport properties of polymer films for food packaging IV. Plastics Progress Through Processing, New York, ANTEC: 38th annual technical conference: 681-683
- Perdikoulias, J.; and Wybenga, W. 1989. Designing barrier film structures. Tappi Journal, Nov.: 107-112.
- Rogers, C. E., Stannett, V. and Szwarc, M. 1960. The sorption, diffusion and permeation of organic vapors in polyethylene. J. polymer Sci. 45: 61.
- Rogers, C. E. 1964. Permeability and chemical resistance of polymers. ch. 9 in "Engineering design for plastics". Bear, E. (ed). Rheinhold, N. Y.
- Rogers, C. E. 1965. Solubility and diffusivity. ch. 6 in "Physics and chemistry of the organic solid state vol. 2". Fox, D., Labes, M. M. and Weissberger, A. (ed). J. Willey & Sons. N. Y.
- Rogers, C. E. 1985. Permeation of gases and vapours in polymers. in "Polymer Permeability". Comyn, J. (ed.), 11-69. Elsevier Applied Science Publishers, N.Y.
- Toi, K. 1978. Pressure dependence of diffusion coefficient for CO_2 in glassy polymers. Org. Coatings and Plastic Chem., vol 39: 178-183.
- Theodorou, E.; and Paik, S. 1992. Effect of organic vapour interaction on permeation rate through polymer films. Packaging Technol. & Sci., 5(1): 21-25.
- Sadler, G. D.; and Braddock R. J. 1991. Absorption of citrus flavor volatiles by low density polyethylene. J. of Food Sci., 56(1): 35-37.
- Salame, M. 1992. The individual contributions of crystallinity and orientation to the over-all barrier properties of PET. Fifth Ryder European Conference on Plastics and Packaging for Food and Beverages, 475-483.
- Strandburg, G.; Delassus, P. T.; and Howell, B. 1991.
 Thermodynamics of permeation of flavors in polymers.
 American Chemical Society Symposium Series, 365: 11-27.
- Stuk, L. G. F. 1990. Journal of Polymer Sci. Part B: polymer Physics, 28: 127 -131.

- Subramanian, P. M. 1985. Permeability barrier by controlled morphology of polymer blends. Polymer Engineering and Sci., 25(8): 483-487.
- Theodorou, E.; and Paik. J. S. 1992. Effect of organic vapour interaction on permeation rate through polymer films. Packaging Technol. & Sci., vol 5: 21-25.
- Varsanyi, I. 1985. Permeability of polymers in food packaging. in "Food Packaging and Preservation".

 Mathlouthi, M. (ed.), 25-38. Elsevier Applied Science Publishers, New York, N.Y.
- Vieth W. R. 1991. "Diffusion in and through polymers". Oxford University Press, New York.
- Yamada, K.; Mita, K.; Yoshida, K.; and Ishitani, T. 1992. A study of the absorption of fruit juice volatiles by the sealant layer in flexible packaging containers. Packaging Technol. & Sci., vol 5: 41-47.

I		
'		

HICHIGAN STATE UNIV. LIBRARIES
31293015673993